EFFECT OF SURFACE FINISH ON BOILING UNDER JET IMPINGEMENT

Effect of Surface Finish on Boiling Heat Transfer at Stagnation Point under Free Liquid Jet Impingement

By

Yasser Selima, B.Sc., M.A.Sc.

A Thesis

Submitted to the School of Graduate Studies

In Partial Fulfillment of the Requirements

For the Degree of

Master of Applied Science

McMaster University

Master of Applied Science	(2011) McMaster University
(Mechanical Engineering)	Hamilton, Ontario

TITLE: Effect of Surface Finish on Boiling Heat Transfer at Stagnation Point under Free Liquid Jet Impingement

AUTHOR: Yasser Selima, B.Sc., M.A.Sc., (Mechanical Engineering) Ain Shams University, Cairo, Egypt

SUPERVISOR: Dr. Mohamed S. Hamed, Associate Professor, Department of Mechanical Engineering

NUMBER OF PAGES: xv, 117

ABSTRACT

Experiments were performed to study the effect of surface finish and jet velocity on the boiling performance at the stagnation point under a free liquid planar jet. A rectangular jet with dimensions 9 mm x 1 mm was used to impinge subcooled water on the center of a copper surface 8 mm width x 20 mm length. Jet velocities ranged from 0.9 to 2.5 m/s while the degree of subcooling was kept constant at 10°C. Three surfaces were prepared using emery paper #1200, #500 and #320 and the arithmetic mean square of the roughness $\mathbf{R_a}$= 18.72, 401.65 and 533.53 nm.

Increasing the jet velocity has shown to increase the heat flux slightly in the single phase regime. Also by increasing the jet velocity, boiling was found to start at higher surface superheat achieving higher values of burn out heat flux BOF for jet velocities $V_j \leq 1.5$ m/s. This trend agrees with studies reported in literature. Some contradicting results occurred at higher jet velocities which is attributed to the flow profile.

For jet velocities lower than 2 m/s, the surface with higher $\mathbf{R_a}$ was found to have a delayed Onset of Nucleate Boiling ONB, higher Burn out Heat Flux BOF, and lower rate of heat transfer in the single phase regime. Surface finish did not show significant effect on boiling performance at higher jet velocities. The contradictions observed at jet velocities higher than 1.5 m/s were attributed to the flow profile.

Results regarding the effect of surface finish on heat transfer in the single phase regime under liquid jet impingement were compared to literature and a reasonable agreement was found. More studies are needed to explain the contradictions found for higher jet velocities.

ACKNOWLEDGEMENTS

First of all praise to God the greatest, the most merciful, the all beneficent, the omniscient, who guided the man to know which he did not know.

I wish to express my gratitude to my supervisor Dr. Mohamed S. Hamed, who helped whenever I was in need. I would also like to express my sincere thanks to my committee members Dr. Ross L. Judd and Dr. James S. Cotton, for their valuable suggestions and remarks throughout all the tasks of the study.

I am also indebted to the technicians of Mechanical Engineering Department at McMaster University; Ron Lodewyks, Jim McLaren, Mark McKenzie, J.P Talon and Joe Verhaeghe, for their help in constructing the experimental test facility.

Many thanks to Dr. Ahmed Omar who assisted me technically and provided help when needed. Also, I would like to thank my friends Dr. Hossam Sadek, Eng. Hassan Morsi and Eng. Mahmoud Marzouk for their help and support.

I also wish to sincerely thank Dr. Marilyn F. Lightstone and Dr. Samir Ziada for their help during the most challenging of times. Many thanks to the department of the Mechanical Engineering and the chair, Dr. Saeid Habibi, for extending the generosity. Last but not least, I would like to thank Dr. Nathan

Cooper for continuous advice and counseling on both professional and personal level.

I want also to express my full and deepest gratitude to my family; especially my wife, my parents, and my in laws for the constant support and love that I received during the past years.

DEDICATION

To My Wife, Mum and Dad

Table of Contents

List of Figures

List of Tables

Chapter 1 Introduction

Boiling heat transfer is considered as one of the best cooling methods that have been used in many applications for centuries. Boiling is heat transfer process coupled with phase change from liquid to vapor. Boiling could be classified into two main types; Pool and Forced convection boiling. Pool boiling happens when the fluid is stagnant while flow boiling happens when the fluid is being forced to flow over or across the heater surface. Flow boiling is also referred to as forced convection boiling.

Forced convection boiling can be classified into; Parallel Flow Boiling where the liquid is flowing parallel to the heated surface, and Jet Impingement Boiling where the liquid is admitted in the form of a jet normal to the heated surface. When a jet is impinged on a heated surface, the flow field could be divided into three main regimes; stagnation zone, developing flow and fully developed flow regime. First regime, stagnation zone, is located under the jet. It is followed by the developing flow regime where the jet spreads in the longitudinal direction forming a thin fluid layer on the heater surface. After a particular distance from the nozzle, the flow becomes fully developed and the thickness of the fluid layer increases. In the last regime, the flow could be treated as an open channel flow in case of using a planar jet.

To distinguish between the characteristics of both jet impingement and parallel flow boiling, we have to draw the boiling curve. The boiling curve is a relation between the heat flux on the vertical axis versus the temperature difference between the heated surface and the liquid saturation temperature on the horizontal axis. This temperature difference is referred to as the degree of superheat. Figure 1-1 shows a schematic sketch of the parallel flow boiling while Figure 1-2 shows the boiling curve for jet impingement boiling. The two figures show the different regimes starting with the single phase/forced convection regime. In this regime a linear relation relates the heat flux with the degree of superheat.

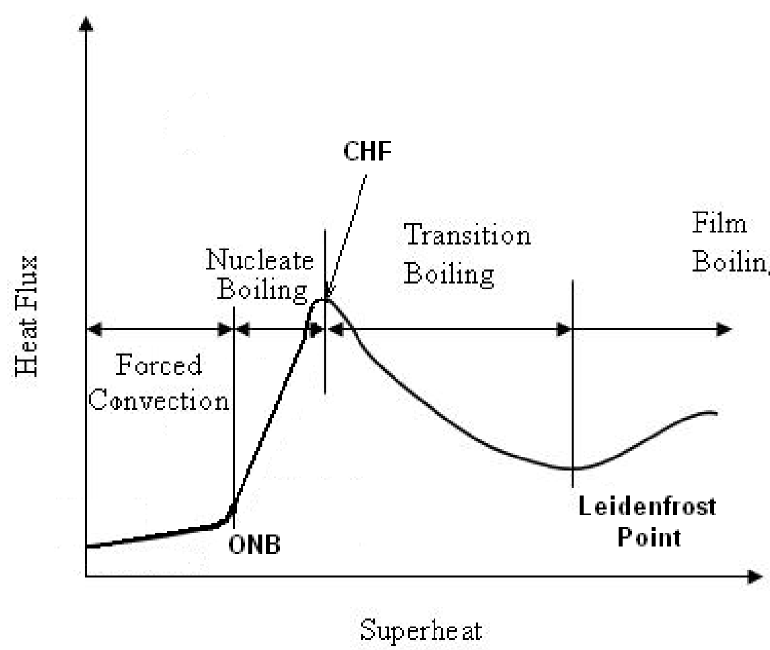

Figure 1-1 Boiling Curve for Parallel Flow Boiling

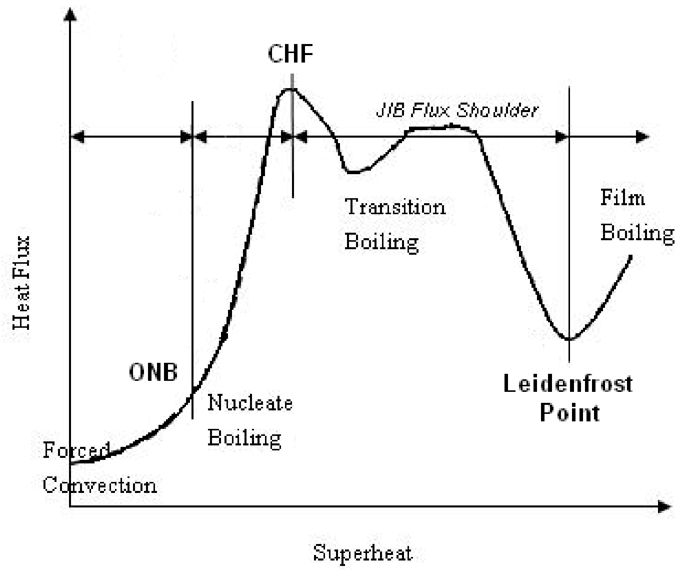

Figure 1-2 Boiling Curve for Jet Impingement Boiling

For both jet impingement and parallel flow boiling, the single phase regime is followed by the Onset of Nucleate Boiling ONB where the Nucleate Boiling regime starts. In the nucleate boiling regime, the rate of increase of heat flux is much higher with increasing surface degree of superheat. At the end of the nucleate boiling regime, the Critical Heat Flux CHF occurs marking the end of nucleate boiling and the beginning of a transition boiling regime. In transition boiling, bubbles occupy large area of the surface which is enough to merge and form large vapor bubbles and so blanket the heated surface. This causes deterioration in the heat transfer rate until it drops to a minimum value at a surface temperature known as the Leidenfrost point. Further increase in surface degree of superheat beyond the Leidenfrost point causes a stable vapor film to cover the entire surface marking the film boiling regime. The difference between flow and jet impingement boiling is the existence of heat flux shoulder after the CHF. This flux shoulder is one of the jet impingement boiling advantages where it keeps high heat transfer rate for a wide range of surface superheat during the transition regime. The other advantage of jet impingement boiling is that it is accompanied by higher heat transfer rate when compared to flow boiling.

Surface roughness is a measure of the texture of a surface. It is quantified by the vertical deviations of a real surface from its ideal form: If these deviations are large, the surface is rough; if they are small the surface is smooth. In general, roughness plays an important role in determining how a real object will interact with its environment. Rough surfaces have higher friction coefficients than smooth surfaces which accelerates the laminar to turbulent transition. Roughness is often a good predictor of the performance of a mechanical component. As one of the surface conditions, surface roughness could affect the boiling heat transfer by affecting the flow field or by increasing the number of surface cavities which acts as bubble nucleation sites.

Many different roughness parameters are being used. $\mathbf{R_a}$ is the most common parameter among them which represents the arithmetic average of the roughness profile. Some other common parameters include $\mathbf{R_z}$ and $\mathbf{R_q}$, sometimes called $\mathbf{R_{rms}}$. By convention every 2D roughness parameter is a capital R followed by additional characters in the subscript. The subscript identifies the formula that was used. $\mathbf{R_q}$ or $\mathbf{R_{rms}}$ represents the root mean square of the measured point. And $\mathbf{R_z}$ represents the average distance between the highest peak and lowest valley in each sampling length.

Due to the liquid jet impingement ability to remove high heat transfer rates for a wide range of surface temperatures, and because of the role of surface parameters on heat transfer performance, this study focuses on the effect of surface roughness on cooling performance at the stagnation point under free Liquid Jet Impingement. Chapter two presents literature review for the studies performed in this topic focusing on the most recent ones. Chapter three will introduce the experimental facility used in this study. It presents the test rig and the experimental procedure. Results and discussions will be presented in Chapter four followed by a conclusions and recommendations in the Chapter five.

Chapter 2 Literature Review

Many studies considered boiling under free jet impingement. Most of these studies focused on the effect of different parameters such as the jet velocity, degree of subcooling, and the distance between the jet and the targeted surface. None of these studies considered the effect of surface roughness/conditions on boiling heat transfer under free jet impingement cooling. This chapter will present briefly some of the most recent experimental work regarding liquid jet impingement as well as the significance of surface roughness parameters on boiling heat transfer.

2.1 Experimental Studies on Liquid Jet Impingement Cooling

Experimental studies, performed with liquid jet impingement, were under either steady state or transient conditions. Transient experiments could be performed by heating the surface to a predetermined degree of superheat and then quenching the surface with the liquid jet. During the transient experiment, the surface temperature decreases with time allowing the study of different regimes; starting from film boiling, transient, nucleate boiling and ending with the forced convection regime. The advantage of the transient experiments is that they are able to predict the actual cooling rates in an industrial process. However, the duration of the experiment does not allow enough time to study the underlying physics behind the boiling process. If the heater block in the transient experiments has large thermal inertia and is being cooled by a low jet velocity with low degree of subcooling, more detailed boiling studies could be performed.

Steady state experiments proceed by controlling the input heat under particular experimental conditions such as fixed jet velocity, nozzle to heater space, and liquid subcooling. The main advantage of conducting steady-state experiments is that there is no time constraint to study the variations in the bubble dynamics at the specified conditions. This gives an opportunity to obtain sufficient data about the nucleation sites, frequency of bubble formation and bubble growth rate.

Steady state experiments could be performed by controlling one of the two parameters; constant surface temperature or constant heat flux. Constant heat flux experiments could be achieved by adjusting the output power from a power source to obtain a certain level of heat flux. Constant surface temperature experiments need a feedback procedure to control the heating power thus fixing the heated surface temperature at the desired condition.

Most of the experimental studies focused on the effect of jet velocity and degree of liquid subcooling on the Onset Nucleate Boiling ONB and the Critical Heat Flux CHF. Other parameters had been studied such as nozzle to surface distance and the use of multiple jets. Examples from the steady state and unsteady experiments will be illustrated below, focusing on the effect of jet velocity and degree of subcooling.

2.1.1 Steady State Experiments

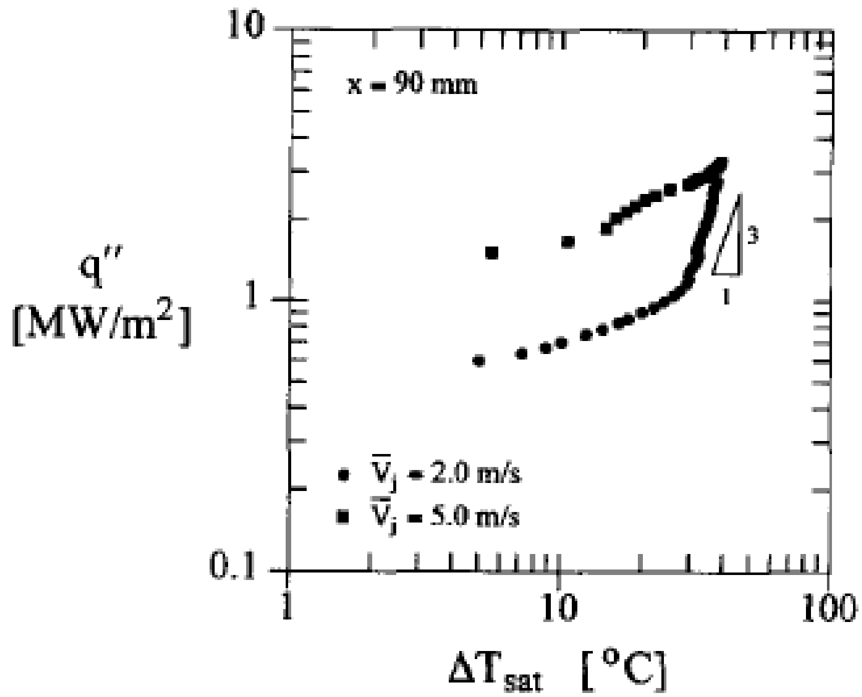

Figure 2-1 Boiling Curve at a Distance x=90 mm from the Stagnation Line, Wolf et al. (1996)

Wolf et al. (1996) studied the boiling of water impinged from a planar free jet on horizontal steel plate in both forced convection and nucleate boiling regimes. The experiments were conducted using jet velocity values between 2 and 5 m/s and heat flux ranging from 0.25 to 6.34 MW/m^2. The degree of subcooling was kept constant at 50°C. The planar jet dimensions were 10.2 mm x 102 mm while the heated plate dimensions were 37.5 mm width x 260 mm length. In the single phase regime, the heat transfer coefficient was influenced by the flow hydrodynamics more than the wall heat flux or the degree subcooling. In the fully developed region, distance from the stagnation was insignificant and the velocity effect on the heat transfer was dominated by the bubble induced mixing and evaporation. Increasing the jet velocity was shown to start the boiling at lower surface superheat while the heat flux and CHF increased as shown in Figure 2-1.

Robidou et al. (2003) studied the effect of jet velocity, water subcooling and nozzle-to-surface distance on boiling under free planar jet. Jet velocities ranged from 0.7 to 0.8 m/s while the experiments were conducted at 7 and 17 $^{\circ}$C of subcooling. The authors examined the whole boiling curve from the single phase regime to the film boiling regime and obtained the results illustrated in Figure 2-2. The heat transfer rate was improved by increasing the water subcooling in the forced convection and the nucleate boiling regimes. Increasing the jet velocity from 0.7 to 0.8 m/s increased the heat flux in the forced convection regime while no effect was reported on the fully developed nucleate boiling regime. However, they reported an increase in the CHF due to an increase of the jet velocity. Local boiling curves showed higher value of CHF at stagnation point than downstream, Figure 2-2. At the stagnation region and up to three jet widths, the authors observed high values of heat flux after the CHF verifying the existence of a flux shoulder in the transition boiling region. This was explained by the jet effect breaking up the agglomerating vapor patches in the unstable transition boiling regime.

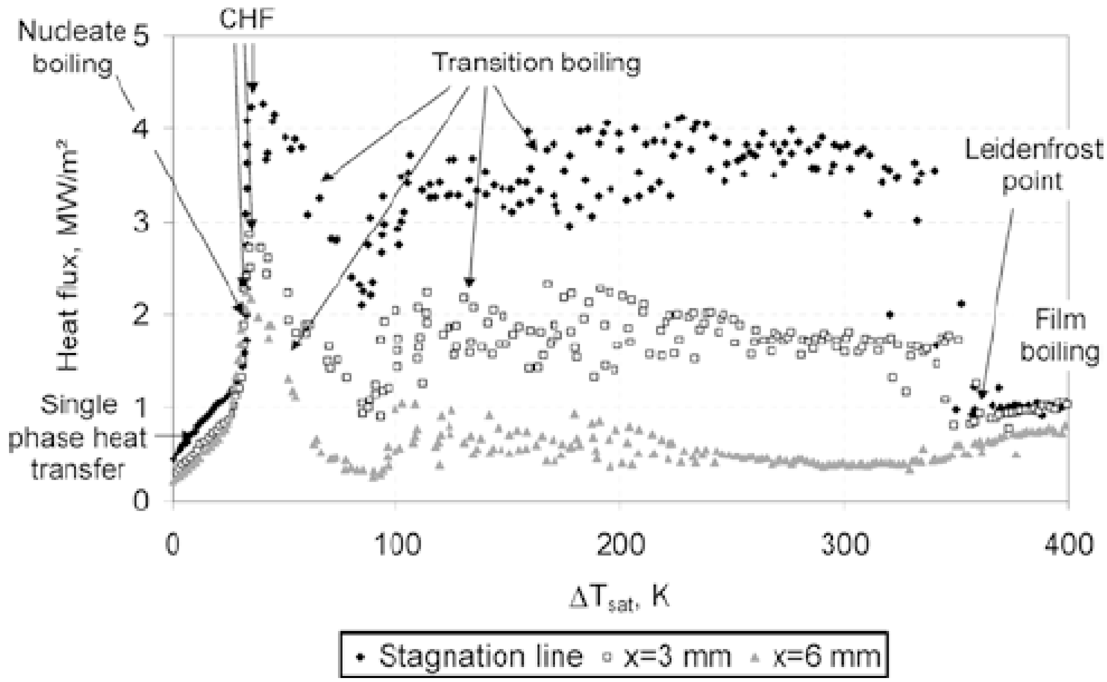

Figure 2-2 Local Boiling Curves, V_n=0.8m/s, ΔT_{sub}=16 K, H_n=6 mm, Robidou et al. (2003)

Omar et al. (2007) studied the effect of jet velocity and the degree of subcooling on liquid jet impingement cooling in the partial and fully developed nucleate boiling regimes. The study was conducted under steady state conditions, controlled surface temperature. Jet velocity ranged from 0.75 to 1.68 m/s, and the water degree of subcooling between 10 to 28°C. The nozzle used was a sudden contraction configuration and had rectangular cross section 1 mm width x 9 mm length. The heater surface was made of copper with dimensions 8 mm x 20 mm. The study used temperature measurements and visual observations to describe the changes to the boiling mechanisms in the partial and fully developed regimes as well as the critical heat flux. Data was analyzed using two approaches. The first approach used a one dimensional analysis to study the effect of jet velocity and the degree of subcooling. Whereas the other approach used a two dimensional analysis under which the relative variations in boiling curve were investigated for stagnation (*x/w=0*) and downstream locations (*x/w = 2 and 4*). Results indicated that increasing jet velocity and subcooling delayed the initiation of net vapor generation and reduced the average bubble size and frequency. Results also verified the existence of a flat flux shoulder after CHF.

Figure 2-3 shows the effect of jet velocity on the boiling performance. The figure illustrates that increasing the jet velocity from 0.75 m/s to 1.68 m/s shifted the ONB from 7.5°C to 13°C of surface superheat, as reported by the authors. Figure 2-4 shows the effect of increasing the degree of subcooling. As seen from the figure, the Onset Nucleate Boiling ONB point is shifted to higher surface superheat with increasing the degree of subcooling. The critical heat flux also increased with increasing the jet velocity and degree of subcooling.

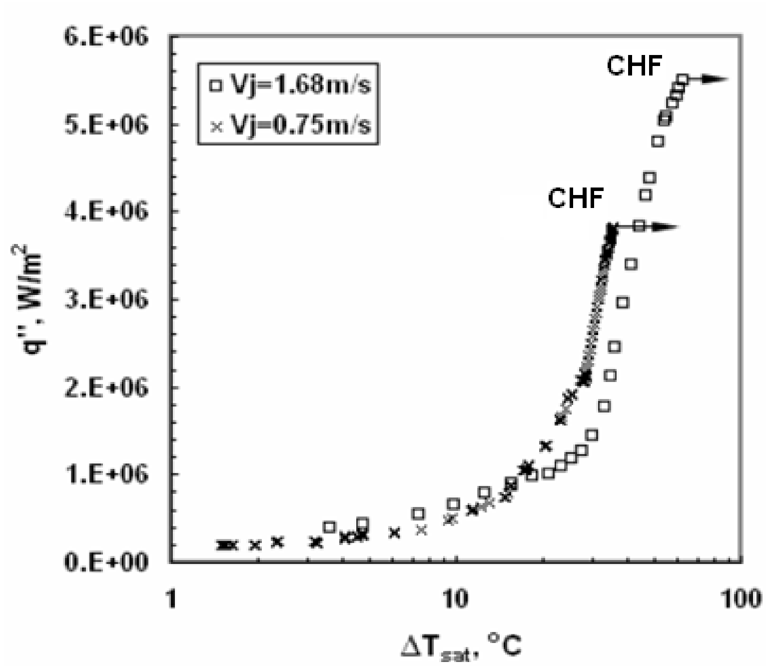

Figure 2-3 Effect of Jet Velocity on Nucleate Boiling Regime and CHF Conditions (ΔT_{sub}=10°C), Omar et al. (2007)

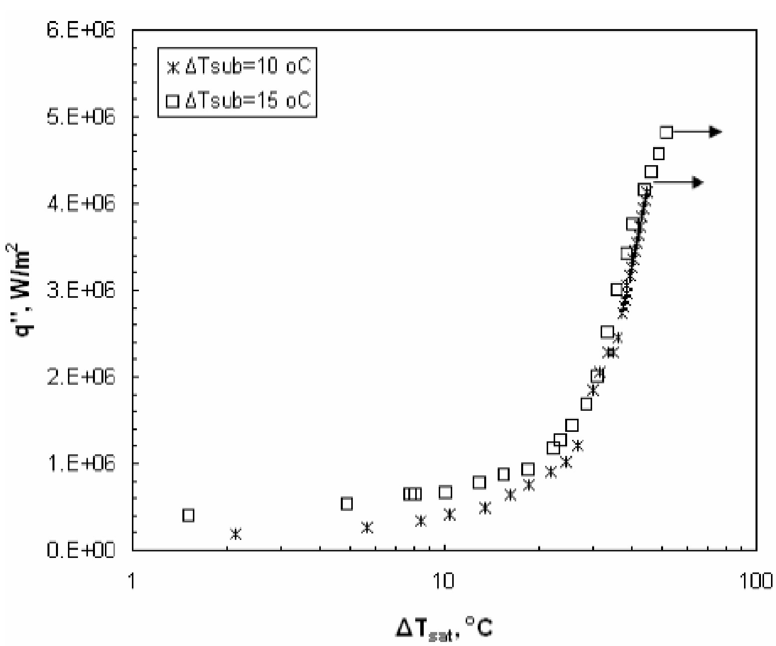

Figure 2-4 Effect of Water Subcooling on Nucleate Boiling Regime and CHF Conditions (V_j= 0.95 m/s), Omar et al. (2007)

Copeland (1970) and Ruch and Holman (1975) performed boiling experiments for jet impinging on a downward facing heated surface. It was found that, for fully developed nucleate boiling, the heat flux was independent of impingement velocity and depended only on the wall superheat. Same results were obtained on an upward facing surface by Ishigai et al. (1978) who used steady and transient methods to investigate the effects of jet velocity on nucleate boiling heat transfer for a subcooled planar free jet of water. The steady state showed that for velocities of 1.0 and 2.1 m/s and a subcooling of 35^{o}C, the flux was independent of velocity. Miyasaka and Inada (1980) and Miyasaka et al. (1980) results showed no effect of jet velocity (1.1 to 15.3 m/s) on nucleate boiling heat transfer for a highly subcooled (85^{o}C ≤ ΔT_{sub} ≤ 108^{o}C), planar jet of water (Wolf et al. 1993).

Katto and Monde (1974) found that even for a jet velocity range as large as 5.3 and up to 60 m/s with saturated water, the fully developed nucleate boiling curve was independent of the jet velocity. It was simply an extension of the data for pool boiling to larger heat fluxes and wall superheats, Wolf et al. (1993).

Cho and Wu (1988) reported fully developed nucleate boiling data for a jet of R-113 at velocities ranging from 0.7 to 8.2 m/s. The authors did not specify the degree of subcooling. For a fixed heat flux, increasing the jet velocity was shown to decrease the surface temperature by as much as 9°C over the range of tested jet velocities, Wolf et al. (1993).

Vader et al. (1992) demonstrated the invariance of fully developed nucleate boiling of a subcooled water jet impinged at the stagnation point from a rectangular nozzle. The jet velocities ranged from 1.8 to 4.5 m/s. However the results were limited to a small region boiling the incipience of nucleate boiling, thereby precluding correlation of the data. The reported boiling curves showed low insignificant effect of jet velocity on the onset of nucleate boiling.

Ishigai et al. (1980) examined the effect of increasing the degree of subcooling from 35°C and 75°C on the nucleate boiling heat transfer for a planar jet of water with a velocity of 2.1 m/s. Despite doubling the subcooling degree, minor heat transfer enhancements were observed for the same wall superheat.

Copeland (1970) studied the effects of increasing the degree of subcooling (4°C – 78°C) on fully developed nucleate boiling. Results detected that increasing the subcooling shifts the boiling curves to a higher heat transfer and surface superheat. Most of the studies found that increasing the degree of subcooling increases the rate of heat transfer for the same surface superheat and shifts the ONB to the right. CHF increases as well by increasing the degree of subcooling, Wolf et al. (1993).

As reported by Wolf et al. (1993) nozzle to surface spacing was also examined by Monde and Katto (1977), Kamata et al. (1988), Wasdsworth (1990) and Nonn et al. (1988) and the results showed the distance between the nozzle and the heated surface was insignificant.

2.1.2 Transient Experiments

Omar (2010) reported in his thesis Liu and Wang in (2001) focused on the transition and film boiling regimes both experimentally and analytically. They quenched a stainless steel plate initially at 1000°C with a 10 mm circular water jet. Five to eighty degrees of subcooling was used while the jet velocity ranged from 1 to 3 m/s. They developed mathematical correlations using the experimental data.

2.1.3 Summary of Experimental Studies on LJIC

Effect of jet velocity was the focus of many studies (Ishiagi et al., 1978, Miyasaka and Inada, 1980, Miyasaka et al., 1980, Vader et al., 1992, Robidou et al., 2003 and Omar et al., 2007). Many contrasts had been shown in literature regarding the effect of jet velocity on the nucleate boiling regime under Liquid Jet Impingement Cooling LJIC. However, most of the research (Robidou et al., 2003 and Omar et al., 2007) agreed that the CHF increases with increasing the jet velocity. Many contradictions on the effect of jet velocity on the rate of heat removing and the location of ONB were reported. Meanwhile most recent studies showed that jet velocity has an insignificant effect on the boiling curve; (Omar et al., 2007 and Robidou et al., 2003 reported that increasing the jet velocity resulted in shifting the boiling curve to a higher heat flux and higher degree of subcooling, some studies (Miyasaka and Inada, 1980, Miyasaka et al., 1980 and Vader et al., 1992)

In general, increasing the jet velocity will increase the mass flow rate of the fluid cooling the surface. As a result, the fluid velocity parallel to the surface will increase, increasing the coefficient of heat transfer and the rate of heat removal in the single phase regime. Also, higher fluid velocity will increase the drag force on the bubbles causing a delay in bubble formation i.e. delaying the ONB. The increase of CHF with higher jet velocity could be the result of the increase of the fraction of heat transferred to the fluid by forced convection or the increase in turbulence which breaks up the vapor blankets and wets the surface delaying the formation of vapor film on the surface. In addition, the increase in bubble collapse rate due to the high drag force makes a higher surface superheat mandatory for bubble formation, thus causing CHF to increase.

Increasing liquid subcooling decreases the bulk fluid temperature. As a result, higher degrees of surface superheats are required to achieve the temperature required to activate the nucleation sites. Hence, the ONB delays with increasing degree of liquid subcooling shifting the whole boiling curve to the right.

Table 2.1 Summary of Experimental Studies on LJIC

Summary of Experimental Studies							
Author	Jet Type	Fluid	ΔT_{sub} (°C)	V_n (m/s)	d or w_n (mm)	z (mm)	Degas
Vader et al (1992)	Planar-free	Water	50-70	1.8-4.5	10.2	89.7	No
Cho and Wu (1988)	Circular-Free	R-113	-	0.7-8.2	0.76	13	-
Monde and Katto (1978)	Circular-Free	Water	0-30	3.9-26.0	2.0-2.5	-	-
Monde (1980)	Circular-Free	Water	<5	0.67-4.2	1	-	-
Miyasaka et al (1980)	Planar-free	Water	85-108	1.5-15.3	10	15	-
Miyasaka and Inada (1980)	Planar-free	Water	85-108	1.1-15.3	10	15	No
Copeland (1970)	Circular-Free	Water	4 -78	0.79-6.4	0.28-0.75	8.0-17.3	-
Ruch and Holman (1975)	Circular-Free	R-113	27	1.23-6.87	0.21-0.433	4.7-9.8	-
Katto and Monde (1974)	Circular-Free	Water	<3	5.3-60	2	30	-
Monde and Furukawa (1988)	Circular-Free	R-113	<2	2.0-3.4	1.1	5	-
Monde and Okuma (1985)	Circular-Free	R-113	<3	0.49-9.9	1.1-4.13	3	-
Ishigai et al (1978)	Planar-free	Water	35-75	1.0-2.1	6.2	15	-
Robidou (2003)	Planar-free	Water	50	0.7-0.8	1	6	Yes
Omar et al	Planar-free	Water	10-28	0.68 -1.7	1	-	Yes

Critical heat flux is the focus of many studies as it represents the maximum possible heat flux at lower surface superheats. CHF was shown to increase with increasing the jet velocity as well as with increasing degree of liquid subcooling. Many attempts had been done to model the critical heat flux empirically as a function of the operating parameters, Wolf et al. (1993). By increasing the surface superheat beyond the CHF, Robidou (2003) and Omar et al. (2007) verified the existence of flux shoulder experimentally.

2.2 Boiling Dynamics and Modeling of Heat transfer

To determine the boiling effect on the overall heat transfer, bubble growth rate, bubble density, and release frequency need to be quantified. High-speed imaging is usually used for this purpose without disturbing the flow field or the active nucleation sites. When the flow field is not easily visualized, intrusive techniques such as optical probe could be used to obtain the necessary information on the bubble dynamics.

Bogdanic et al. (2009) used an intrusive optical probe to study the bubble release frequency and the characteristics of the vapor boundary layer over the entire boiling curve during planar free surface jet impingement. The probe tip was thinned to 10 microns to allow for the detection of very small bubble. The available information on the bubble frequency was obtained only at the stagnation region and for a single jet velocity (0.4 m/s) and water subcooling (20 K) values. No further information has been reported on the other parameters to develop quantifying models. Bogdanic et al. (2009) suggested that a sampling frequency of at least 250 kHz should be used for measuring the bubble generation frequency under the stagnation of the impingement jet.

Omar et al. (2007) used FASTEC Imaging Troubleshooter high speed camera at a rate of 250 fps and resolution of 640x480. The study shows sequence of bubble growth, sliding and coalescence of three bubbles as shown in Figure 2-5. Upstream bubble diameter at departure was measured from the pictures to be in the order of 0.35 mm while the agglomerated diameter was approximately 1.2 mm. The authors captured that big bubbles were rolled off the surface quicker than the smaller ones when commencing to slide and this attributed to the large drag force on the big bubbles. By increasing the surface superheat, it was clear that boiling intensity increases rapidly over a narrow range of surface temperature increase.

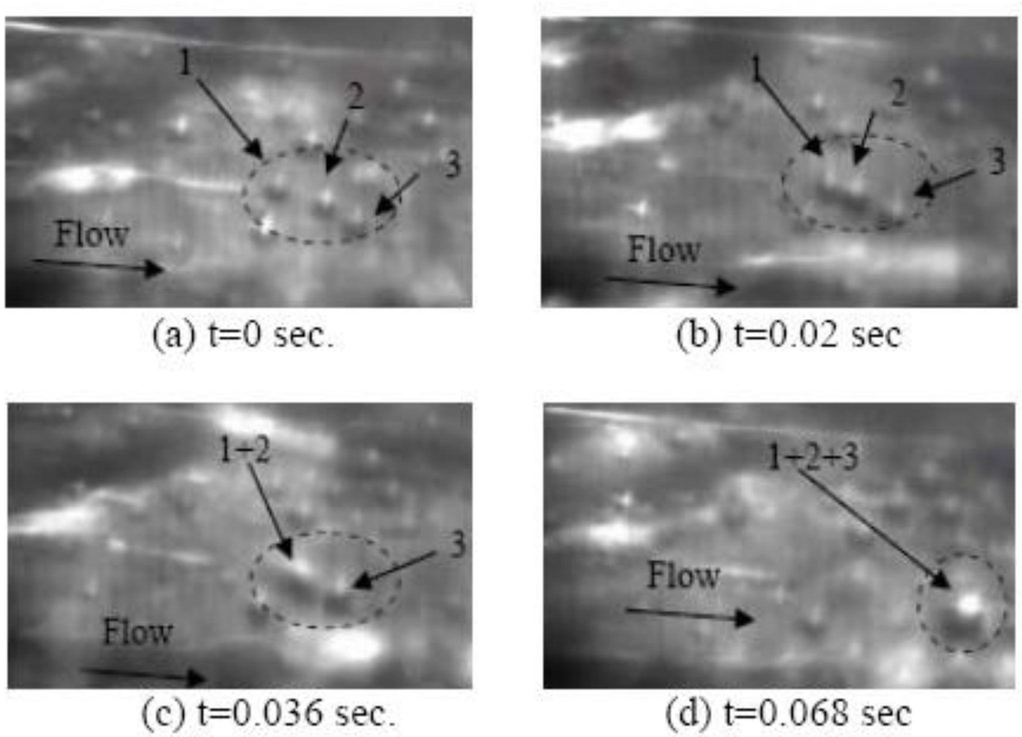

Figure 2-5 Sequence of Bubble Sliding and Coalescence at $\Delta T_s = 14^{\circ}C$, Omar et al. (2007)

Several modeling approaches have been implemented in the previous literature to quantify the wall heat flux at different regimes. An empirical correlations approach was intensively developed in this context to describe the different flow regimes.

Another approach to model the flow and thermal fields during jet impingement cooling is analytical modeling. In this approach, modifications are applied to the terms of the conservation equations to account for the flow particulars.

A mechanistic modeling approach provides an appropriate tool to quantify the wall heat flux based on modular format of the governing transport mechanisms. This approach assigns partitions or fractions of the process time and heater area to individual mechanisms. Time averaging of the heat transfer due to different mechanisms accounts for the wall heat flux at given cooling conditions. Various scenarios were considered in the partitioning. Judd and Hwang (1976) proposed three different mechanisms to be responsible for the heat transport in pool boiling configurations at the wall: the free convection, transient conduction, and the evaporation of a liquid layer entrapped beneath the growing bubble.

Omar et al. (2009a) modeled wall heat flux from a horizontal heated surface exposed to an impinging planar water jet using the concept of wall flux partitioning. The wall heat flux in the nucleate boiling regime is comprised of three components namely: forced convection heat flux, transient conduction heat flux, and evaporation heat flux. The proposed model was complemented with sub-models for the bubble departure diameter and bubble population using experimental data obtained by high speed imaging. The experiments were conducted using water at atmospheric pressure, mass flux range of 388-1649 kg/m^2.s, degree of subcooling (ΔT_{sub}) in the range of 10-28 $^{\circ}$C, and surface temperature in the range (T_s) of 75-125 $^{\circ}$C.

The heat transfer by forced convection is assumed to occur continuously wherever no bubble nucleation occurs on the exposed heated surface. The boiling process was divided to three main regions: forced convection area, bubble projected area, and the effective area that experience transient conduction as bubble departs or collapses. Each flux partition was modeled independently and constitutive sub-models for the closure of the problem have been presented. The sub-models were obtained from an original set of experimental data obtained specifically under jet impingement cooling conditions. The model was validated in the studied range using experimental data.

Omar et al. (2009b) introduced a new scenario identification procedure (SIP) proposed for the bubble growth termination during subcooled flow boiling under an impinging free planar jet. Two mechanisms are considered in the proposed SIP:

1. The thermal equilibrium between the surrounding fluid, the heater surface, and the bubble
2. The dynamic equilibrium of the forces acting on the growing bubble

The scenario of bubble growth termination and the bubble maximum diameter under specific impingement conditions was attributed to the earlier of the two equilibrium conditions. Depending on the controlling mechanisms, a bubble would collapse at its nucleation site if the thermal equilibrium precedes the dynamic equilibrium or it would depart and slide along the heated surface otherwise.

The proposed SIP has been validated using experimental data obtained from the high speed imaging of the subcooled flow boiling on a horizontal surface under various conditions of free planar jet impingement. The jet velocity varied from 0.4 m/s to 1.7 m/s. The degree of water subcooling varied from 10°C to 28°C. The surface superheat varied from 0°C to 30°C along a span of the heated surface from the stagnation down to ten jet widths. The model was investigated by applying thermal and force balances on the bubble in order to estimate the probability of the bubble growth, slide or collapse in its location.

The validation process showed that the proposed SIP is not only capable of capturing the right growth termination scenario but it can also predict reasonably the maximum bubble diameter.

2.3 Effect of Surface Roughness on Boiling Heat Transfer

It is a fact that surface roughness has an effect on boiling heat transfer and number of active nucleation sites. However, studying the effect of surface roughness on flow or pool boiling heat transfer has not been aggressively tackled as expected. Studying the effect of surface roughness on boiling heat transfer under LJIC will facilitate the selection of suitable surface parameters, enabling manufacturers to eventually select between several surface parameters to obtain the required heat transfer rate within their temperature limits.

Bubble formation during nucleate boiling is affected by the shape of the surface. The existence and density of cavities affect the Onset of Nucleate Boiling ONB as well as the number of active nucleation sites at particular surface superheat. The increase of the active nucleation sites enhances the heat transfer at the same surface superheat and same boiling conditions. Cavity's shape, depth, and mouth diameter are some factors that can affect the cavity's ability to trap vapor or gas residue and hence to act as an active nucleation site. Measurement of these factors is very difficult and depends on the measurement techniques as well as the resolution of the measurement device. As a result, much of the research that studied the relationship between the surface shape and nucleate boiling heat transfer took the roughness parameters as an indication of the surface shape.

The idea that the surface roughness can affect the boiling performance started in 1931 when Jakob and Fritz studied the effect of surface roughness on the boiling performance. They boiled water from a sandblasted surface and a surface having a square grid of machined grooves (0.016 mm square with 0.48 mm spacing). The sandblasted surface provided 15% improvement while the grooved surface initially yielded boiling coefficients about three times higher than smooth surface. However, the heat transfer enhancements ended in few days.

This was referred to as the aging effect which was explained by unstable vapor trap cavities – formed by roughening the surface – and has eventually degassed leaving no vapor to sustain the nucleation process, Webb (2004).

Griffith and Wallis (1960) proposed the first fundamental understanding of how an artificial nucleation site may function. They showed that the cavity geometry is important in two ways. First, the mouth diameter determines the superheat needed to initiate boiling. Second, the cavity shape determines its stability after the boiling has begun. Figure 2-6a shows the re-entrant cavity shape proposed by Griffith and Wallis while Figure 2-6b shows $1/r$ versus bubble volume. The authors observed that the term $1/r$ is proportional to the liquid superheat required to maintain a vapor nucleus. Even when the vapor radius of curvature is negative, the vapor nucleus may continue to exist in the presence of subcooled liquid. So, the re-entrant cavity can react as a very stable vapor trap.

Hsu (1962) extended this analysis to include the effects of the thermal boundary layer and showed that only a certain range of cavity sizes can serve as active nucleation sites, Webb (2004).

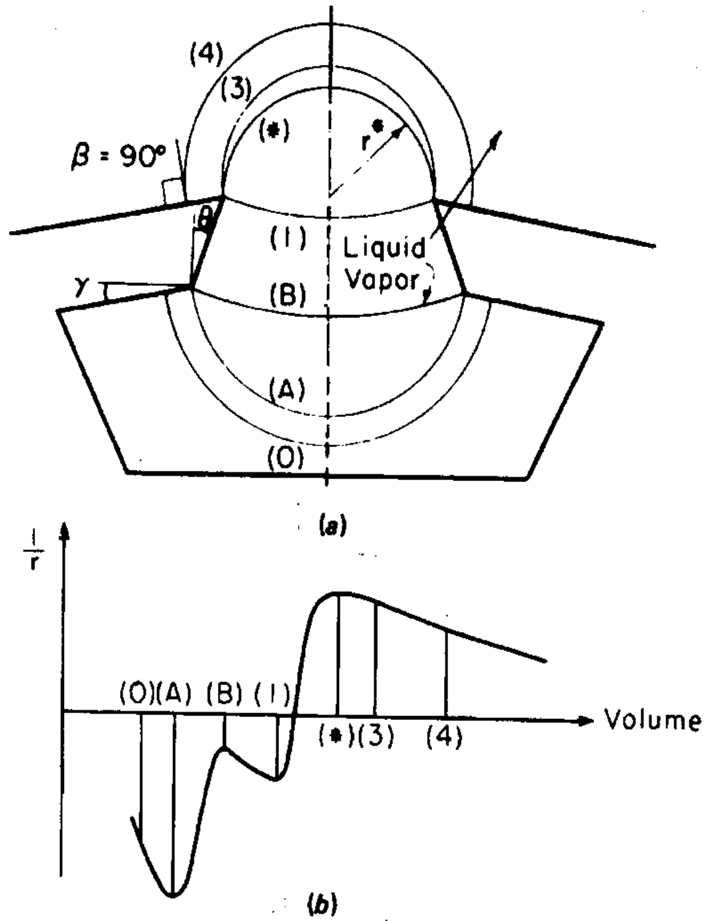

Figure 2-6 a. States of The Liquid–Vapor Interface in a Re-Entrant Cavity
b. Reciprocal Radius l/r Versus Vapor Volume for 90° Contact Angle, Griffith and Wallis (1960)

Many attempts were done to find a relation between the surface roughness and the coefficient of heat transfer or heat flux. The contradiction between the results and the theory was an enough reason for scientists to search the feasibility of selecting the roughness parameter as an indicator of the surface behavior under boiling heat transfer. Mpholo et al. (2010) summarized the difficulties of using surface roughness as a measurement of the surface behavior in three points:

1. The resolution of the measuring instrument affects the measured surface resolution. As the resolution of the measurement device increases, more details about the surface shape could be measured
2. The parameters that are used as a measurement of the surface roughness are statistical values. So, their values depend on the sample size and the height of measured points
3. Roughness does not account for some important parameters like the angle of the cavity or the mouth radius. Entrapment of the vapor in the cavity depends on the angle cavity, while the mouth radius controls the minimum superheat required to activate the cavity

Based on the above points, many research investigations replaced the roughness by another parameter such as the mouth radius or cavity depth as a factor affecting of the boiling performance.

Many researchers studied the effect of surface roughness on pool boiling heat transfer. Some examples will follow:

Berenson (1962) studied the boiling of *n*-pentane on surfaces of varying roughness and found large variations in the heat transfer coefficient, of up to 600%, due to the differences in surface characteristics, Webb (2004).

Jung and Kwak (2006) studied the boiling performance on three prepared surfaces. The first RSHF was prepared using hydrofluoric acid and the RMS was around 307 µm. The maximum height of the roughness was 1.56 µm while its surface area increased by 52% due to the roughness, although the authors did not detail the increase in surface area measurement procedure. The second PSDMF was prepared using dimethylformaide with R_{rms} = 136 µm while its surface area increased by 3% and the maximum height of the roughness was 0.61 µm. The third surface SiBare was left without any special treatment. Figure 2-7 shows the resulting boiling curve for the three surfaces. The interesting result was the directly proportional relationship between the area increase -due to surface roughness- and the CHF, as shown in Figure 2-8.

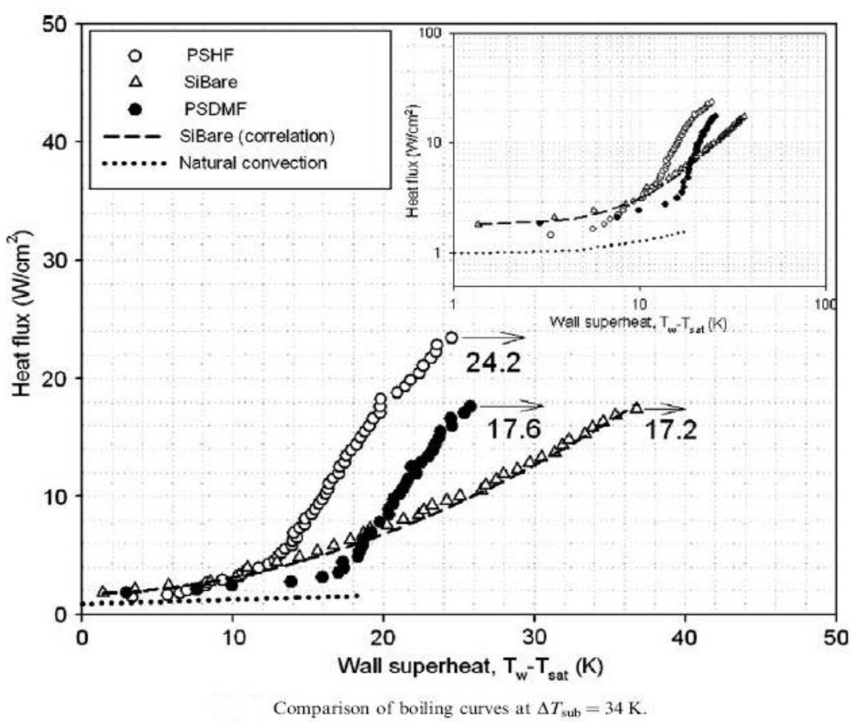

Figure 2-7 Boiling Curve for Different Surfaces, Junk and Kwak (2006)

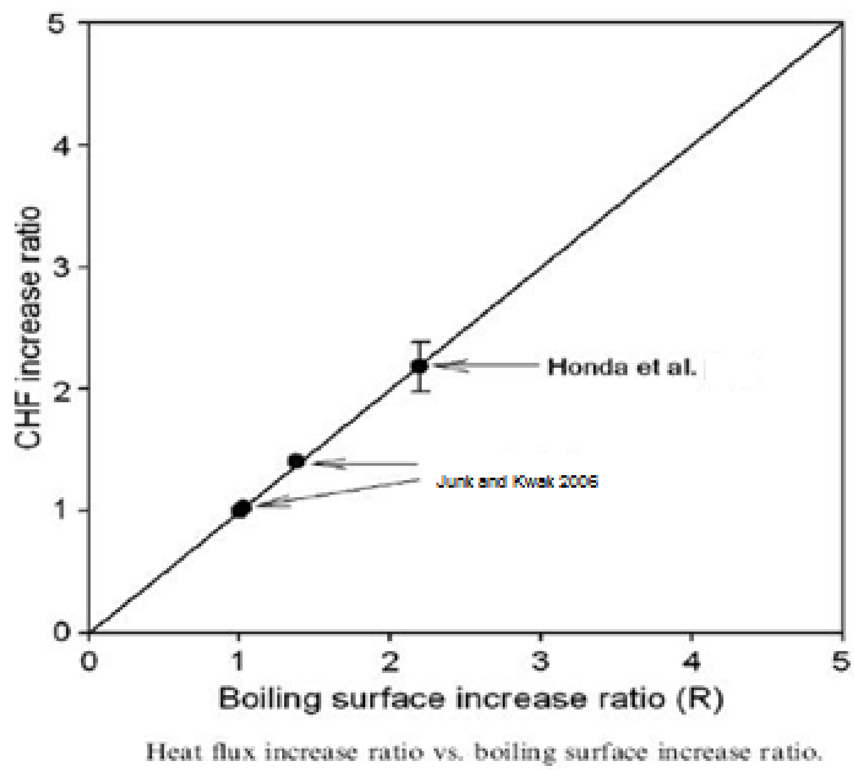

Figure 2-8 Relation between the CHF and the Increase in Surface Area, Junk and Kwak (2006)

Takata et al. (2009) studied the boiling of water droplets dripped on a hot surface. They studied the effect of surface roughness and droplet velocity. A high speed camera was used to record the behaviour of the droplet. Droplet velocity was changed from 1 to 2.5 m/s. Steel surfaces with roughness mirror, P_a=0.2, 3, and 10 was used in the experiment. As no heat transfer was measured during the experiment, the authors defined contact time between the droplet and the surface as an indication of the heat transfer time. The maximum droplet spread was taken as an indication of the heat transfer area. The results showed an increase in contact time with the increase in surface roughness. However, the droplet spread was decreased as surface roughness increased.

Jones et al. (2009) studied the influence of surface roughness on nucleate pool boiling heat transfer. A total of six test pieces of varying surface roughness were tested. The finest roughness was obtained by polishing the surface while electrical discharge machining (EDM) was used to obtain the rough surfaces. The table below shows the surface roughness measurements for the six surfaces.

Table 2.2 Surface Parameters Used By Jones et al., (2009)

	Surface roughness parameters			
Surface preparation	R_a (μm)	R_q (μm)	R_p (μm)	R_z (μm)
Polished (water)	0.038	0.062	0.81	0.58
Polished (FC-77)	0.027	0.039	0.18	0.35
EDM	1.08	1.37	6.09	8.24
	2.22	2.81	12.0	16.7
	5.89	7.37	24.5	37.1
	10.0	12.5	32.4	56.5

The results show little improvement in heat transfer coefficient for roughness beyond R_a=1.08 μm, except for a very rough 10.0 μm surface, which had significantly higher heat transfer coefficients, as shown in Figure 2-9. On the same set of surfaces, FC-77 exhibited a different trend with continuously increasing heat transfer coefficient with respect to surface roughness, at a fixed heat flux.

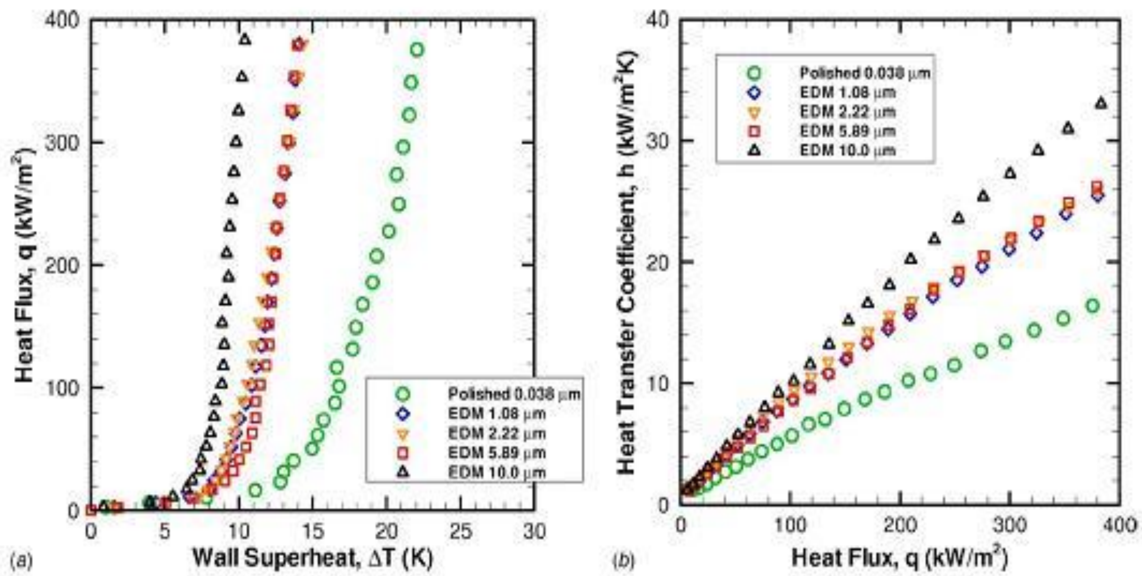

(a) Heat Flux Versus Wall Superheat (b) Heat Transfer Coefficient Versus Heat Flux

Figure 2-9 Boiling Curves for Water, Jones et al. (2009)

John et al. (2009) used high-speed visualizations (8000 fps) of pool boiling at atmospheric pressure from smooth and roughened surfaces, using a perfluorinated hydrocarbon (FC-77) as the working fluid. Aluminum surfaces, polished in the case of the smooth surface and prepared by electrical discharge machining (EDM) in the case of the roughened surface, were used as boiling surfaces. The roughness values were $\mathbf{R_a}$ = 0.03 and 5.89 μm for the polished and roughened surfaces, respectively (these two surfaces were tested by Jones et al., 2009, Figure 2-9). Analysis of the recorded motion pictures shows that the bubble diameter at departure increased with increasing wall superheat, but the surface roughness was also shown to have an influence. Active nucleation site density was shown to increase with both wall superheat and surface roughness.

Mpholo et al. (2010) has performed a 2D dimensional analysis on five surfaces used by Jones and Graimella (2007) to predict the incipience of nucleate boiling. 2D measurements were taken for the fives surfaces at different locations using surface profiler. The smoother surface was polished while the other four surfaces were obtained by EDM. The results were analyzed by Matlab algorithm to predict the radius, angle of the cavities, and mini cavities which are included in large ones. By using Qi et al. (2004) criterion (ϴ> 180- 2ø) and Griffin and Wallis (1960) criterion (ϴ> 0.5 ø<ϴ<40) to determine the active cavities - where ϴ is the contact angle and ø is the cavity angle - the cavities were categorized. The authors were able to divide the cavities into active independent cavities which might include mini cavities or not; and inactive large cavities which includes many independent cavities; and a third type which is inactive large cavity which includes inactive mini-cavities.

No active cavities were recorded when using the smooth surface ($\mathbf{R_{rms}}$ = 0.062 µm). For the other surfaces, the results show that the main depth of the cavity was greater than the measured roughness. This was explained by ignoring the effect of the peaks and concentrating only on the identified cavities.

With the exception of the rougher surface (**R_{rms}**= 12.53 μm), large number of active mini-cavities were found which implies that the majority of the big cavities, containing them, are inactive. Although no trend was found between the mean radii of the cavities and the **R_{rms}** roughness, the percentage of the big cavities on the rougher surface was higher than the other surfaces. Since these cavities have larger mouth radii, lower degree of surface superheat is needed to initiate boiling.

Sathe and Mahjan (1981) showed an inverse relation between the surface roughness and rate of heat transfer experimentally. Four surfaces (**R_{rms}** = 3.83μm, 5.25 μm, 8.56 μm, and V-grooved surface) were used in the experiments. The authors could not measure the roughness of the v-grooved surface. The results showed higher heat transfer at the same surface superheat for (3.83 μm) surface. When the degree of subcooling was decreased from 44°C to 31°C, higher heat transfer rate was obtained by the V-grooved surface, than the (3.83 μm). The rougher surface resulted in worse heat transfer characteristics for both degrees of subcooling. The authors explained the results by suggesting that the (3.83 μm) surface would have maximum number of cavities in this range of subcooling when compared to the other two surfaces. The author suggested using the expression “rougher with respect to boiling” instead of using RMS of roughness to express the surface which has more cavities in the range of active sites.

Although many studies have focused on the effect of surface roughness on pool boiling heat transfer, few studies focused on flow boiling. Example of these studies was conducted by Kandlikar and Spiesman (1998). They performed flow boiling experiments on a 3 mm x 40 mm horizontal channel using four different surfaces. Three surfaces were prepared using different grit papers. The smoothest surface was polished using 1 µm silica particles in water solution and then by 0.03 µm silica particles in water solution to obtain a mirror finish. The average roughness of the surfaces was measured to be (0.188, 0.363, 0.716 and 3.064 µm). Using Image-Pro software, the authors was able to obtain an approximate count of the surface cavities and measuring their average diameters. Although the surface roughness values were different, the cavity size distribution plots were quite similar. Also, the roughest surface performed slightly better than others, meanwhile the other surfaces did not perform in the order of their roughness. When the authors increased Re number from 2253 to 7136, the roughest and smoothest surfaces performance were very close to each other and higher than the other two surfaces.

Yu et al. (1998) correlated the two phase convection multiplier factor with the cavity size R_c instead of the roughness parameter. They conducted experiments on boiling of refrigerants flowing in two smooth tube; Tube A ($\mathbf{R_{rms}}$=0.52 µm) and Tube B ($\mathbf{R_{rms}}$=0.29 µm). The results showed higher heat transfer coefficient for the rougher surface (A). The correlation was then validated by data from literature and a good agreement was found. The authors clarified experimentally that the effect of surface condition on flow boiling comes from the nucleate boiling component and related it to the nucleate cavity size.

Very few studies focused on effect of surface roughness under LJIC. Kugler and Dhir (1996) performed an experimental study on the effect of enhancing the surface under three jet impingements. The work was an extension of what the same authors had published earlier on using the same way of enhancing heat transfer under single jet. A comparison between the two publications was held. Two jet velocities (1.4 and 5.6 m/s) were tested. The two jet velocities were obtained by passing the same mass flow rate (18.93 l/h from each jet) from 2.2 and 1.1 mm diameter nozzles. Three heated surfaces were used during the experiments and the results were compared to a plane surface. The plane surface was polished by # 600 silicon sand paper. Macro structured surface was obtained by machining radial grooves (1 mm width and 1-3 mm depth) on the surface. A micro-structured surface was obtained by sintering a porous copper coating into the heater surface by flame spraying copper powder in oxygen rich atmosphere. Void fraction (volumetric fraction of vacuum) of the sintered layer was 30-40% with a total thickness of 0.4 mm. A third enhanced surface macro/micro structure was treated by both the above methods; machined radial grooves and sintering a porous powder.

The results show that the jet velocity at low superheats affects the heat flux, while there is no significant effect at higher surface superheats. The macro surface showed a 50% heat transfer increase over the plane surface. For higher superheats, the heat flux exhibited three to four times improvement. The porous layer on the micro structured surface behaved as re-entrant nucleation sites, increasing the number of nucleation sites for boiling inception. The surface with the porous matrix was able to sustain long periods of nucleate boiling at relatively low superheats. The macro/micro structured surface showed better heat transfer enhancement. The study showed that using multiple jets while increasing the surface area with proportionally has a slight effect on heat flux.

Gabour and Lienhard (1994) studied the roughness effect on heat transfer under the stagnation regime. The study was limited to the single phase forced convection regime. The experiments were performed using 10 surfaces with roughness root mean square R_{rms} ranging from 0.3 μm for S0 to 28.2 μm for S10. Table 2.3 shows the root mean square roughness heights as reported by the authors. Three nozzle diameter were tested; 4.4, 6.0 and 9.0 mm. The authors reported significant increase in the values of Nu number with the increase of surface roughness at constant Re number. Figure 2-10 shows the effect of surface roughness on Nu number for 4.4 mm diameter nozzle.

Table 2.3 Root-mean-square roughness heights for the ten heater surfaces, Gabour and Lienhard (1994)

SURFACE	RMS ROUGHNESS (μm)
S1	0.3
S2	4.7
S3	6.3
S4	8.6
S5	13.1
S6	14.1
S7	20.1
S8	25.9
S9	26.5
S10	28.2

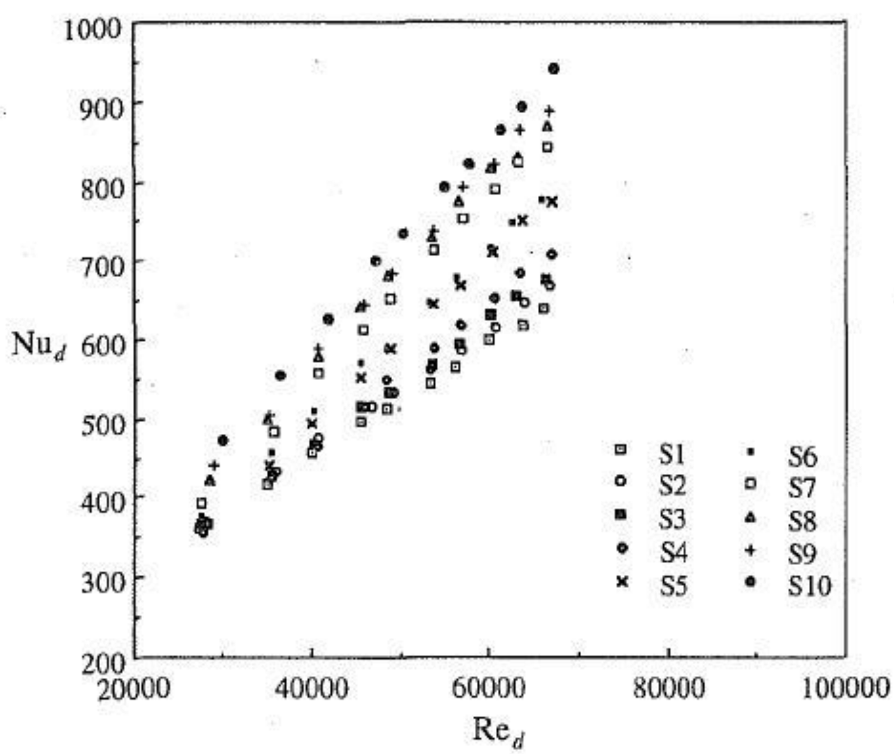

Figure 2-10 Effect of Surface Roughness on Nu Number for the Ten Tested Surfaces, Gabour and Lienhard (1994)

Wolf et al. (1993) discussed Aihara et al.(1993) nucleate boiling data for circular, submerged jet of saturated liquid nitrogen impinging on a concave, radically confined, hemispherical heater. Data was provided for sanded (emery paper no. 500), machined, and mirror finishes of the copper surface. Whereas the nucleate boiling curves for the machined and mirror finishes were indistinguishable, the sanded finish produced slightly lower wall superheats (~ 10%) for a fixed heat flux and V_n = 1 m/s.

Guo et al. (2011) conducted experiments to study the performance of subcooled flow boiling heat transfer combined with jet impingement of FC-72 over silicon chips (10 x 10 x 0.5 mm^3). Four kinds of micro-pin-fins, shown in Figure 2-11, with dimensions of 30 x 60, 30 x 120, 50 x 60, 50 x 120 mm^2 (thickness t x height h) were fabricated on the chip surfaces by using dry etching technique. A smooth surface was also tested for comparison. Two different liquid subcooling (25°C and 35°C), three different jet velocities V_j (0, 1, 2 m/s) and three different crossflow velocities V_c (0.5, 1, 1.5 m/s) were tested. Best heat transfer enhancements were found at particular combinations of jet and flow velocity. Results showed that for a fixed condition, all micro-pin-fined surfaces undergo a considerable heat transfer enhancement compared to the smooth surface. Figure 2-12 shows a comparison of heat transfer characteristics between a smooth surface and the micro-pin-fins, shown in Figure 2-11.

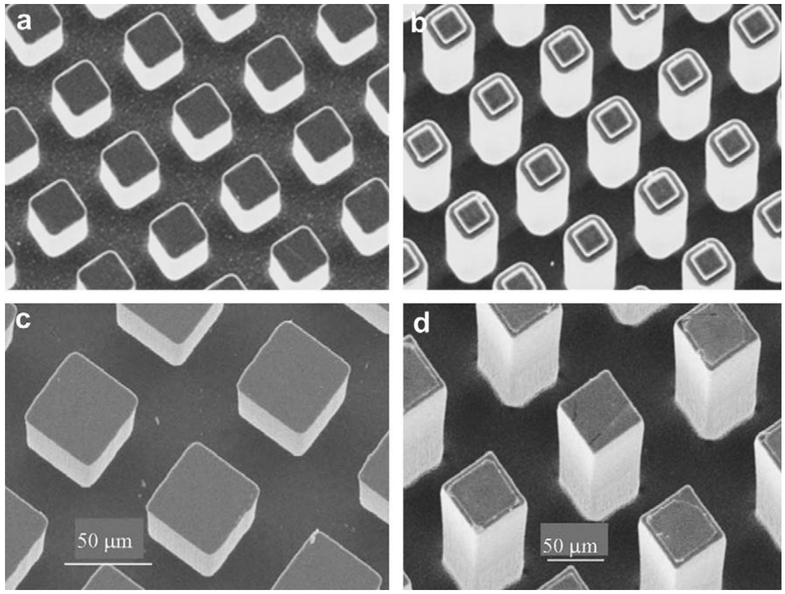

(a) Chip PF30-60. (b) Chip PF30-120. (c) Chip PF50-60. (d) Chip PF50-120
Figure 2-11 Scanning Electron Microscope Images of Micro-Pin-Fins, Guo et al. (2011)

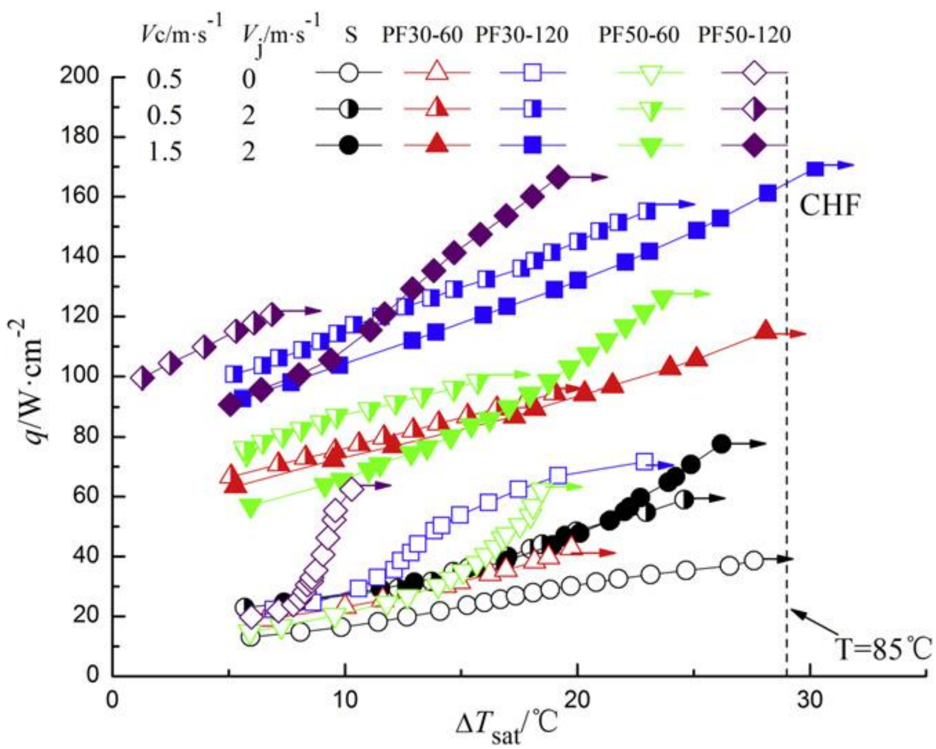

Figure 2-12 Effects of Micro-Pin-Fins, ΔT_{sub} = 35°C, Guo et al. (2011)

Sinha, J. (2003) studied the effect of roughness in the quenching process by imparting different degrees of roughness to an Inconel–Al2O3 rod by means of sandpaper and emery cloth. The average RMS roughness for the unroughened rod was 50 μin. (1.27×10^{-6} m). The average RMS roughness for the rod polished by 80-gritsandpaper was 150 μin. (3.81×10^{-6} m), meanwhile the average RMS roughness for the rod polished by 40-grit sandpaper was 260 μin. (6.604×10^{-6} m). Figure 2-13 shows the effect of increasing the roughness on the transient boiling curve.

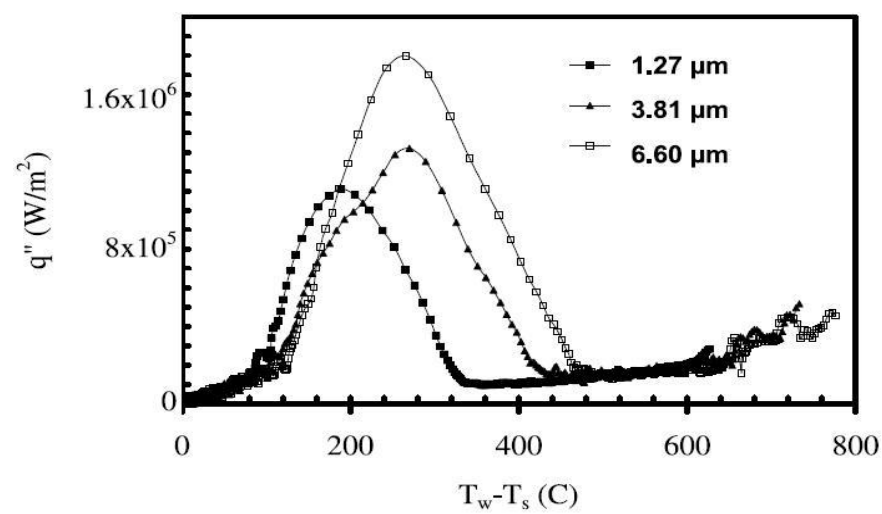

Figure 2-13 Effect of Surface Roughness on Boiling Curve under Quenching Process (T_s=925°C & ΔT_{sub}=5°C), Sinha, J. (2003)

2.3.1 Summary of the Effect of Roughness on Nucleate Boiling Heat Transfer

From the above studies regarding the effect of roughness on both pool and flow boiling, most of the results reported boiling enhancement due to increasing the roughness. However, it was difficult to determine a relationship between the roughness parameters and the heat flux. This is due to the fact that the roughness parameters are statistical values which can not represent the existence or the density of cavities that are able to act as active nucleation sites. Instead of relating the enhancement of boiling to the roughness parameters, some studies related the enhancement of boiling to other parameters such as the mouth radius. Although that the research regarding this topic started in early thirties, the relation between the boiling heat flux and the surface roughness/conditions in both pool and flow boiling are still undetermined until today. The effect of roughness under LJIC is still in its early stages where there are only few publications attempting to shed light on this topic.

The increased understanding of the role of surface condition has led to commercially available enhanced surfaces for improved boiling performance. Many of these boiling enhancements are designed to create re-entrant-type cavity structures which are more difficult for the liquid to fully wet than simple cavity shapes, Jones et al. (2009). Table 2.4 shows summarize the experimental findings on the effect of surface roughness on boiling heat transfer

Table 2.4 Summary of The Experimental Findings on The Effect of Surface Roughness on Heat Transfer

Study	Purpose	Findings
Jones et al. 2009	Influence of surface roughness on nucleate pool boiling heat transfer	Little improvement in heat transfer coefficient for roughness beyond Ra=1.08 μm, except for a very rough surface Ra=10.0 μm surface
Gabour and Lienhard 1994	Effect of roughness on single phase heat transfer at the stagnation point under circular jet impingement	Higher heat flux observed with increasing the roughness
Sinha, J. 2003	Effect of roughness on the boiling process in the case of quenching process	Increasing the Roughness rapids the transfer from film to transient and then to nucleate boiling. CHF also increased
Guo et al. 2011	Performance of subcooled flow boiling combined with jet impingement of FC-72 over silicon chips with micro-pin-fins	Best heat transfer enhancements were found at particular combinations of jet and flow velocity
Aihara et al. 1993	Effect of surface roughness under impinged circular jet	Higher heat flux obtained by the sanded surface (emery #500)
Kugler and Dhir 1996	Effect of enhancing the heat transfer by sanding, grooves on the surface (macro), powder sintering (micro) or combination of grooves and sintering (macro/micro) under circular jet impingement	The macro/micro structured surface showed better heat transfer enhancement
Sathe and Mahjan, 1981	Effect of Roughness on pool boiling	Inverse relation between the surface roughness and rate of heat transfer
John et al. 2009	High-speed visualizations (8000 fps) of pool boiling	Active nucleation site was increased with increasing the surface roughness
Takata et al. 2009	Visualization of boiling of water droplets dripped on a hot surfaces with different roughness	Increase in contact time and decrease in droplet spread with surface roughness increase.
Jung and Kwak 2006	Pool boiling performance on three prepared surfaces with different roughness	Higher heat flux with increasing the roughness

2.4 Flow Profile under Free Liquid Jet Impingement

When a smooth planar jet falls on a horizontal rectangular plate bounded by walls to form a flow channel, the jet spreads in the direction parallel to the surface forming a thin layer. After a particular distance from the stagnation point, the flow depth becomes much greater, which is called a hydraulic jump. Watson, (1964) studied the motion in the thin layer analytically and empirically for a laminar and turbulent flow impinged from a circular jet on a circular disk.

Wolf et al. (1993) divided the flow field into three main regions; stagnation, developing flow and fully developed flow. The stagnation region located between the stagnation line under the jet centerline and up to half of the jet width. The developing region is where the fluid accelerates to the fluid velocity within few percent. In the parallel flow region, the effect of impingement is no longer realized.

Omar (2010) showed the existence of a hydraulic jump at a distance X_{hj} from the stagnation point. Figure 2.14 shows a schematic sketch for the 2D flow field in an open channel after liquid jet Impingement. As shown in the figure, a rather abrupt rise occurs in the liquid surface at a distance X_{hj} measured from the stagnation point in the direction of flow. The rapidly flowing liquid is abruptly slowed and increases in height, converting some of the flow's initial kinetic energy into an increase in potential energy. Omar (2010) determined an empirical correlation to calculate the distance X_{hj}, equation (2.1).

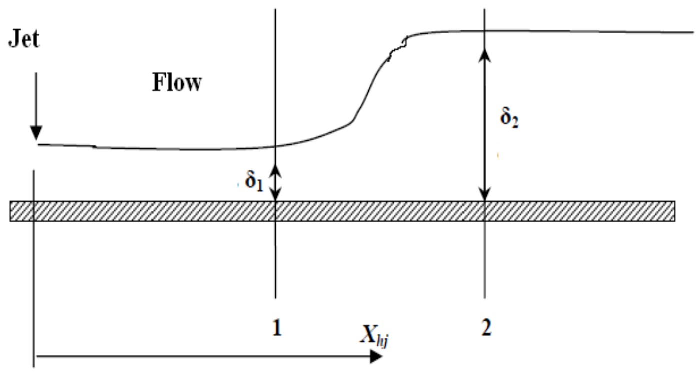

Figure 2-14 Schematic Sketch for The 2D Flow Field in an Open Channel, Omar (2010)

$$\frac{X_{hj}}{w} = 6.51\, V_n^{2.67} \qquad (2.1)$$

Where, w is the jet width, X_{hj} is the distance between the jet centerline to the hydraulic jump location and V_n is the jet velocity at the nozzle exit

2.5 Summary of Literature Review

Effect of jet velocity was the focus of many studies (Ishiagi et al., 1978, Miyasaka and Inada, 1980, Miyasaka et al., 1980, Vader et al., 1992, Robidou et al., 2003 and Omar et al., 2007). Many contrasts had been shown in literature regarding the effect of jet velocity on the nucleate boiling regime under Liquid Jet Impingement Cooling LJIC. However, most of the research (Robidou et al., 2003 and Omar et al., 2007) agreed that the CHF increases with increasing the jet velocity. Many contradictions on the effect of jet velocity on the rate of heat removing and the location of ONB were reported. While the most recent studies

(Omar et al., 2007 and Robidou et al., 2003) reported that increasing the jet velocity resulted in shifting the boiling curve to a higher heat flux and higher degree of subcooling, some studies (Miyasaka and Inada, 1980, Miyasaka et al., 1980 and Vader et al., 1992) showed that jet velocity has an insignificant effect on the boiling curve.

In general, increasing the jet velocity will increase the mass flow rate of the fluid cooling the surface. As a result, the fluid velocity parallel to the surface will increase, increasing the coefficient of heat transfer and the rate of heat removal in the single phase regime. Also, higher fluid velocity will increase the drag force on the bubbles causing a delay in bubble formation which delays the ONB. The increase of CHF with higher jet velocity could be the result of the increase of the fraction of heat transferred to the fluid by forced convection or the increase in turbulence which breaks up the vapor blankets and wets the surface delaying the formation of vapor film on the surface. In addition, the increase in bubble collapse rate due to the high drag force makes a higher surface superheat mandatory for bubble formation, thus causing CHF to increase.

Increasing liquid subcooling decreases the bulk fluid temperature. As a result, higher degrees of surface superheats are required to achieve the temperature required to activate the nucleation sites. Hence, the ONB is delayed with increasing degree of liquid subcooling, shifting the whole boiling curve to the right.

Critical heat flux is the focus of many studies as it represents the maximum possible heat flux at lower surface superheats. CHF was showed to increase with increasing the jet velocity as well as with increasing the degree of liquid subcooling. Many attempts had been done to model the critical heat flux empirically as a function of the operating parameters.

Although measuring the roughness parameters is the most common way used in literature to predict the surface performance in boiling heat transfer, there are many problems in taking that as granted. The first problem is that the measured roughness parameters are dependent on the resolution of the measuring device. Second problem is that the roughness parameters are just statistical values which would change from a location to another on the same surface. They could even be affected by the length tested. Finally, although that roughness can indicate the densities of cavities on the surface there is no indication at all regarding how many of these cavities will act as active cavities.

The data reported in the literature indicates that the roughness has an effect on the boiling performance. However, some research did not report that effect and instead no or an inverse effect was reported. Many researches do not agree with taking the roughness as a measurement of the surface conditions. It is suggested that using average cavity size and/or cavities density would give better indication of the surface performance. Some correlations were reported to relate the coefficient of heat transfer/heat flux with the cavity size in pool boiling experiments. Going further, mathematical algorithms were used to categorize the cavities depending on the size and predict which cavities are able to act as an active nucleation site.

No studies to the author's knowledge focused on the effect of roughness on steady state nucleate boiling under LJIC except one which is in Japanese language and reported by Wolf et al. (1993).

2.6 Objective of Research

From the above literature survey, it can be seen that the effect of surface finish on boiling under liquid jet impingement have not been investigated. In addition, there are some contradictions regarding the effect of jet velocity. The main objective of this research is to study the effect of jet velocity and surface finish on both single phase and nucleate boiling regime at the stagnation point under a free liquid jet impingement.

Chapter 3 Experimental Test Facility

3.1 Experimental Test Rig

3.1.1 The Flow Loop

A test rig was constructed to conduct experimental investigations of liquid jet impingement boiling. Experiments were conducted in the Thermal Processing Laboratory (TPL), McMaster University. The test rig contains a flow loop which has been used to investigate steady-state nucleate boiling under a free planar water jet impinging on a flat surface. A schematic of the flow loop is shown in Figure 3-1.

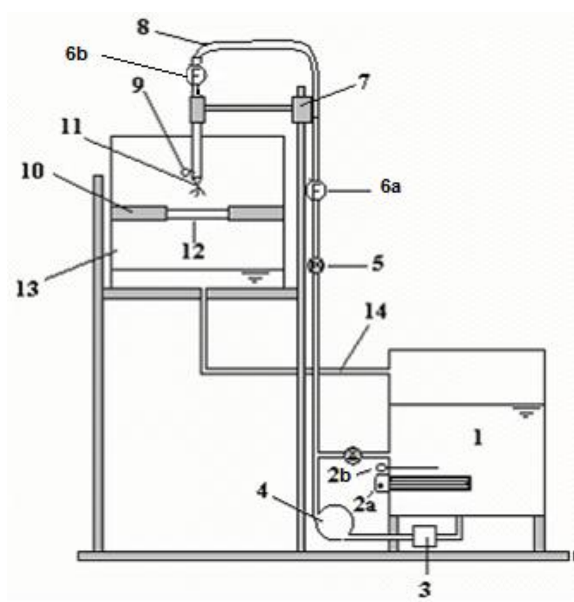

1-Water tank, 2a- Water heater, 2b-Thermocouple, 3-Strainer, 4-Pump, 5-Valve, 6a-High flow meter, 6b- Low Flow meter, 7-Nozzle holder, 8- Hose, 9-Thermocouple, 10-Test Section Holder, 11-Nozzle, 12- Test Section, 13-Collecting tank, 14-Drain

Figure 3-1 Schematic of Flow Loop

The flow loop is shown in Figure 3-1. It contains two tanks; a water supply tank (1) where the 5 KW water heater (2a) is immersed, and a collecting tank (13). The heater is used to heat the supply water to a predetermined temperature. The predetermined temperature is slightly higher than the subcooled set point in order to account for heat losses All experiments reported in the current work were performed at 10˚C degree of subcooling unless mentioned otherwise. Water is delivered to the 1 x 9 mm nozzle (11) at the desired flow rate using one of two parallel pumps (4). The first pump is a centrifugal pump while the second is a gear pump (OBERDORFER N2000). The gear pump was added to the test rig to enable achieving higher jet velocities. Water passed through the test section (12) into the collecting tank (13) and returns back to the supply water tank (1) by gravity. Two flow meters were used to measure the mass flow rate to the nozzle (11); a low flow turbine meter (6b) (Omega FTB-9504, maximum flow rate of 0.016 l/s), and high flow meter (6a) (Omega FTB-9509, maximum flow rate of 0.058 l/s). The two flow meters were used to cover the whole range of velocities tested. The nozzle (11) used was of sudden contraction configuration type. The test section details will be illustrated later in this chapter.

To achieve the desired jet velocity, a regulating valve (5) was used to control the water flow rate into the nozzle. Another needle valve, at the nozzle inlet, was used for fine velocity control. A T type thermocouple (2b) was used to measure the water temperature in the tank and to adjust the water temperature. Another K type thermocouple (9) was placed before the nozzle (11) to measure the supply water temperature before the test section (12). The test section details will be discussed later in this chapter.

3.1.2 The Test Section

As shown in Figure 3-2, the test section consists of two plates of machinable ceramic (Cotronics series 900, k = 1.08 W/m.K) (1). The flow channel was constructed by gluing two quartz plates (2) on the upper ceramic plate (1) at the sides of the heated (boiling) surface (6). Each quartz plate was 1 cm high. The reason for using quartz plates was to form an open channel to keep the water flow parallel to the heated surface. The flow channel dimensions are 8 mm X 20 mm where the rectangular nozzle (9 mm X 1 mm) was projected on the center of the flow channel allowing 10 mm of flow on each side of the jet. Although the nozzle to surface distance has no significant effect according to the literature (Monde and Katto, 1977, Kamata et al., 1988, Wasdsworth, 1990 and Nonn et al., 1988), the distance was fixed at 15 mm during all experiments.

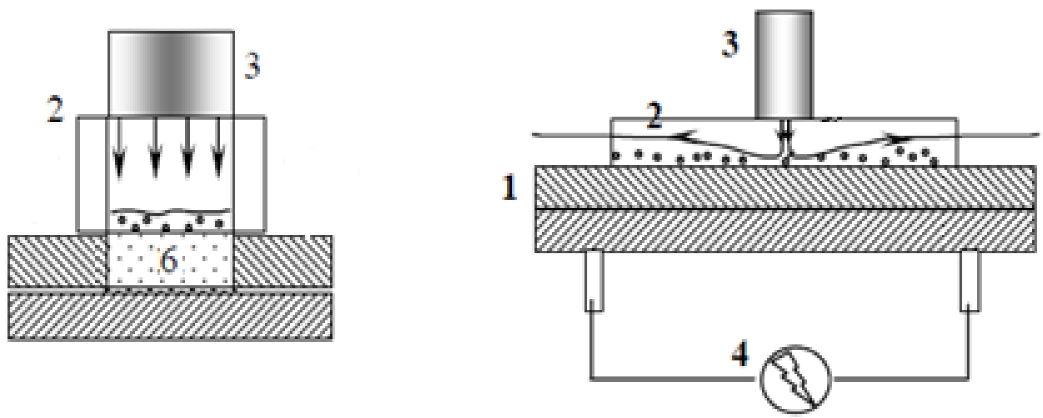

1-Ceramic plates, 2- Quartz plates, 3- Planar nozzle, 4- DC Power supply, 5- High speed camera, 6- Heated surface
Figure 3-2 Schematic of the Test Section

A 2.6 kW DC power supply (XANTREX XFR 20-130, 0-20V 0-130A) was used to provide heat through a 50 microns thick NiCr 80/20 foil placed beneath a copper block. An aluminum oxide layer was placed between the copper block and the heating foil to electrically insulate the copper block from the foil. Figure 3-3 shows a sketch of the assembled test section while photographs for the test section are provided in Figure 3-4.

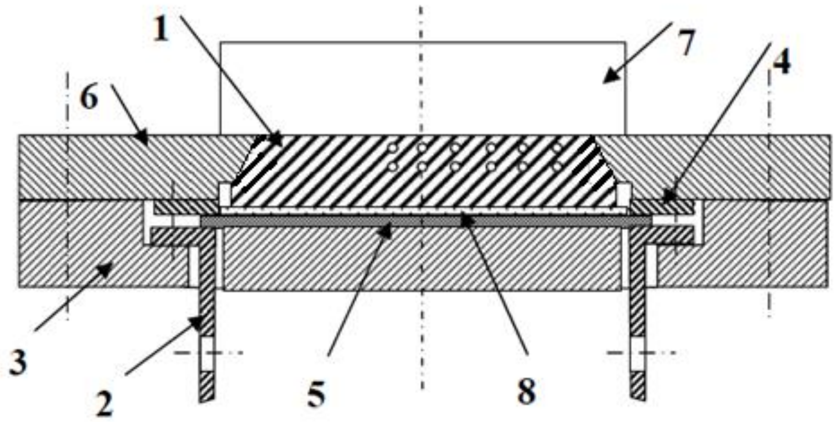

1- Copper block, 2- Power lugs, 3- Lower ceramic plate, 4- Clamps, 5- Ni/Cr foil, 6- Upper ceramic plate, 7- Quartz plate, 8- Al_2O_3 insulation layer
Figure 3-3 Assembly of the Boiling Module

Three boiling blocks were made of high purity copper (grade C110) with average thermal conductivity k_{cu} = 380 W/m.K over the temperature range of interest in the current research, i.e. between 90°C and 130°C. The thermal conductivity of the boiling block has been assumed constant as its value varied by only 3% over such temperature range. Twelve holes, 4 mm depth, 0.52 mm in diameter were drilled into the side of each copper block. Figure 3-5 shows the locations of the drilled holes that were drilled at two different distances from the exposed surface, with six holes at each distance. Each of these holes was 4 mm in depth.

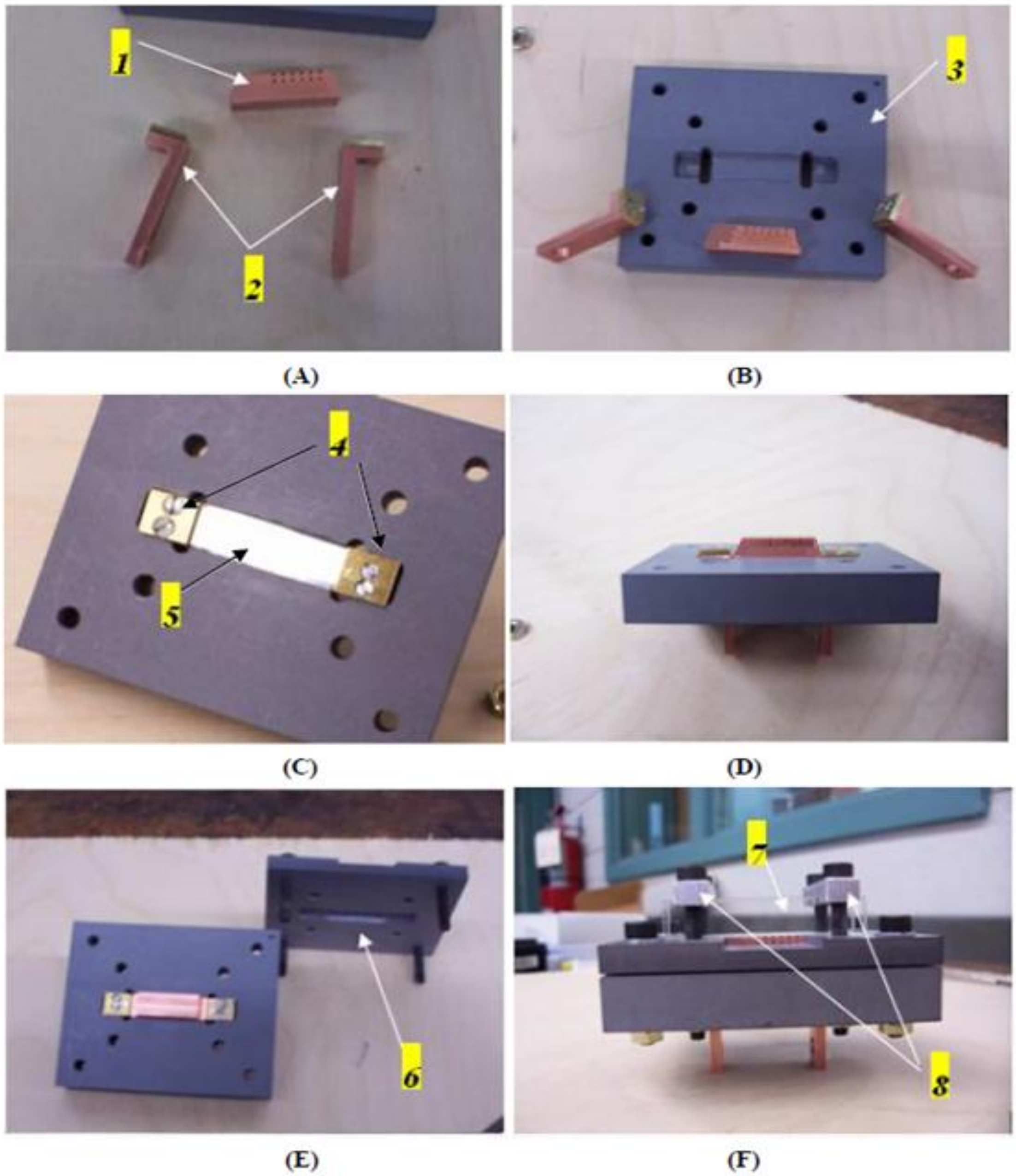

1- Boiling block, 2-Power lugs, 3- Lower Ceramic plate, 4- Heating foil clamps, 5- Ni/Cr heating foil (50 microns thick), 6- Upper ceramic plate, 7- Quartz side plates, 8- Quartz plates' clamps.

Figure 3-4 Photographs of the Test Section Assembly Steps, Omar (2010)

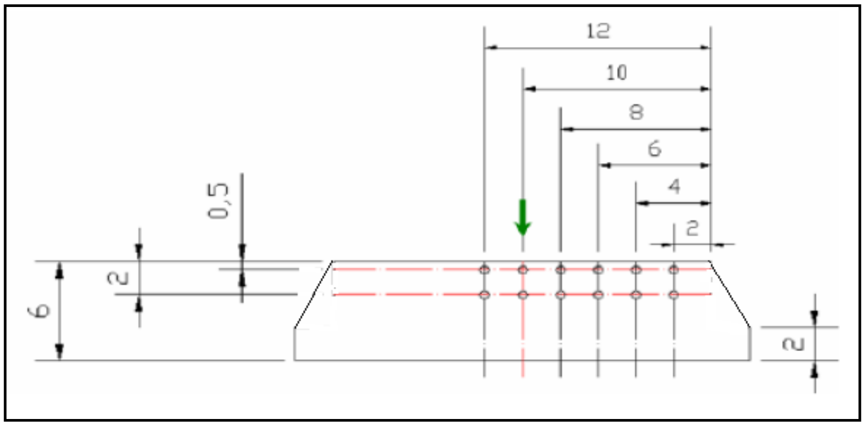

Figure 3-5 Locations of Thermocouples' Holes

To measure the interior temperatures of the boiling blocks, twelve 0.5 mm outer diameter, sheathed, ungrounded K-type thermocouples were inserted in these holes. These temperature readings were used to determine the surface temperature and the heat flux at the stagnation point. During assembly, the holes of the copper block were filled with heat transfer oil and the thermocouples were painted with silver paste. Silicon rubber was used to fix the thermocouples on the ceramic plate and to insulate the side of the copper block.

As mentioned before, three copper blocks were manufactured; each was placed in upper ceramic plate and was connected to 12 separate calibrated (± 0.1°C) thermocouples. The upper surface of each block was sanded using specific emery paper to obtain different surface roughness. More details regarding the roughnesses will be presented later. Thermocouples were connected to data acquisition card (NI SCXI-1000).

3.2 Analysis of Experimental Heat Transfer Data

Steady state, constant surface temperature was used. The right lower surface thermocouple (highest temperature) was controlled using a proportional controller. Each reading was taken when the controlled temperature reaches steady state. Then the set point was changed to a higher value for the next reading.

Data was analyzed using MATLAB code produced by Omar (2010). The code extrapolates the temperature readings to obtain the interior temperatures at the insulated end of the copper block, where no thermocouples were placed, and then it uses Finite Difference Analysis to predict the interior temperatures. The surface temperatures at different locations were calculated later by best fitting the determined interior temperature. Hence, the heat flux and the coefficient of heat transfer could be calculated. The code was validated using CFX simulations. The Finite Difference Algorithm is explained in more details in Appendix B.

3.3 Boiling Surfaces

Three surfaces with different roughness were used during the experiments. Each surface was sanded by a particular emery paper in the direction of flow. Sanding started by a rough emery paper followed by a smoother one in the cross direction and so on until the required sand paper. The final sanding direction was chosen in the flow direction to allow sanding the surface before each experiment without removing the glued quartz plates before each experiment. Emery paper of grade #1200 was used for sanding the smoothest surface S1, while Emery papers #600 and #320 were used for preparing the surface S2 and S3 respectively.

Surface roughness parameters were measured using Zygo 3D surface profiler. Seven samples, each of dimensions 0.36 mm x 0.27mm were measured for each surface and the roughness parameters were determined for each sample. Then the average of each parameter and its standard deviation were calculated. Table 3.1 shows the average roughness parameters for the three surfaces and the standard deviation of the measurements. Figure 3-6, Figure 3-7 and Figure 3-8 show a sample for each surface of the 3D surface profile measured at the stagnation line (the center of the copper surface).

Table 3.1 The Average Roughness Parameters and the Standard Deviation of the Measured Samples

	S1		***S2***		***S3***	
	Average	***σ***	***Average***	***σ***	***Average***	***σ***
R_a nm	*18.72*	*2.47*	*401.65*	*41.18*	*533.53*	*96.09*
R_z nm	*348.47*	*77.14*	*6884.00*	*990.08*	*8320.33*	*2150.07*
rms nm	*27.41*	*3.82*	*546.70*	*64.24*	*744.14*	*135.13*

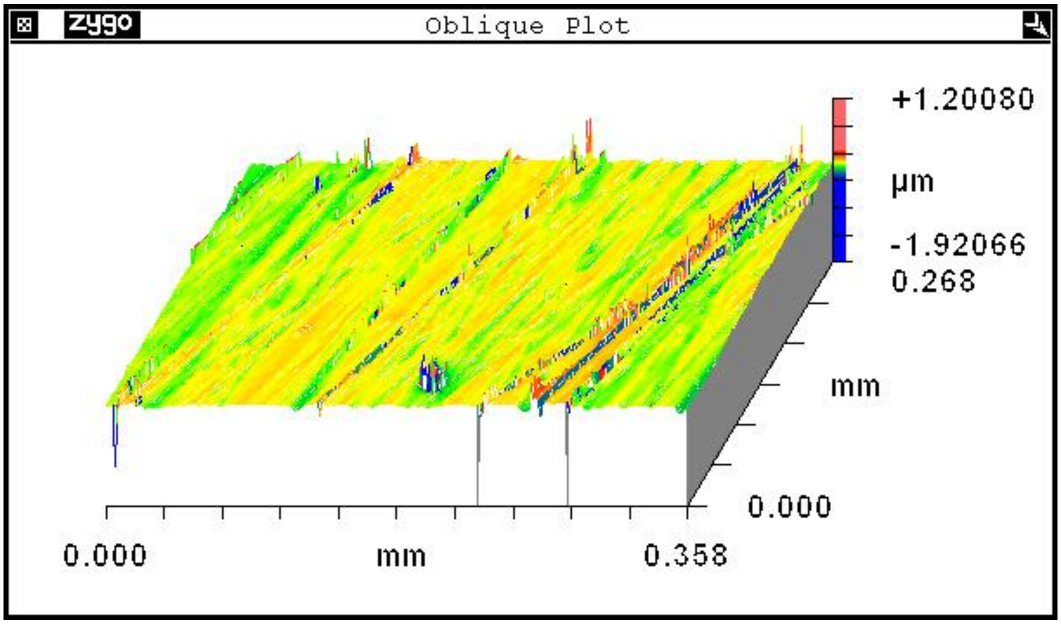

Figure 3-6 Surface S1 Profile

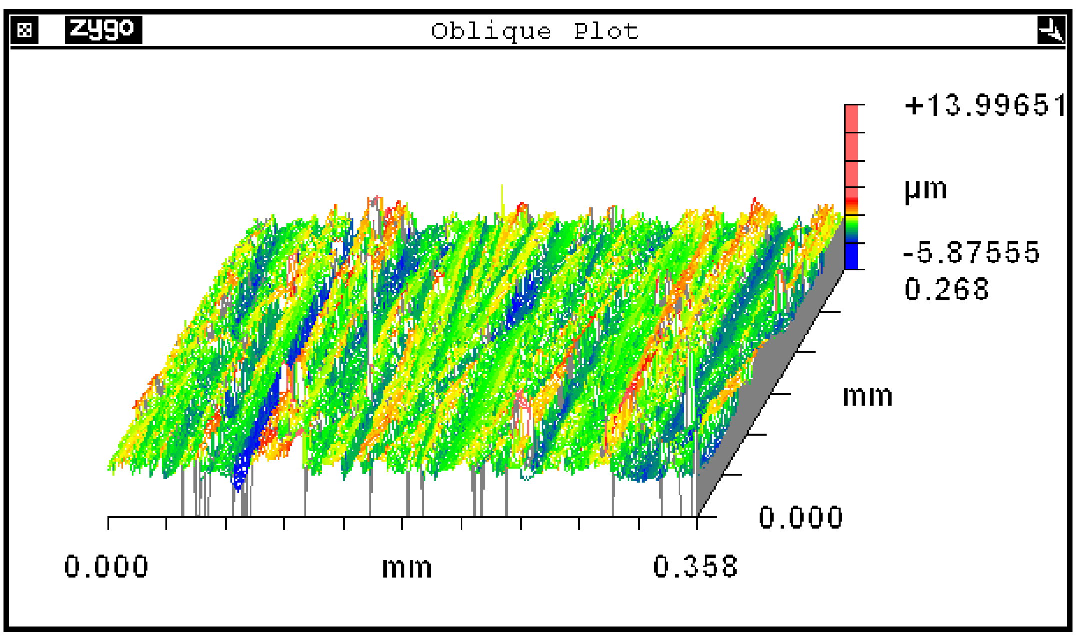

Figure 3-7 Surface S2 Profile

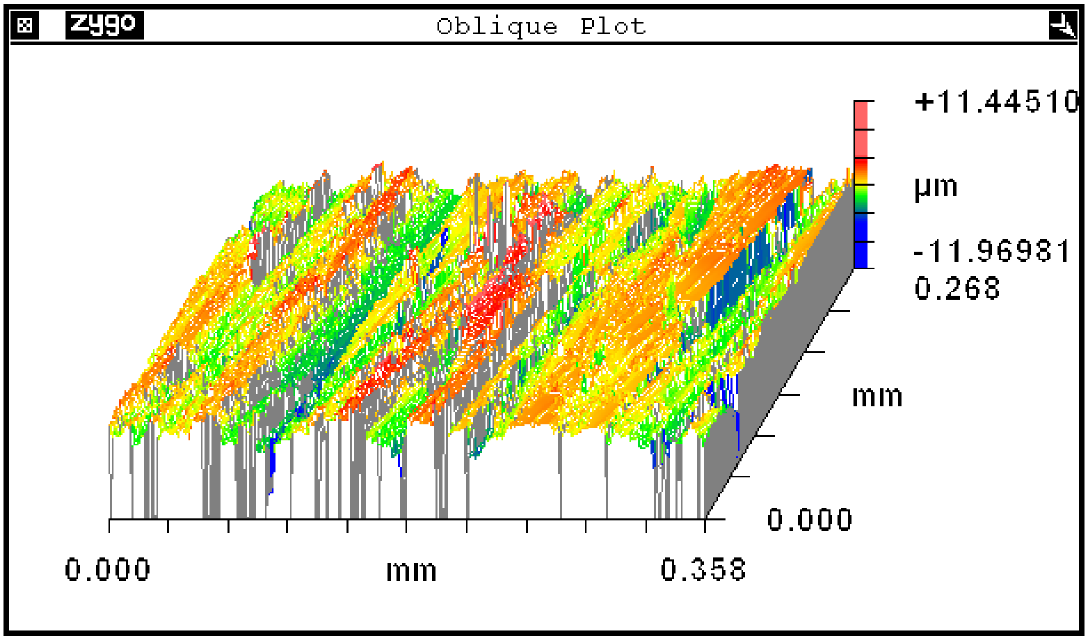

Figure 3-8 Surface S3 Profile

3.4 Experimental Procedure

Prior to each experiment the boiling surface was cleaned by sanding using emery paper specified for this surface in the flow direction and then washed with acetone. Surface roughness measurements were repeated prior to some selected experiments to ensure consistency. The following steps were conducted in each experiment:

1- The test section was de-assembled to change the burned out heating foil
2- The water in the supply tank was heated to a temperature close to the boiling temperature. Then the water was degassed by opening the valves and circulating the water for about 30 minutes

3- The valves were adjusted to achieve the required jet velocity using the needle valve at the nozzle inlet

4- The water temperature was adjusted using the immersed heater in the water tank

5- Both water temperature and jet velocity were monitored throughout the run to enable readjustment if necessary. The deviation in the velocity readings was within ±0.05 m/s, while the fluctuations in the water temperature were within ±2°C of the desired values

6- The heated surface temperature was adjusted using the proportional controller of the power supply output. The controller adjusts the power supply output based on the difference between the temperature reading of the farthest thermocouple inside the copper block from the jet stagnation and a pre-selected set temperature input into the controller. All the experiments were performed as controlled temperature experiments

7- After reaching a steady-state, readings of the block thermocouples were recorded at 50Hz for thirty seconds. Steady state criterion is when the monitored temperature first decimal digit is steady for more than 1 minute. Reaching the steady state conditions takes a minimum of 2 to 3 minutes and takes longer in the forced convection regime

8- The set point temperature was increased by increments of 0.5°C to 3°C until foil burnout. Starting by 2°C to 3°C as increment step in the single phase regime then, it was set to 1°C in the nucleate boiling regime and then to 0.5°C near the foil burn out

9- Steps 6, 7 and 8 were repeated until foil burnout occurred

Chapter 4 Experimental Results and Discussions

4.1 Introduction

Experimental results, analysis and discussions will be presented in this chapter. The spatial temperature distribution was obtained using the interior temperature measurements. Then the spatial rate of heat flux distribution was obtained. This was done by using the finite difference analysis FDA algorithm, developed by Omar (2010) mentioned in the previous chapter. As the aim of this study was to study the effect of surface roughness on boiling under liquid jet impingement at the stagnation point, only data relevant to the stagnation point will be presented in this thesis.

This chapter will present and discuss the results obtained. The next section, 4.2, will include a discussion of the jet impingement flow field observed during the experiments and some digital photographs will be presented. In section 4.3, the effect of jet velocity on boiling performance at stagnation point under liquid jet impingement will be illustrated and discussed; also, boiling curves at stagnation point and the coefficient of heat transfer will be presented at different jet velocities followed by a discussion. The effect of surface finish on boiling curves will be presented in section 4.4. It is worth mentioning that the literature surveyed did not present the effect of surface finish on heat transfer performance except in the forced convection regime. Section 4.5 will focus on the forced convection regime and a comparison with Gabour and Lienhard (1994) study will be conducted.

As mentioned in the previous chapter, three surfaces have been used in this study. Tap water was used as cooling fluid during all experiments. The degree of subcooling was fixed at 10±2°C during all experiments, measured at the nozzle inlet. Five values of jet velocity: Vj = 0.9, 1.2, 1.5, 2.0 and 2.5 ± 0.05 m/s were tested on each surface. All runs continued until foil burnout. All measurements were taken at steady state conditions.

4.2 Flow Profile of a Liquid Jet Impinged on an Open Channel

This section focuses on the flow field obtained during the boiling experiments. Although that no high speed camera was used, some digital photos were captured during the experiments. As mentioned in the literature, a hydraulic jump occurs after a distance X_{hj} from the stagnation line. Figure 4-1 shows a schematic sketch for the 2D flow field in an open channel after liquid jet impingement. As shown in the figure, a rather abrupt rise occurs in the liquid surface at a distance X_{hj} measured from the stagnation point in the direction of the flow. The rapidly flowing liquid slows abruptly and increases in height, converting some of the initial kinetic energy into potential energy. Omar (2010) developed an empirical correlation to calculate the distance X_{hj}, equation (4.1).

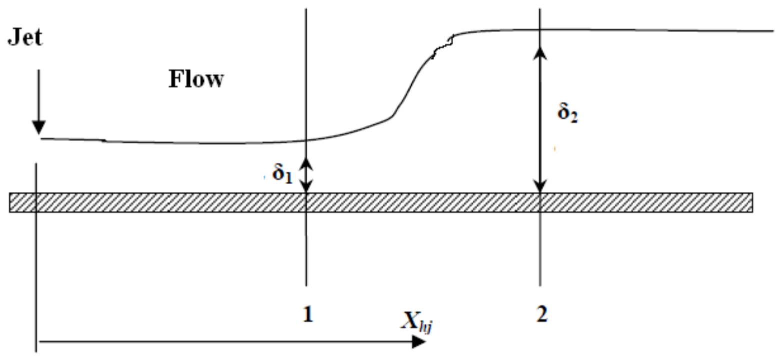

Figure 4-1 Schematic Sketch for the 2D Flow Field in an Open Channel, Omar 2010

$$\frac{X_{hj}}{w} = 6.51\, V_n^{2.67} \tag{4.1}$$

where *w* is the jet width and V_n is the jet velocity at the nozzle exit

Figure 4-2 shows a digital photograph taken for the flow field at jet velocity V_j = 0.9 m/s on surface S2. From the figure, a hydraulic jump could be seen clearly at a distance $X_{hj} \approx 5$ mm from the stagnation line. This agrees well with equation (4.1). Table 3.1 shows the values of the hydraulic jump for all jet velocities tested in the current study calculated using equation (4.1). From the table, for all values of jet velocity tested, except the smaller jet velocity (0.9 m/s), the hydraulic jump happens at a distance X_{hj} > 10 mm. These values of X_{hj} are larger than half length of the flow channel which means that the hydraulic jump occurs outside the heated surface.

Figure 4-3 shows a digital photograph for the flow field taken at jet velocity of 1.5 m/s on surface S2. The photograph seems to agree with the result obtained by equation (4.1) where the hydraulic jump could be seen just outside the heater surface.

Table 4.1 Hydraulic Jump Location Downstream the Jet, *Calculated using Equation (4.1)*

V_j m/s	X_{hj} mm
0.9	4.91
1.2	10.59
1.5	19.22
2.0	41.43
2.5	75.18
3.0	122.32

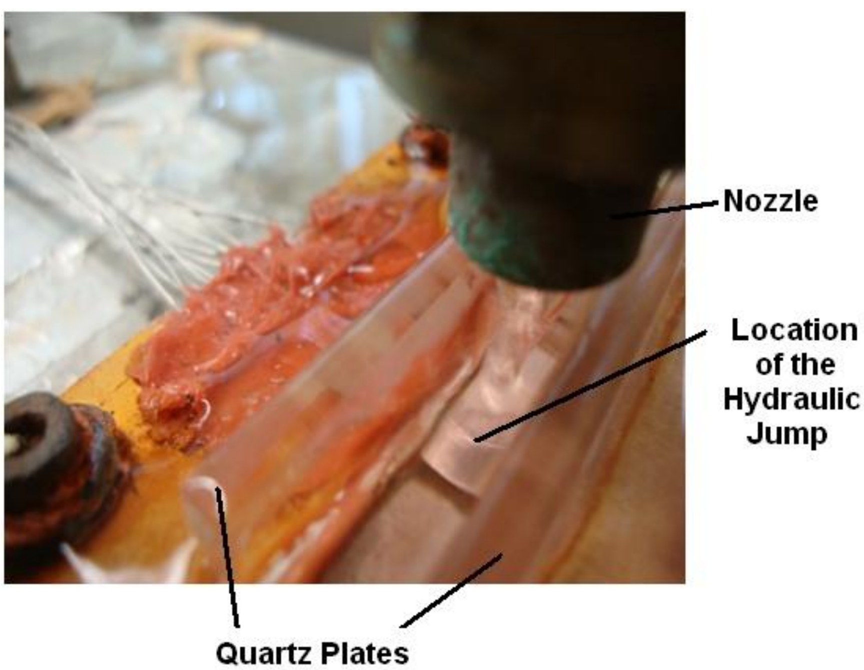

Figure 4-2 Photograph of the Flow Field taken at Jet Velocity of 0.9 m/s

Figure 4-4 shows a digital photograph captured for the flow field taken at a jet velocity of 2.5 m/s on surface S2. Because of the high jet velocity, the water splashed for a long distance resulting in a huge amount of water flow along and across the quartz plates.

From the figures, it could be noticed that flow field could not be treated as a two dimensional flow for jet velocities higher than 1.5 m/s as Vj > 1.5 m/s, the two dimensional open channel flow was changed to a non-uniform flow, see Figure 4-4.

Figure 4-3 Photograph of the Flow Field taken at Jet Velocity of 1.5 m/s

Figure 4-4 photograph for the flow field taken at jet velocity of 2.5 m/s

4.3 Effect of Jet velocity

4.3.1 Boiling Curve at Stagnation Point

Figure 4-5 shows the boiling curve at the stagnation point at a jet velocity V_j = 0.9 m/s on surface S1. Trend lines are presented on the graph to show the slope in the forced convection regime, partial and fully developed nucleate boiling regimes. Determination of the Onset of Nucleate Boiling ONB was done by observing noticeable change in the slope after the single phase regime. From Figure 4-5, we can see that the ONB located at 10.9°C of surface superheat. Similarly, the fully developed nucleate boiling started at 13°C of surface superheat. Omar (2010) reported an ONB at 12°C of surface superheat at the stagnation point at a jet velocity V_j = 0.95 m/s which agrees well with the current results.

During the experiments, at the same experimental conditions, foil burn out was occurring at different values of surface heat. So, there is no confidence that the maximum obtained heat flux represents the actual critical heat flux. For this reason, the maximum heat flux obtained, where foil burn out occurred, will be called burn out heat flux BOF instead of critical heat flux.

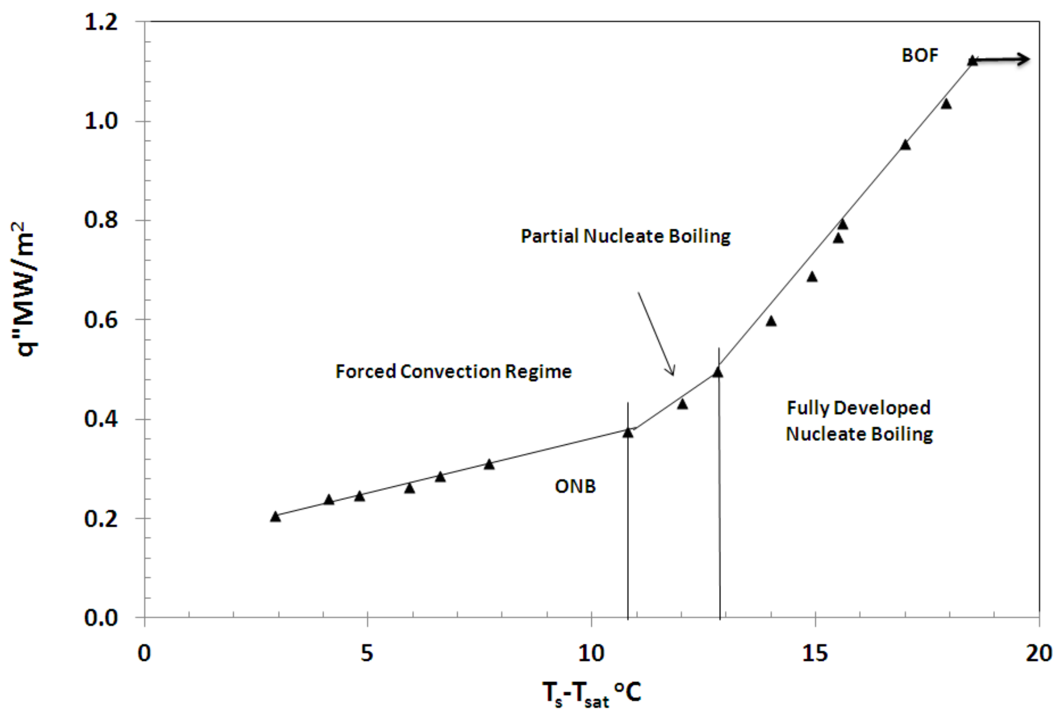

Figure 4-5 Boiling Curve V_j = 0.9 m/s, Surface S1

Figure 4-6 compares between the boiling curve obtained in the current work at V_j = 1.2 m/s on surface S1 and that observed by Omar (2010) at the stagnation line. From the figure, a good agreement could be noticed in the single phase, partial nucleate boiling regimes. The deviation between Omar (2010) and the current work in the nucleate boiling regime could be explained by the surface roughness or the direction of sanding the surface. Omar (2010) did not report the exact value of surface roughness but it was mentioned that R_a was less than 1 µm.

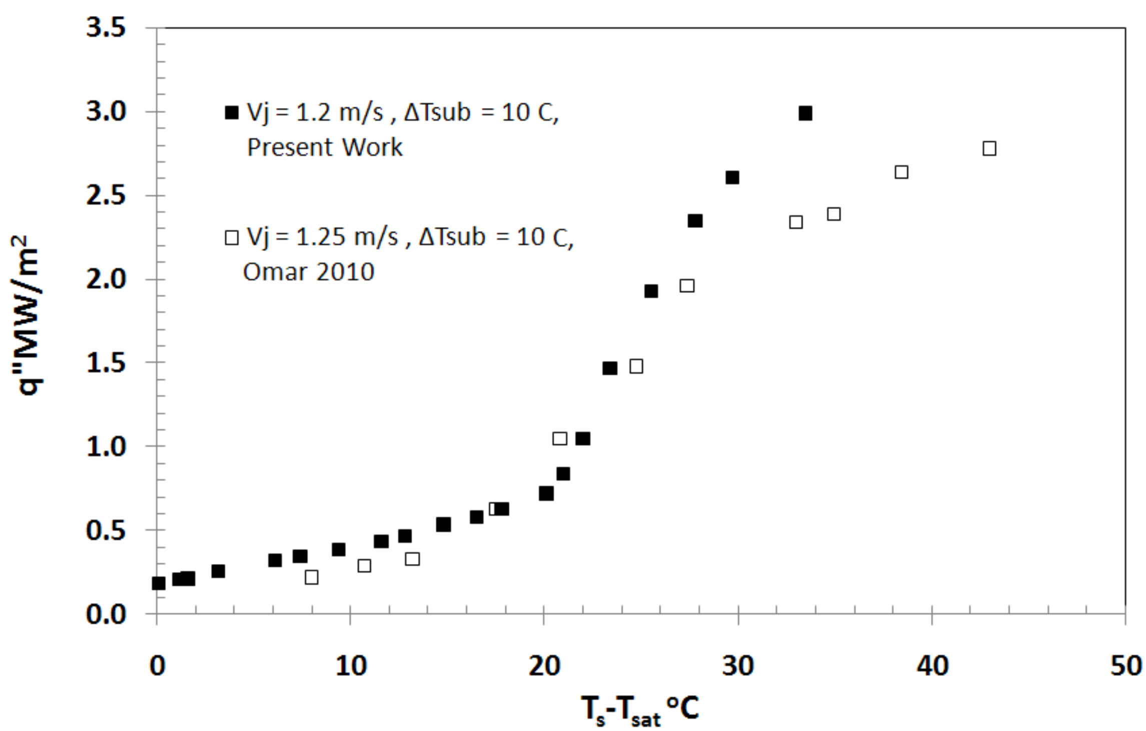

Figure 4-6 Comparison between the Boiling Curves Obtained by the Present Work and Omar (2010)

Figure 4-7 compares between the boiling curve obtained in the current work at V_j = 0.9 m/s on surface S1 and those observed by Robidou et al. (2003) at the stagnation line at 7 and 17°C of subcooling at jet velocity V_j = 0.7 m/s. The deviation between the current work's boiling curve and that obtained by Robidou et al. (2003) could be explained by the different geometry where the experimental setup used by Robidou et al. (2003) did not include side walls. Also the surface used by Robidou et al. (2003) was nickel plated. Robidou et al. (2003) did not report roughness measurement of the nickel plated surface. Omar (2010) reported an ONB at 12°C of surface superheat at the stagnation point at a jet velocity V_j = 0.95 m/s which agrees well with the current results.

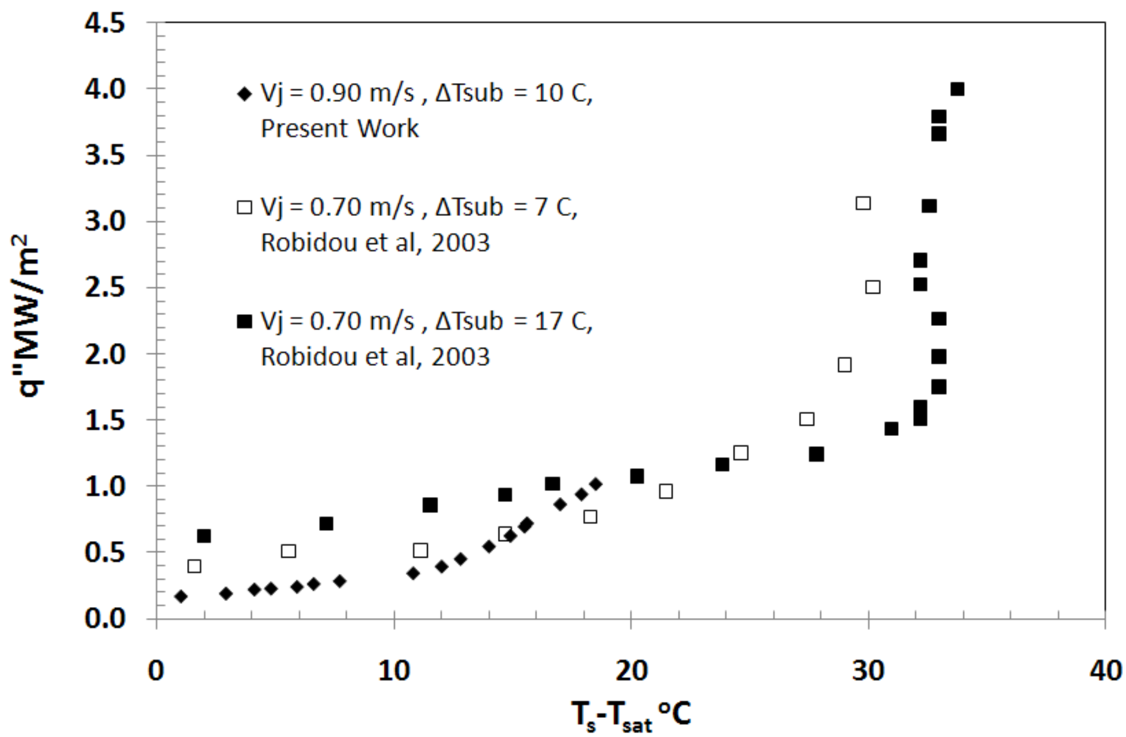

Figure 4-7 Comparison between the Boiling Curves Obtained by the Present Work and Robidou et al. (2003)

4.3.2 Effect of Jet Velocity on the Boiling Curve at Stagnation Point

Figure 4-8 shows the boiling curves at the stagnation point for surface S1 at two different jet velocities. Increasing the jet velocity from 0.9 to 1.2 m/s has insignificant increase of heat transfer in single phase regime. Also, the Onset of Nucleate Boiling was delayed from 10.9˚C to 18.2˚C. The burn out heat flux BOF increased from 1.1 to 2.88 MW/m^2. This trend agrees well with data reported in literature by Omar et al. (2007) and Robidou et al. (2003). However, the values of the BOF are much lower than that reported Robidou et al. (2003) which could be explained by the different geometry.

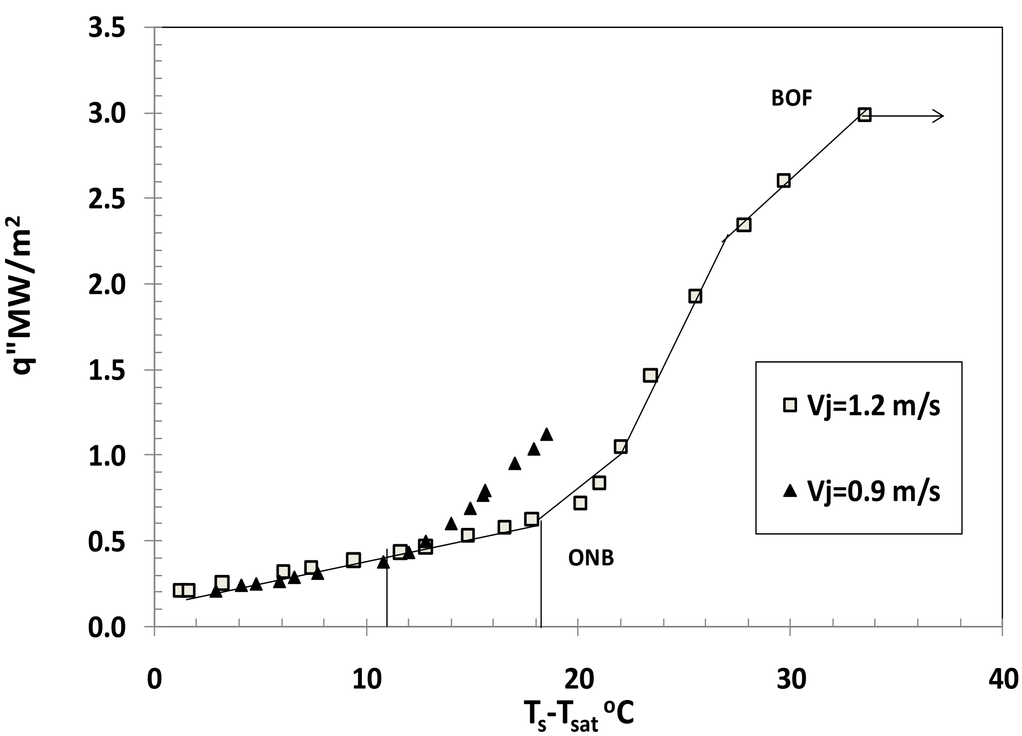

Figure 4-8 Boiling Curve at Stagnation Point, Surface S1

To evaluate the effect of jet velocity on the single phase regime, uncertainty analysis is presented in Appendix A. Figure 4-9 shows the forced convection regime, magnified on a logarithmic scale with error bars calculated as in Appendix A. From the figure, the increase in the rate of heat flux in the forced convection regime lies in the experimental error. Figure 4-9 also shows the horizontal error bars which represent the uncertainty in the surface superheat.

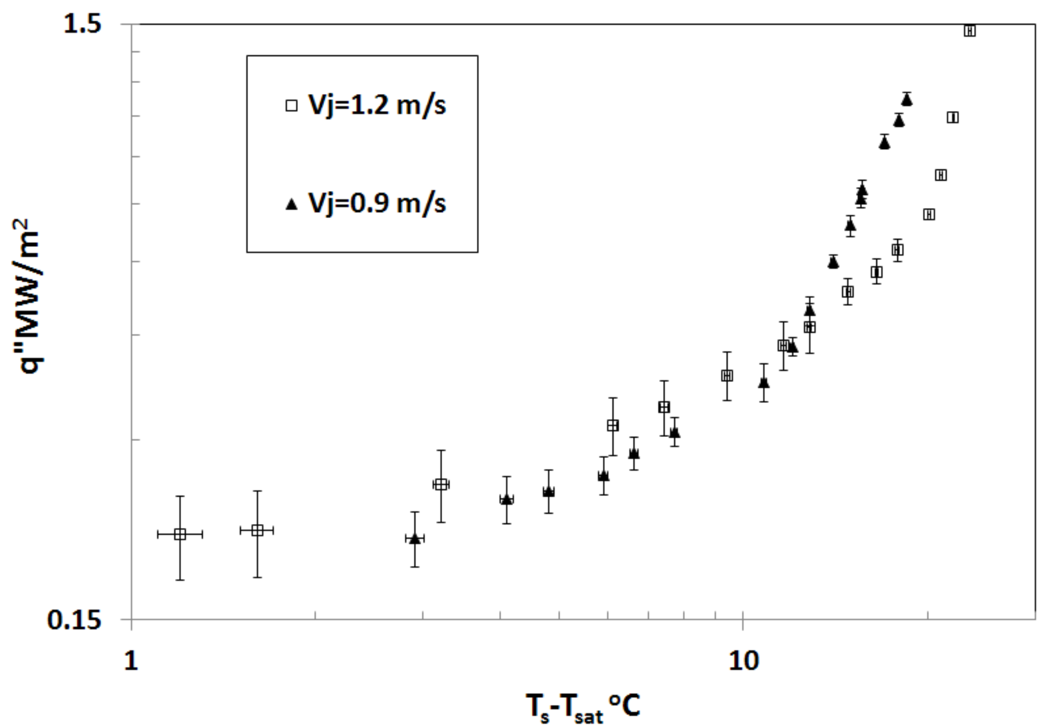

Figure 4-9 Boiling Curve at Stagnation Point, Surface S1, Logarithmic Scale

The same trend continued to occur when increasing the velocity from 1.2 to 1.5 m/s. This can be seen in Figure 4-10 where the rate of heat flux in the single phase regime increased insignificantly with increasing the jet velocity. The

BOF also increased to 3.4 MW/m^2. The surface superheat at the ONB was slightly increased to 18.5°C.

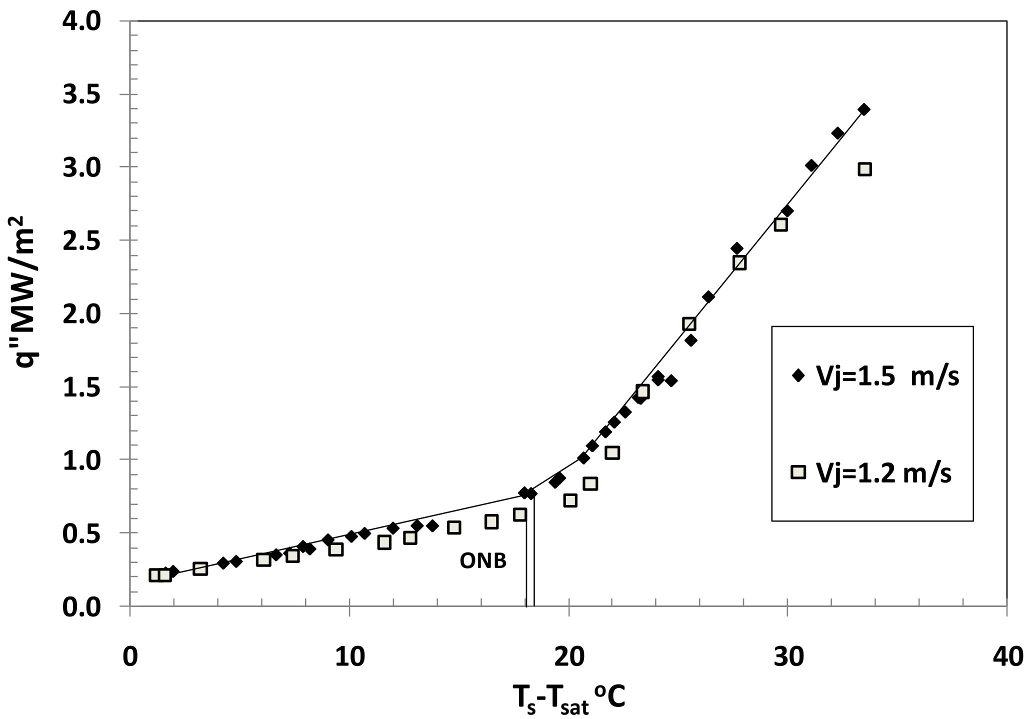

Figure 4-10 Boiling Curve at Stagnation Point, Surface S1

When the jet velocity was increased from 1.5 to 2 m/s, some contradictions occurred. As seen in Figure 4-11, ONB occurred at 12.8°C of surface superheat at V_j = 2 m/s instead of 18.5°C at V_j = 1.5 m/s. As well the value of the BOF decreased to 2.6 MW/m^2. The rate of heat transfer in the single phase regime had a significant increase with increasing jet velocity. The drop in the surface superheat at the ONB could be explained by the change in the flow field observed at high jet velocities where a significant amount of water flow over the two quartz plates as shown in Figure 4-4.

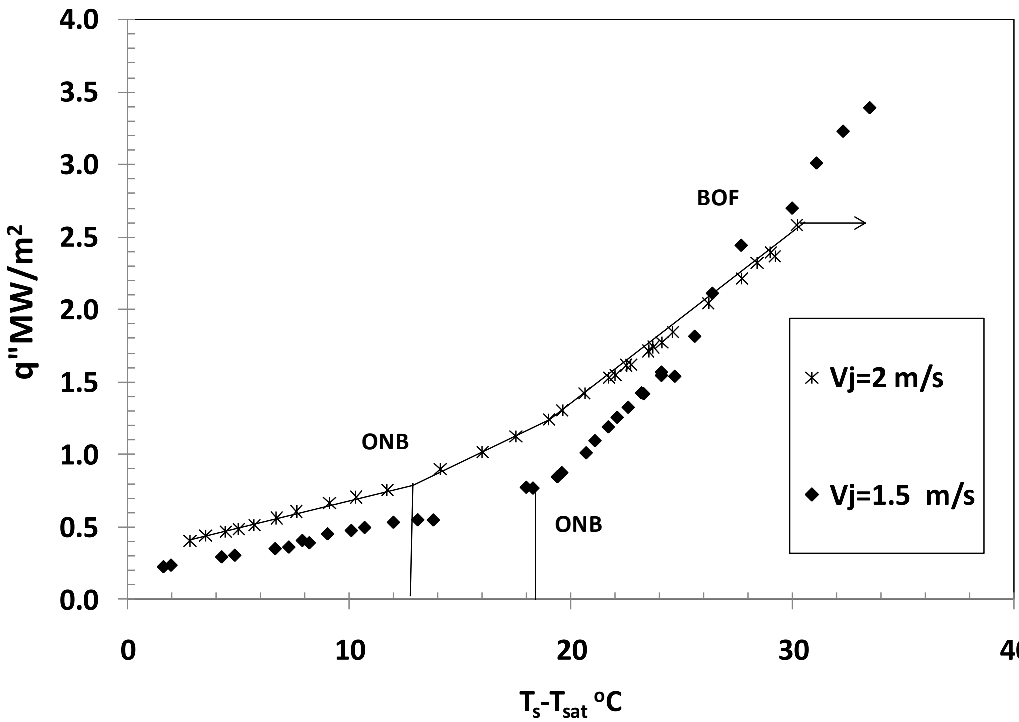

Figure 4-11 Boiling Curve at Stagnation Point, Surface S1

When the jet velocity increased to 2.5 m/s, Figure 4-12, the same trend in the BOF continued and the ONB occurred at lower surface superheat. However, the BOF increased slightly. Heat flux was slightly increased in the forced convection regime. Significant increase in heat flux in the nucleate boiling regime was observed. These non monotonic changes in the ONB and the BOF could be attributed to the significant changes observed in the flow field, see Figure 4-4.

Figure 4-13 shows the boiling curves at the five tested jet velocities on surface S1 using a log log scale.

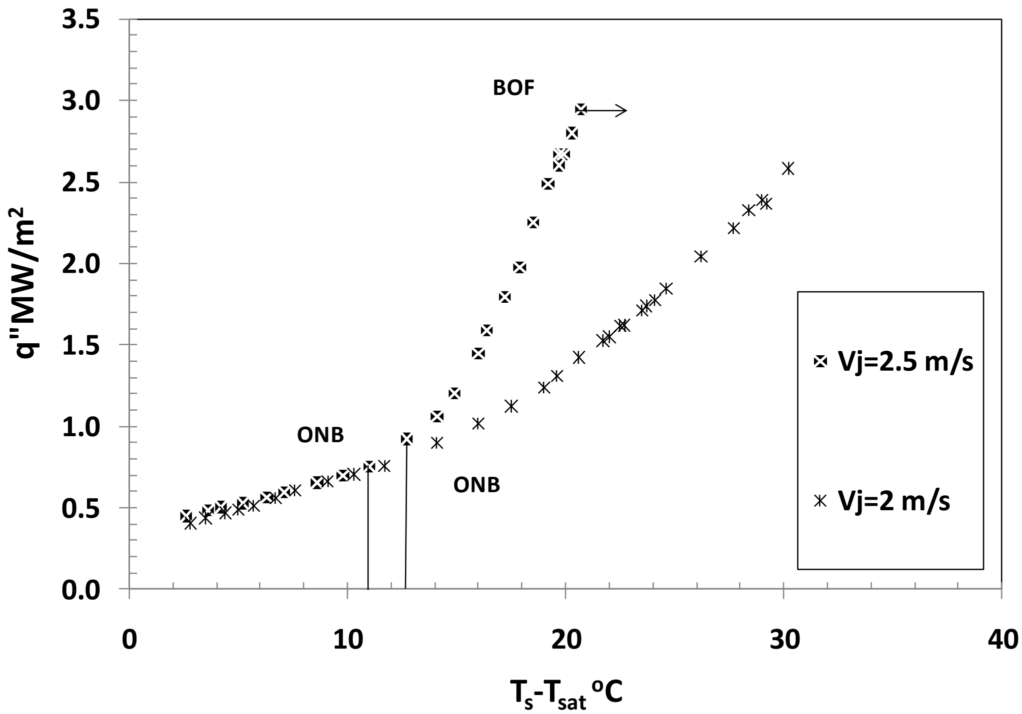

Figure 4-12 Boiling Curve at Stagnation Point, Surface S1

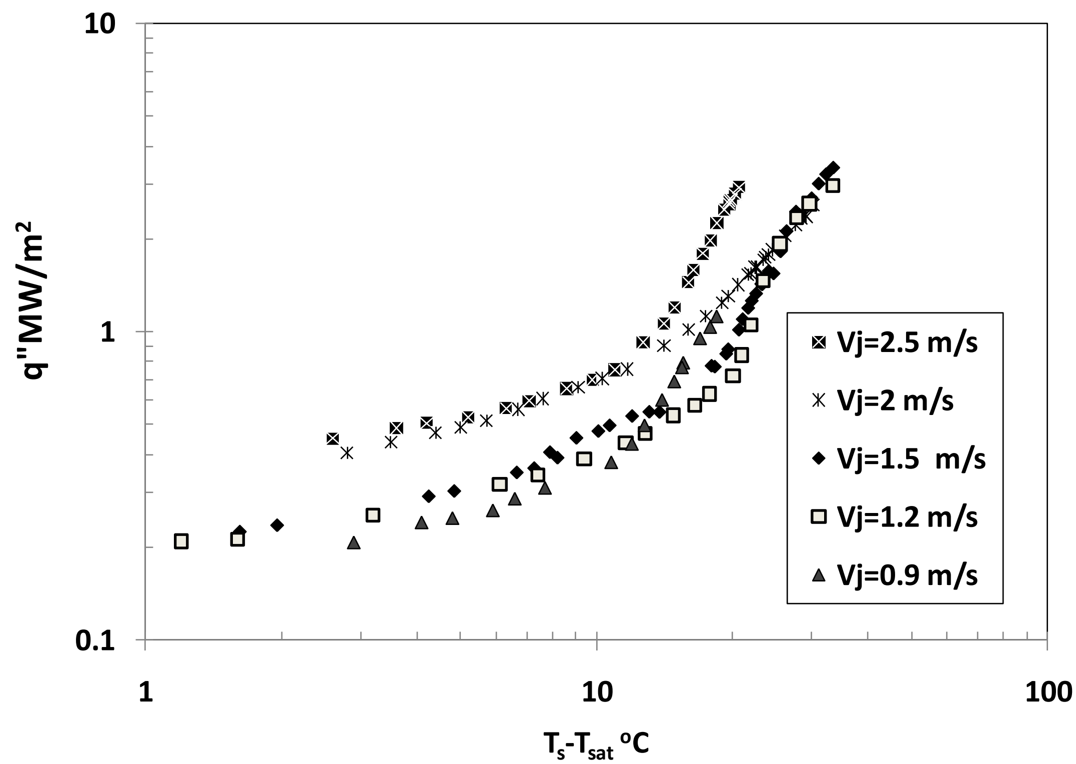

Figure 4-13 Boiling Curve at Stagnation Point, Surface S1, Logarithmic Scale

Figure 4-14 and Figure 4-15 show the effect of jet velocity on the boiling performance for surface S2. As seen in the figures, the rate of heat flux increased with increasing the jet velocity for the whole range of jet velocities studied. This increase was insignificant for jet velocities below 1.5 m/s at low degrees of surface superheat. The surface superheat at the ONB increased with increasing the jet velocity until V_j = 1.5 m/s. Further increase in jet velocity decreased the superheat required to initiate boiling. The BOF also increased with increasing jet velocity until V_j= 2 m/s. Increasing the jet velocity from 2 to 2.5 m/s decreased the value of BOF again. These non monotonic changes in the ONB and the BOF could be attributed to the significant changes observed in the flow field, see Figure 4-4.

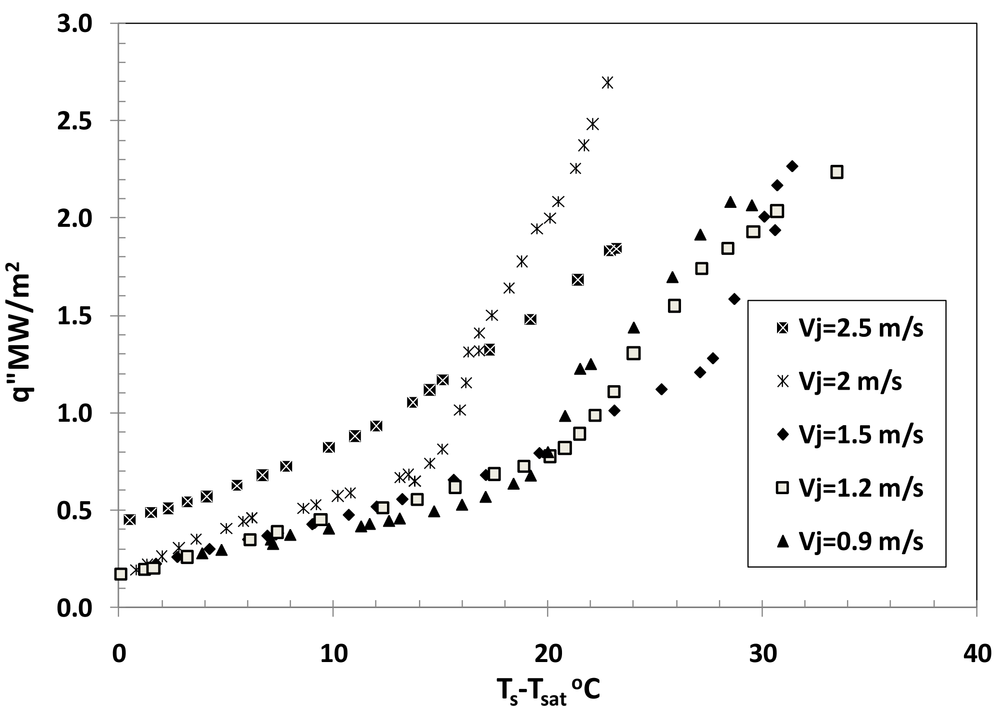

Figure 4-14 Boiling Curve at Stagnation Point, Surface S2

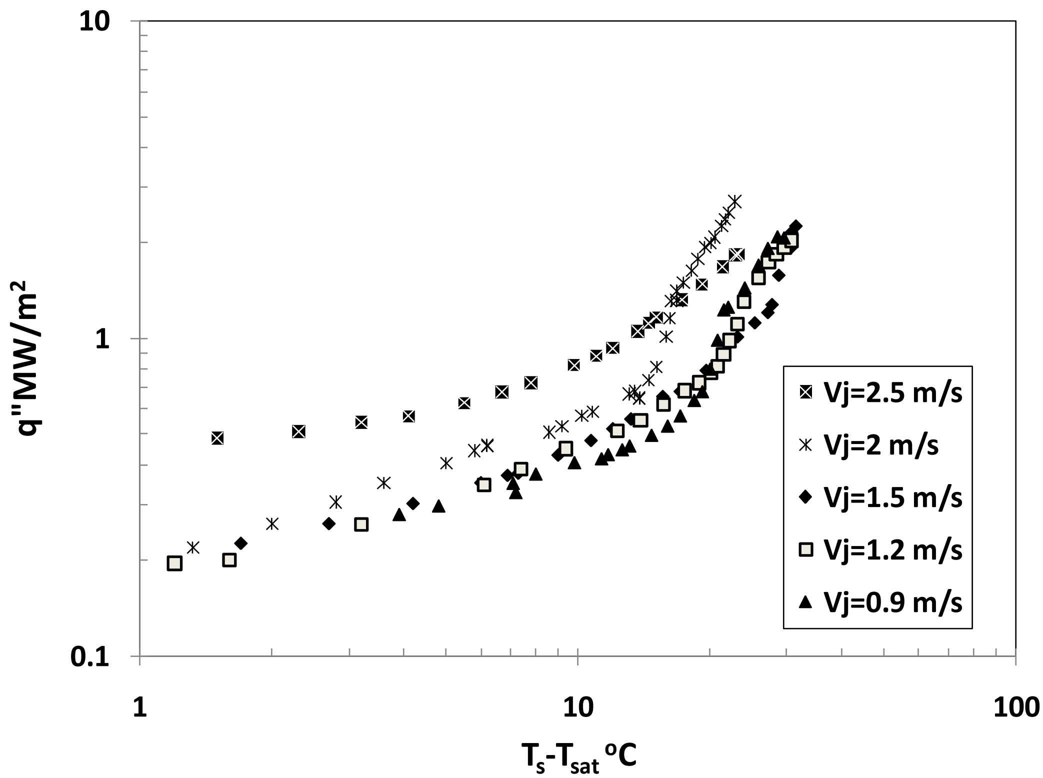

Figure 4-15 Boiling Curve at Stagnation Point, Surface S2, Logarithmic Scale

The same trend noticed for surfaces S1 and S2 was repeated for surface S3 as shown in Figure 4-16 and Figure 4-17. The rate of heat flux increased with increasing the jet velocity for the whole range of jet velocities studied. The surface superheat at the ONB increased with increasing the jet velocity until V_j=1.5 m/s. Further increase in jet velocity decreased the superheat required to initiate boiling. The BOF also increased with increasing jet velocity until V_j= 1.5 m/s. Increasing jet velocity to 2.0 m/s decreased BOF which increased again when the jet velocity was increased to 2.5 m/s. These non monotonic changes in the ONB and the BOF could be attributed to the significant changes observed in the flow field, see Figure 4-4.

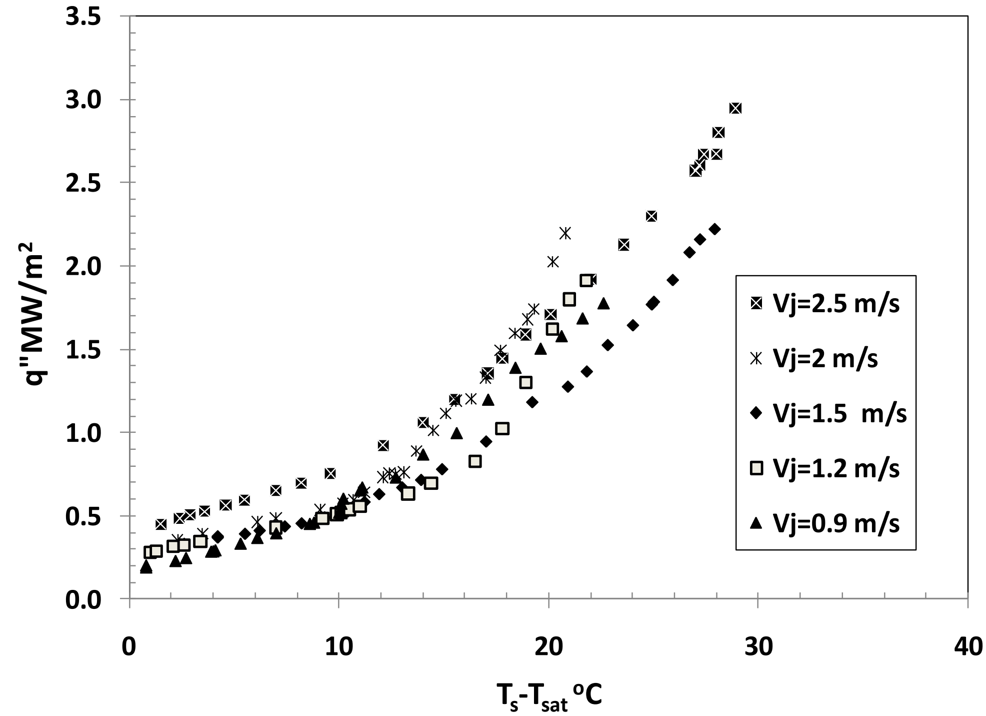

Figure 4-16 Boiling Curve at Stagnation Point, Surface S3

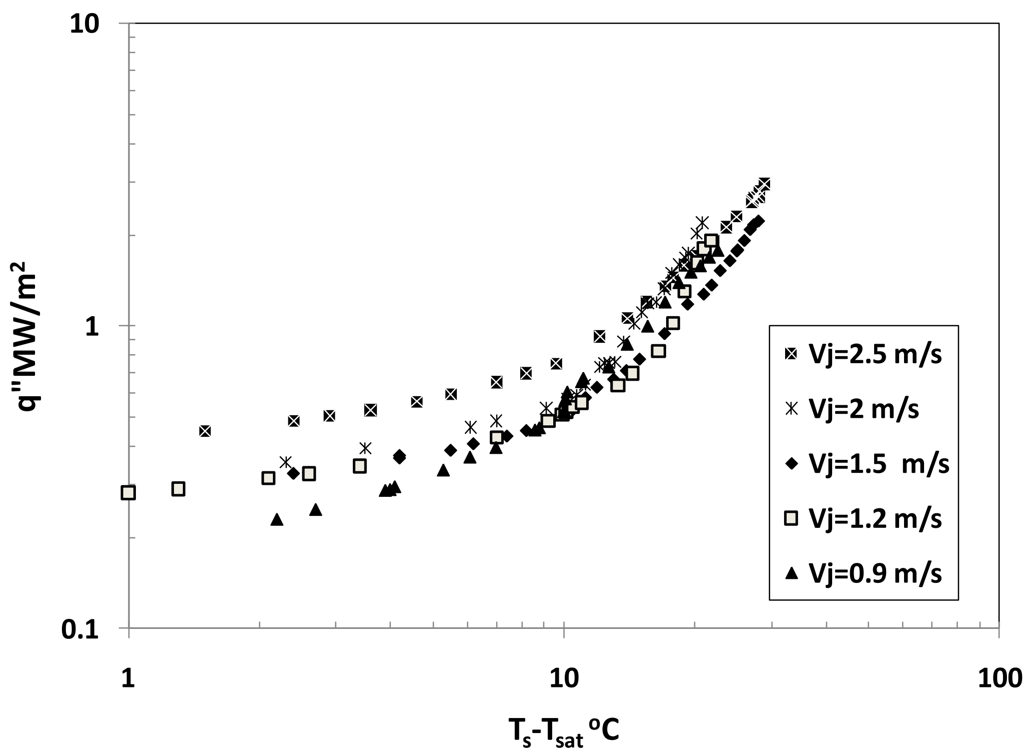

Figure 4-17 Boiling Curve at Stagnation Point, Surface S3, Logarithmic Scale

4.3.3 Discussion on the Effect of Jet Velocity

From the above we can conclude that with increasing jet velocity:

- The rate of heat flux in the single phase regime increased for the tested range of jet velocities. However, this could not be confirmed at low jet velocities and low surface superheat as the heat transfer incremental increase lies in the uncertainty
- The ONB was delayed to a higher degree of surface superheat for $V_j \leq$ 1.5 m/s but an opposite trend was observed at higher jet velocities. This opposite trend is attributed to the flow profile occurred at $V_j > 1.5$ m/s
- The BOF increased for $V_j \leq 1.5$ m/s, then a non monotonic behavior occurs for $V_j > 1.5$ m/s. This behavior is attributed to the significant change in the flow field observed at $V_j > 1.5$ m/s

The increase in heat flux in the single phase regime with increasing jet velocity at the same surface superheat could be explained by the decrease of thermal boundary layer thickness. The heat flux enhancement was insignificant for the smoothest surface because of that the thermal boundary layer was still much thicker than the surface peaks. In addition, higher velocity from the same nozzle increases the mass flow rate responsible of removing heat. The relationship between Nusselt number, Nu versus Reynolds number, Re in the single phase regime will be discussed later in this chapter.

Figure 4-18 shows the effect of jet velocity on the degree of superheat at the ONB boiling. It could be noticed that for the free tested surfaces, ONB location is delayed with increasing jet until a local maximum occurs at Vj = 1.5 m/s. Then an opposite trend occurs for larger jet velocities.

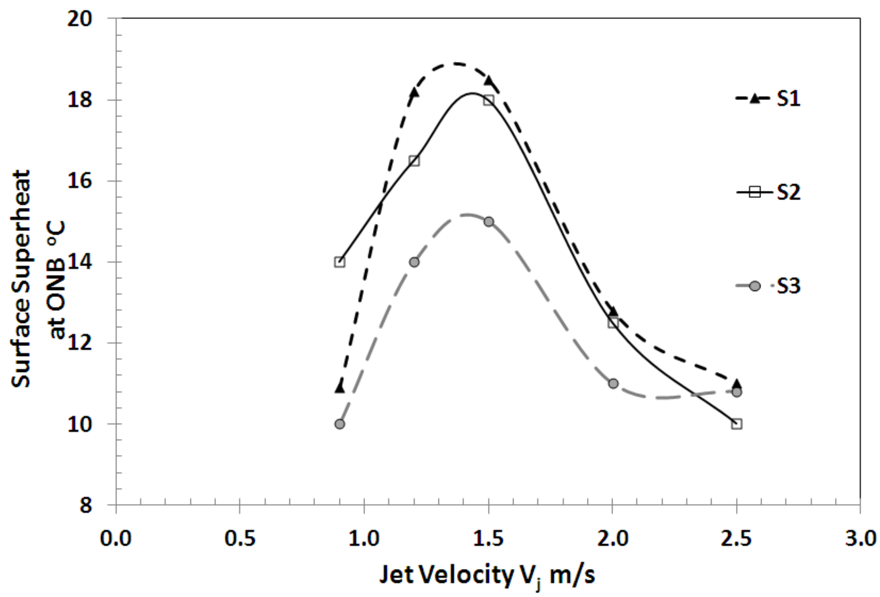

Figure 4-18 Relation between ONB and Jet Velocity

The trend of surface superheat required for ONB at stagnation point should have been affected by the flow downstream the jet. Because of high jet impact and lower fluid temperature, it is expected that the boiling process will not start at the stagnation point before it starts downstream the jet. Increasing the jet velocity increases the flow inertia in the parallel flow regime. For the same value of surface superheat, higher inertia will prevent bubbles from departing and cause them to collapse. This means that the initiation of boiling in the parallel flow regime required a higher degree of surface superheat. Once the boiling starts in the parallel flow regime, it propagates quickly to the whole surface including the stagnation point. Boiling propagation happens because of the bubbles formation which increases the pressure drop and restricts the flow. This can explain the delay of ONB to a higher surface superheat with increasing the jet velocity up to V_j = 1.5 m/s.

The behavior for V_j > 1.5 m/s can be explained from the flow profile discussed earlier in this chapter. As discussed before, at higher jet velocities, a certain amount of fluid flows along and over the sidewalls. This decreases the actual amount of mass flow rate flowing on the heater surface, which in turn decreases the thickness of the liquid layer through the channel, and hence, the boiling process starts sooner somewhere downstream of the jet. Then boiling propagates quickly through the flow channel to the stagnation regime. Boiling propagation happens because of the bubbles formation which increases the pressure drop and restricts the flow. It is worth mentioning here that some studies (Miyasaka and Inada, 1980, Miyasaka et al., 1980 and Vader et al., 1992) that were performed by impinging high jet velocities from a planar jet did not observe a significant effect of jet velocity on the boiling curve because in these studies the jet was free.

The burn out heat flux BOF increased with increasing the jet velocity until V_j=1.5 m/s, which agrees well with Omar (2010) and Robidou (2003). This could be explained by the higher flow inertia that sweeps the bubble formed on the surface thereby rewetting the surface. This prevents bubbles from forming vapor film and blanketing the and hence; higher heat transfer rates could be obtained. Further increase in jet velocity after V_j=1.5 m/s produced fluctuations in the BOF. This could be explained by the thin liquid layer on the boiling surface that initiated the boiling. When the bubble density increases, bubbles could cover a small area of the surface; which decreases the rate of heat transfer at this location and increases the surface temperature very quickly. This may result in foil burnout before the actual critical heat flux CHF.

4.4 Surface Finish Effect on the Boiling Curve at Stagnation point

4.4.1 The Effect of Surface Finish on Boiling at Stagnation Point under Liquid Jet Impingement

This research investigation aims mainly at studying the effect of surface finish on boiling heat transfer. As discussed in chapter two, there are many surface parameters that can affect the boiling performance. However, because it is easier to be measured in the industrial applications, the surface roughness parameters were selected to represent the surface finish.

Three surfaces have been used in the current study. Surface parameters have been presented in the previous chapter in Table 3.1. The arithmetic average of the roughness profiles were $\mathbf{R_a}$= 18.72, 401.65 and 533.53 nm for surfaces S1, S2 and S3 respectively. This section will discuss the effect of surface roughness on the boiling curve at the stagnation point.

Figure 4-19 and Figure 4-20 show the boiling curves for the three surfaces studied at the stagnation point for jet velocity V_j = 0.9 m/s. For the single phase regime, it can be noticed from the figure that increasing the surface roughness increases the heat flux. However, this increase lies within the uncertainty range in the single phase regime. Figure 4-19 and Figure 4-20 also show that the ONB occurred at lower surface superheat for surface S3 than surface S2. Also it shows that BOF decreased in case of surface S3 than that in case of surface S2. However, the boiling curve for surface S1 at the same jet velocity had a different trend. Boiling started at lower surface superheat on surface S1 than that on surface S2.

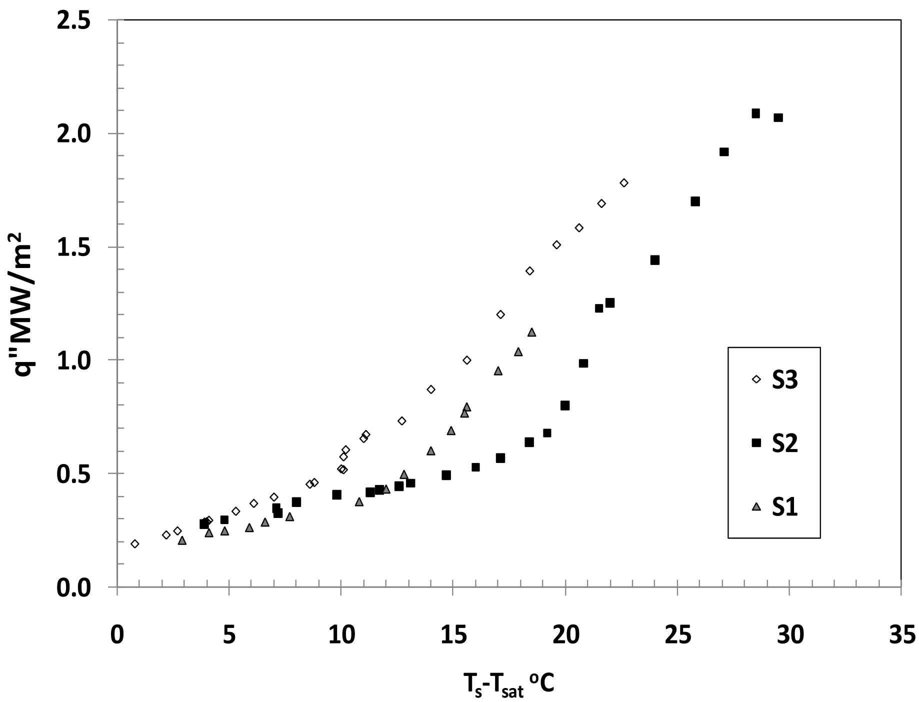

Figure 4-19 Boiling Curve at Stagnation Point, V_j=0.9 m/s

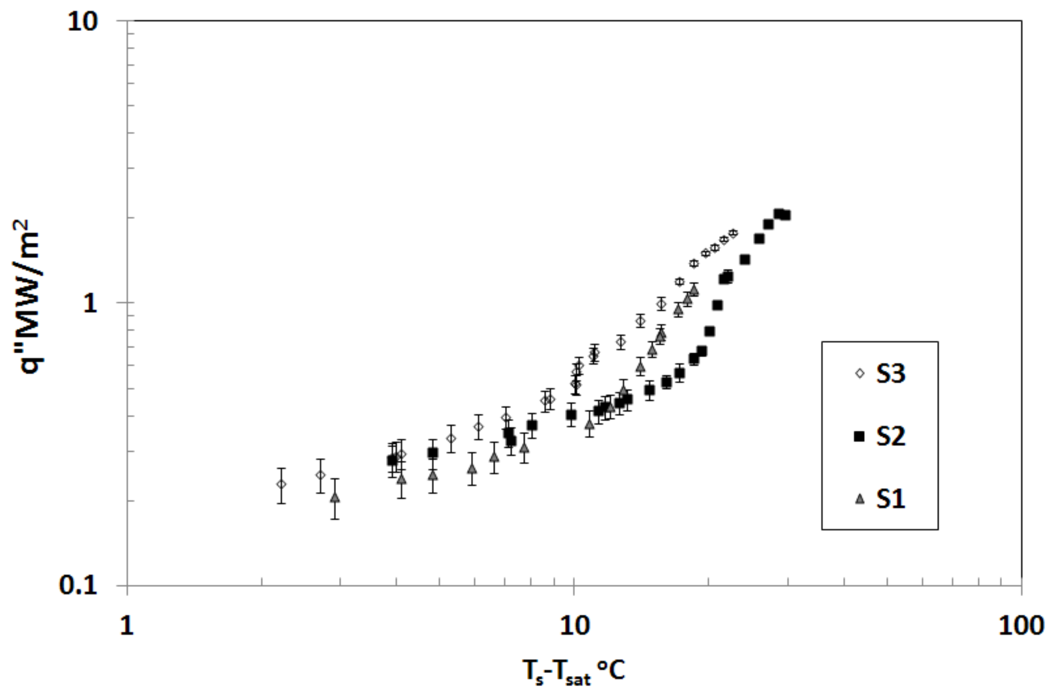

Figure 4-20 Boiling Curve at Stagnation Point, V_j=0.9 m/s, Logarithmic Scale

Figure 4-21 and Figure 4-22 show the boiling curves for the three surfaces studied at the stagnation point for jet velocity V_j = 1.2 m/s. For the single phase regime, it can be noticed from the figure that increasing the surface roughness increases the heat flux at the same wall superheat.

Boiling started sooner on the roughest surface S3, while the location of the ONB with respect to the surface superheat seems to be unchanged between surfaces S2 and S1. The BOF increased with increasing the roughness from S1 to S2 but opposite trend was observed when the roughness increased to surface S3.

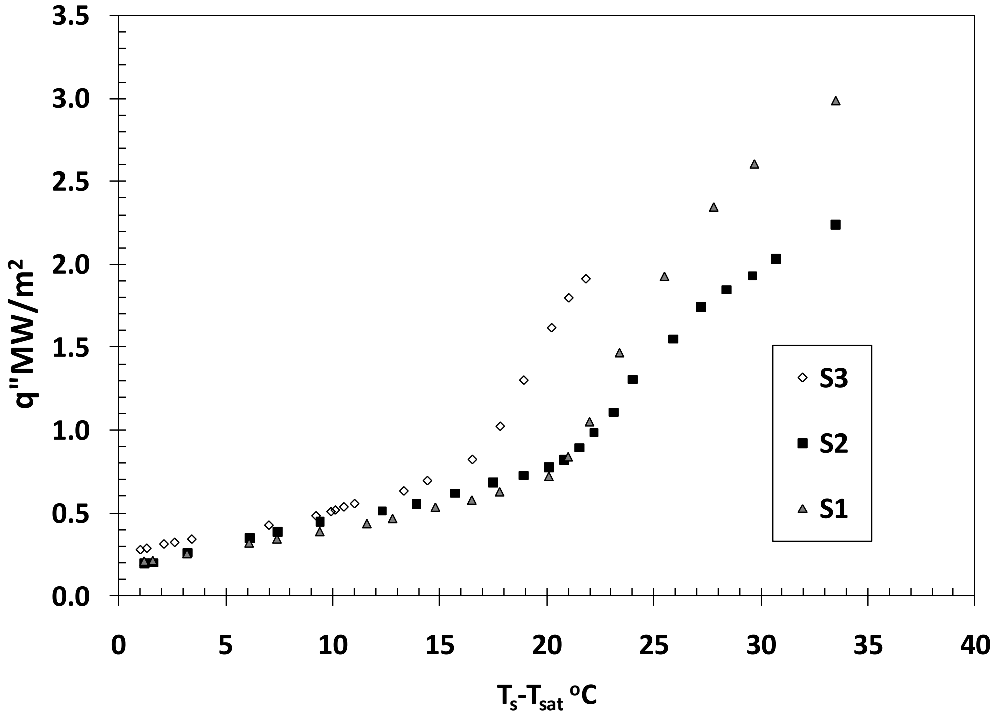

Figure 4-21 Boiling Curve at Stagnation Point, V_j=1.2 m/s

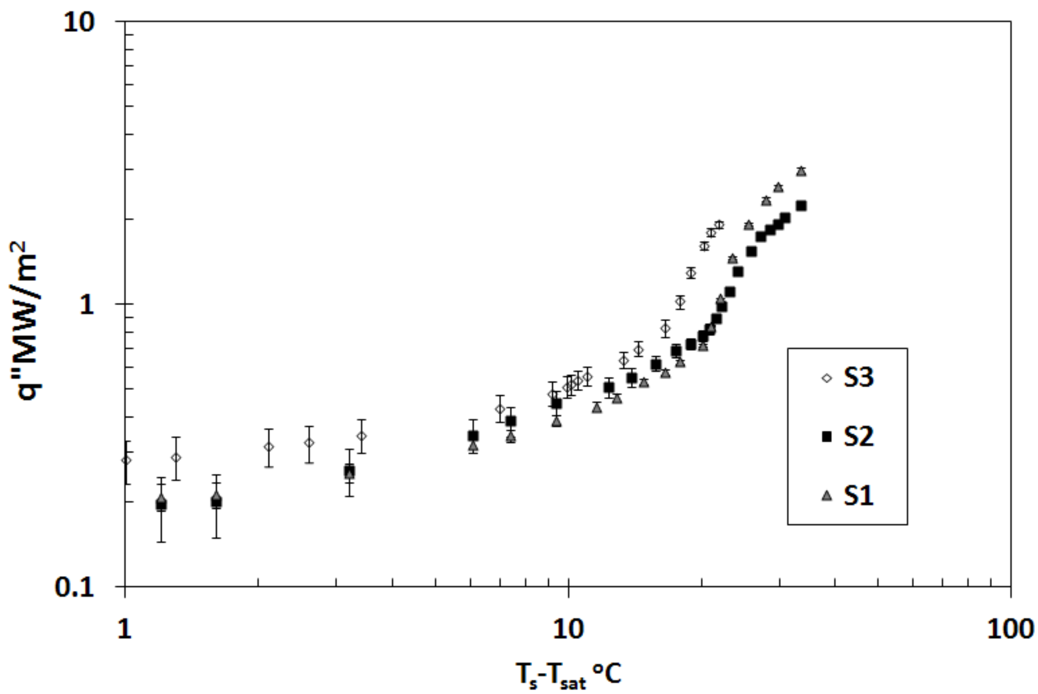

Figure 4-22 Boiling Curve at Stagnation Point, V_j=1.2 m/s, Logarithmic Scale

When the velocity was increased to V_j = 1.5 m/s, the same trend occurred, Figure 4-23 and Figure 4-24. The heat flux increased with increasing the roughness in the forced convection regime. The BOF decreased with increasing the surface roughness. Surface superheat required for initiating boiling, ONB did not change significantly between surfaces SI and S2, while boiling started earlier on surface S3.

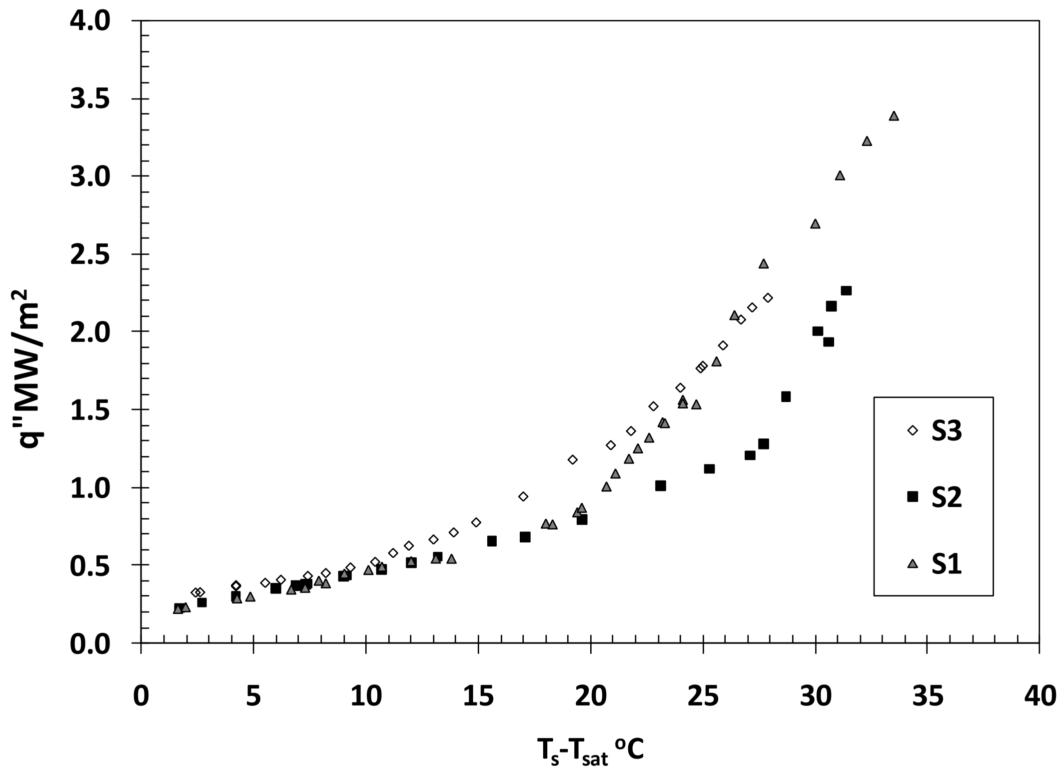

Figure 4-23 Boiling Curve at Stagnation Point, V_j=1.5 m/s

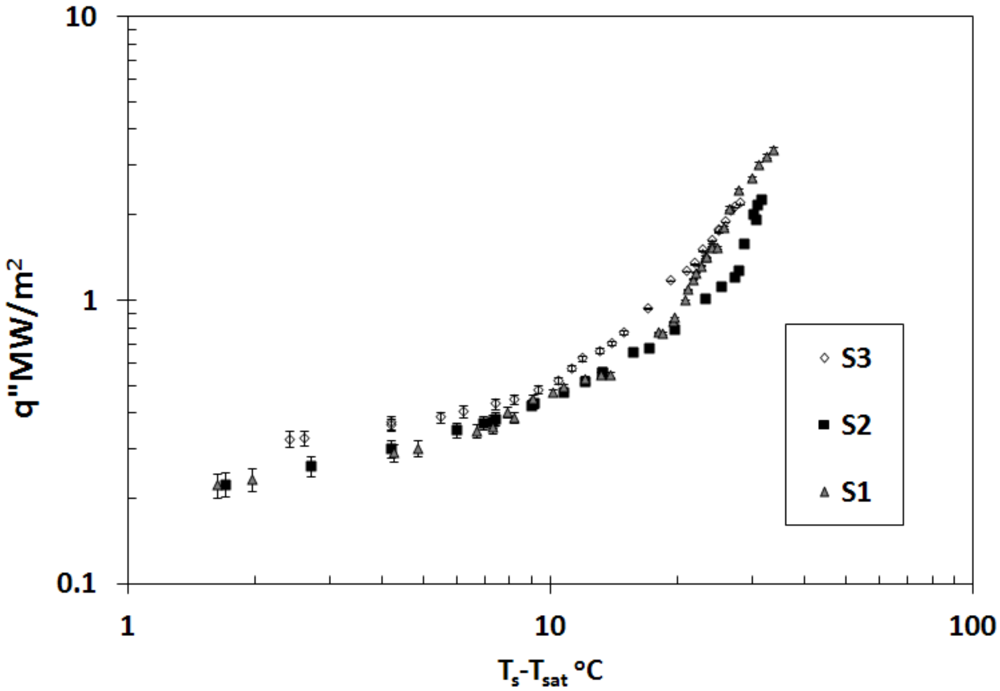

Figure 4-24 Boiling Curve at Stagnation Point, V_j=1.5 m/s, Logarithmic Scale

By increasing the jet velocity to V_j = 2 m/s, surface roughness does have a significant effect on the ONB nor the single phase heat transfer, Figure 4-25 and Figure 4-26. However, the nucleate boiling heat flux was lower for the smoothest surface S1 than both surfaces S2 and S3. The behavior of the boiling curves observed at this jet velocity V_j = 2 m/s could be attributed to the flow profile, see Figure 4-4.

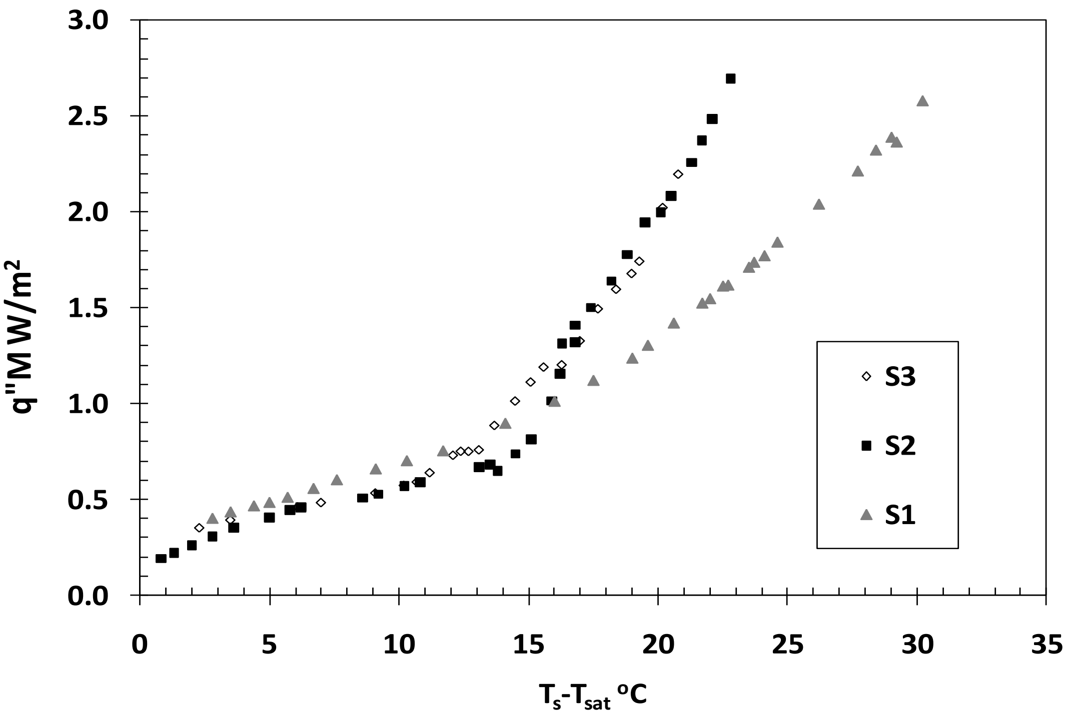

Figure 4-25 Boiling Curve at Stagnation Point, V_j=2.0 m/s

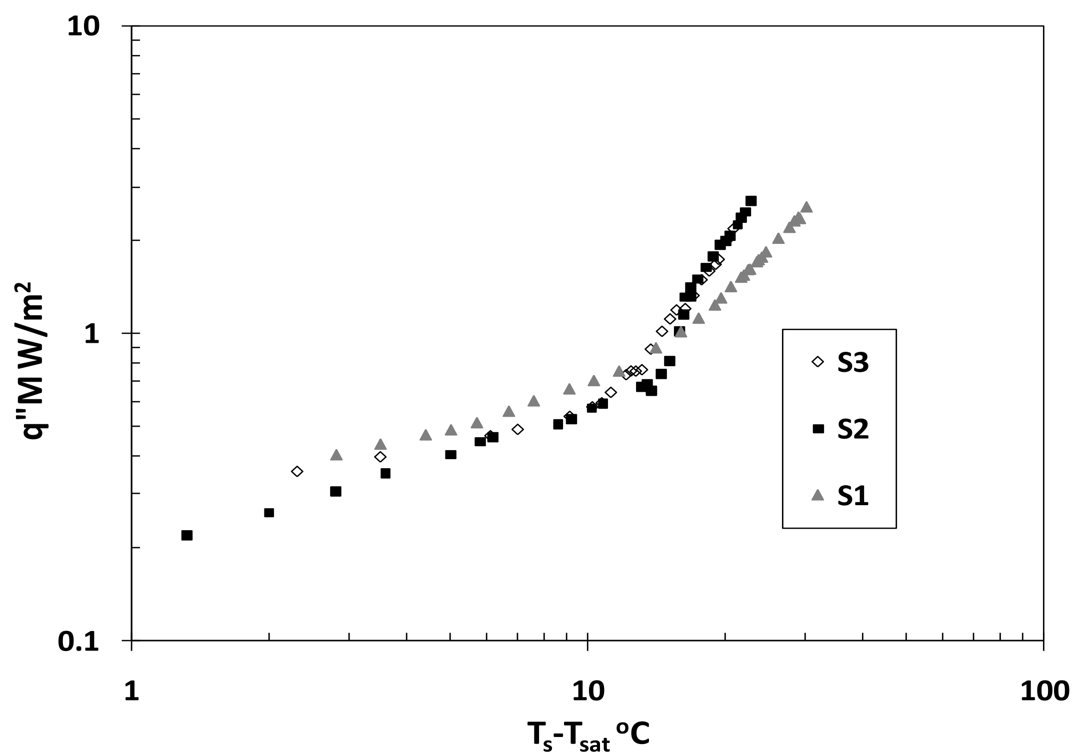

Figure 4-26 Boiling Curve at Stagnation Point, V_j=2.0 m/s, Logarithmic Scale

When the jet velocity increased to V_j = 2.5 m/s, Figure 4-27 and Figure 4-28, the effect of roughness was insignificant on both the single phase regime and the ONB. However, the nucleate boiling heat flux was higher for the smoothest surface S1 than both surfaces S2 and S3, which is opposite to the trend obtained at V_j = 2 m/s, see Figure 4-25. This could be attributed to the thin fluid layer occurred because of the flow profile, see Figure 4-4.

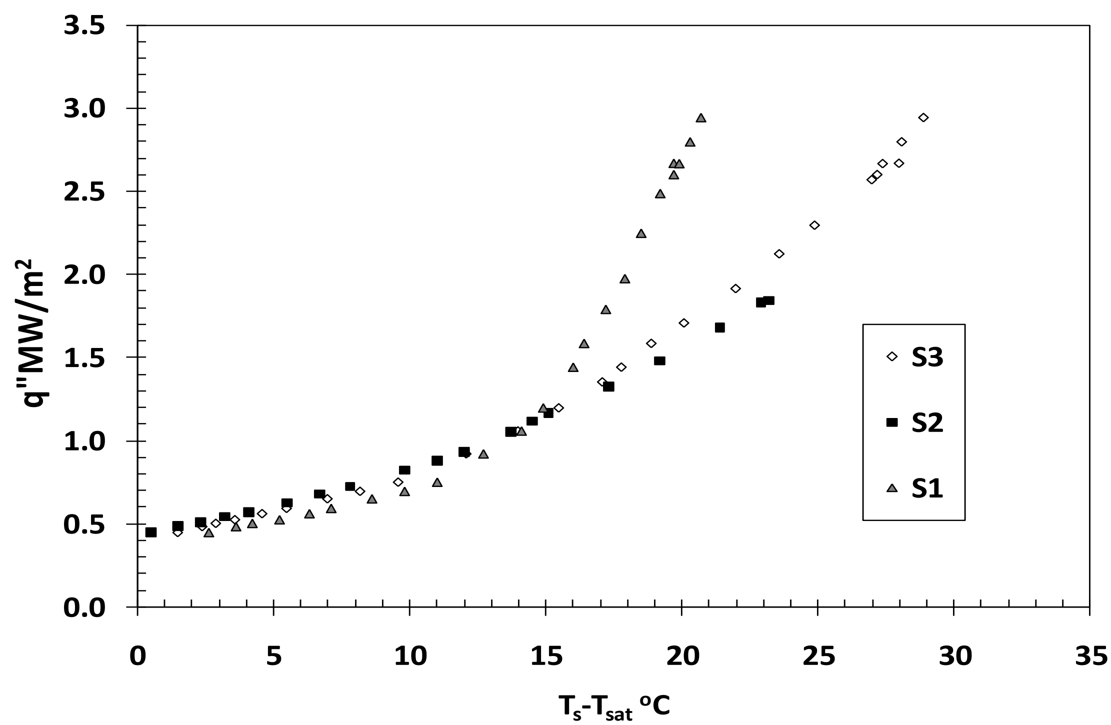

Figure 4-27 Boiling Curve at Stagnation Point, V_j=2.5 m/s

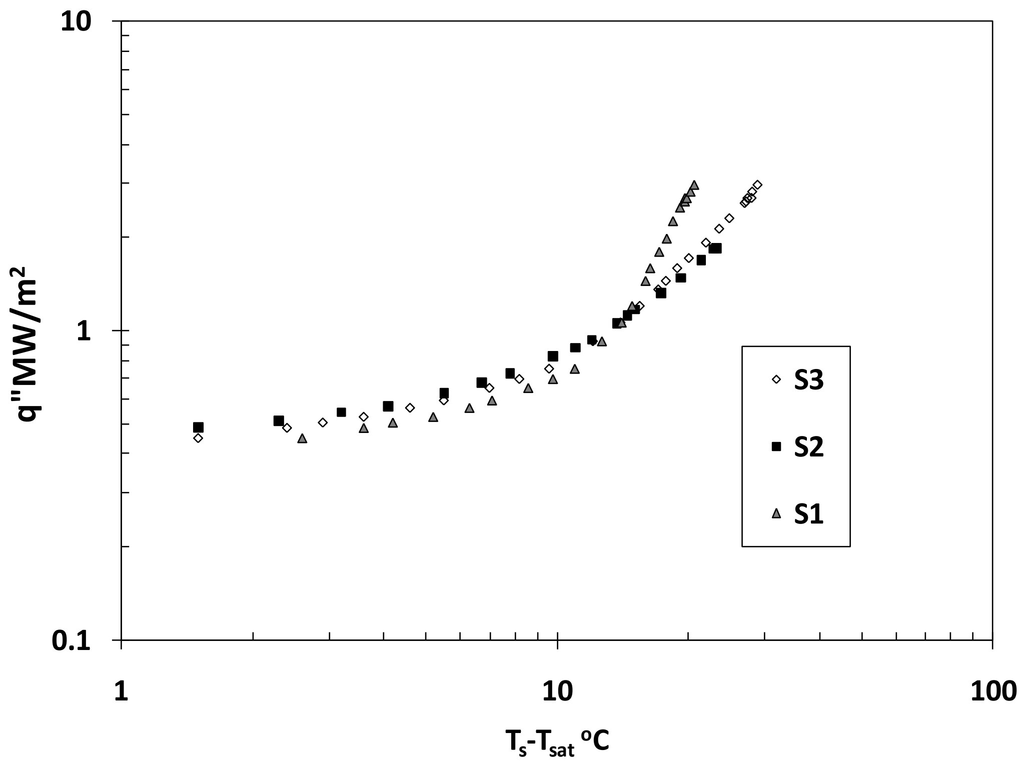

Figure 4-28 Boiling Curve at Stagnation Point, V_j=2.5 m/s, Logarithmic Scale

4.4.2 Summary and Discussions on the Effect of Surface Finish on Boiling at Stagnation Point under Liquid Jet Impingement

An inverse effect of surface roughness on the ONB Boiling could be noticed from the boiling curves at V_j = 1.2 and 1.5 m/s for the three surfaces studied. The ONB occurred slightly earlier when the roughness increased from surface S1 to S2. This effect was magnified when increasing the roughness in case of surface S3. The burn out heat flux BOF was also affected inversely by the surface roughness. The highest value of BOF occurred for surface S1 then S2 and finally S3. Same trend could be noticed at V_j = 0.9 m/s between surfaces S2 and S3 but surface S1, unexpectedly, had a different trend.

At high jet velocities, V_j > 1.5 m/s, the effect of surface roughness on the single phase heat flux and the ONB was insignificant. However, it affected the BOF and the heat flux in the fully developed nucleate boiling regime. No consistent trend could be observed, which could be attributed to the change in the flow field.

In the single phase regime, the increase in heat flux with increasing surface roughness is expected due to the increase in turbulence disturbing the thermal boundary layer. This occurred for jet velocity $V_j \leq 1.5$ m/s. The contradictions which occurred at higher jet velocities could be explained by the decrease of the actual flow rate and the significant change in the open channel flow.

At jet velocity $V_j \leq 1.5$ m/s, boiling was observed to start at lower surface superheat when increasing the surface roughness. The earlier ONB at lower surface superheat could be explained by the possible increase in the number of cavities associated with increasing roughness. These cavities act as nucleation sites which starts the boiling process downstream of the jet. The only exception to the rule was surface S1 at jet velocity $V_j = 0.9$ m/s.

The increase in surface roughness was observed to increase the BOF for jet velocity $V_j \leq 1.5$ m/s. The exception to that was for surface S1 at jet velocity $V_j = 0.9$ m/s. Increasing the roughness increased the large surface cavities which can act as active nucleation sites at lower surface superheat.

Jet velocities $V_j > 1.5$ m/s, resulted in inconsistent trends in ONB and BOF due to significant change in the open channel flow discussed earlier, see Figure 4-4.

4.5 Effect of Surface Roughness on the Single Phase Regime

A single study was reported in the literature that studied the effect of surface roughness on heat transfer under liquid jet impingement in the stagnation region. This study was performed by Gabour and Lienhard (1994). The study focused on the single phase regime and did not approach the nucleate boiling regime. Three round jets were used with jet diameters ranging from 4.4 to 9 mm which directed cold water on ten surfaces with root mean square roughness ranging from 0.3 to 28.2 μm. Although different roughness and different geometries were used, a comparison with this study will be conducted in this section.

To compare the results, the forced convection regime will be extracted from the boiling curves for jet velocities $V_j \leq 1.5$ m/s and the value of the convection coefficient of heat transfer was calculated. Because of the flow profile observed at high jet velocities, the results will be removed from this section. Nusselt Nu and Reynolds Re numbers were calculated based on the nozzle diameter and water film temperature. A relationship between Nusselt number Nu and Reynolds number Re was graphed and compared with the results obtained by Gabour and Lienhard (1994).

4.5.1 Convection Coefficient of Heat Transfer

Data was extracted from the linear relationship between the heat flux and temperature difference before ONB. Figure 4-28, Figure 4-29 and Figure 4-30 show the relationship between heat flux and the temperature difference. Temperature difference is the difference between the heater surface temperature at the stagnation point and the water temperature. As all the data were being calculated at the stagnation point, it was assumed that the water temperature was equal to the jet temperature. A linear correlation was fitted for each curve. The slope value was taken to be the local coefficient of heat transfer at the stagnation point at this value of jet velocity for this surface.

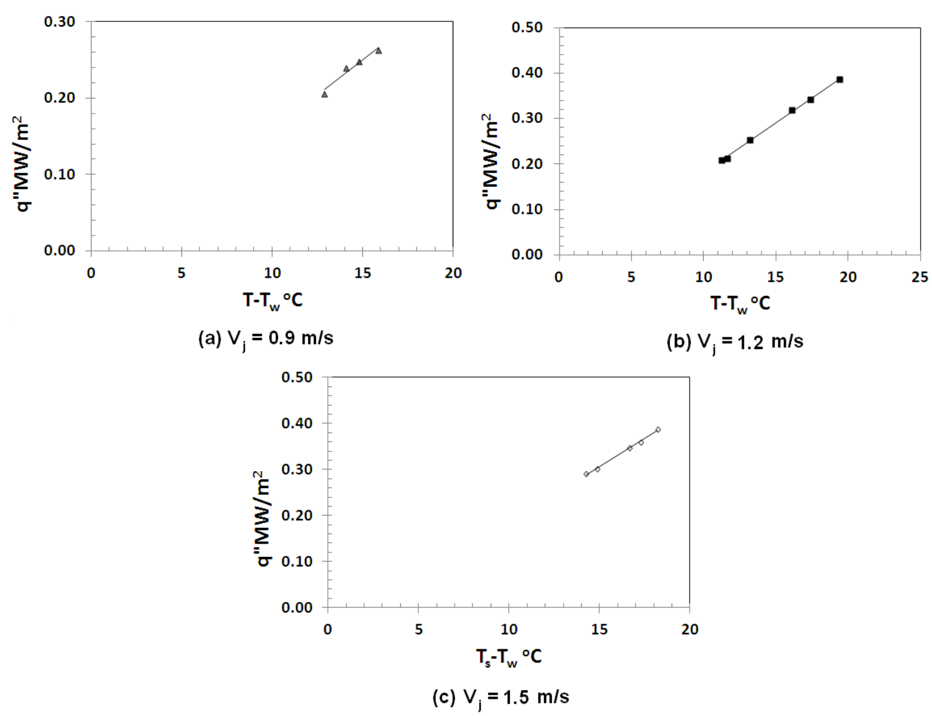

Figure 4-29 Relationship between Heat Flux and Temperature Difference for the Single Phase Regime, Surface S1

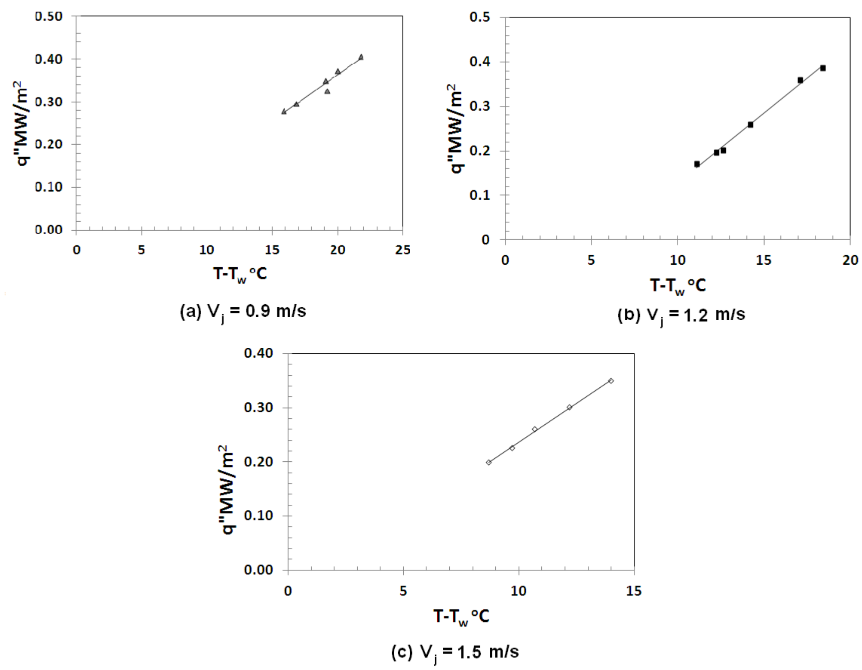

Figure 4-30 Relationship between Heat Flux and Temperature Difference for the Single Phase Regime, Surface S2

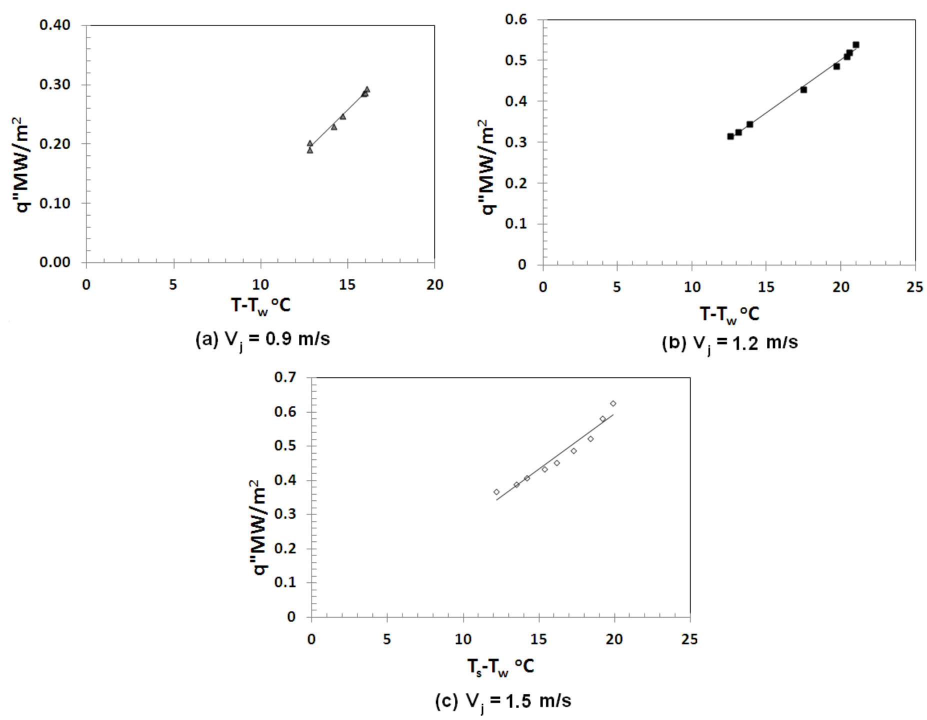

Figure 4-31 Relationship between Heat Flux and Temperature Difference for the Single Phase Regime, Surface S3

Nusselt number Nu and Reynolds number Re were calculated, according to equations (4.2) and (4.3) respectively, based on jet hydraulic diameter ($D_h = 4*A_c/P_w = 1.8\ mm$) as a characteristic length and water properties at the film temperature $T_f = 1/2\ (T + T_w)$. Table 4.2,

S1			
V	h	Re	Nu
0.9	18407	5567	48.9
1.2	22044	7422	58.5
1.5	24263	9278	64.4

Table 4.3 and Table 4.4, show the values of the calculated Re and Nu numbers for the three surfaces respectively.

$$Re = \rho_w V_j D_h / \mu_w \qquad (4.2)$$

$$Nu = h D_h / k_w \qquad (4.3)$$

Where ρ_w, μ_w and k_w are the water density, viscosity and thermal conductivity at the film temperature, respectively

Table 4.2 Values of Re and Nu Numbers for the Single Phase Regime, Surface S1

S1			
V	h	Re	Nu
0.9	18407	5567	48.9
1.2	22044	7422	58.5
1.5	24263	9278	64.4

Table 4.3 Values of Re and Nu Numbers for the Single Phase Regime, Surface S2

S2			
V	h	Re	Nu
0.9	21640	5567	57.5
1.2	31282	7422	83.0
1.5	28717	9278	76.2

Table 4.4 Values of Re and Nu Numbers for the Single Phase Regime, Surface S3

S3			
V	h	Re	Nu
0.9	29168	5567	77.4
1.2	31953	7422	84.8
1.5	51631	9278	137.1

Figure 4-32 shows the relationship between Nusselt Nu and Reynolds Re numbers for the three surfaces with error bars calculated as in Appendix A. It could be noticed that at low Re number, the difference between the values of Nu lie in the uncertainty range. However, as can be seen from the figure, the slope is higher for surface S3 than S2 than S1. This agrees well with results obtained by Gabour and Lienhard (1994).

Figure 4-33 compares Nu versus Re relations obtained by this study and that obtained by Gabour and Lienhard (1994) using a 4.4 mm diameter nozzle. Gabour and Lienhard (1994) were using a circular jet and a much wider range of surface roughness. Taking into account the different range of the studied parameters, different geometry and different surface material, a reasonable qualitatively agreement could be noticed.

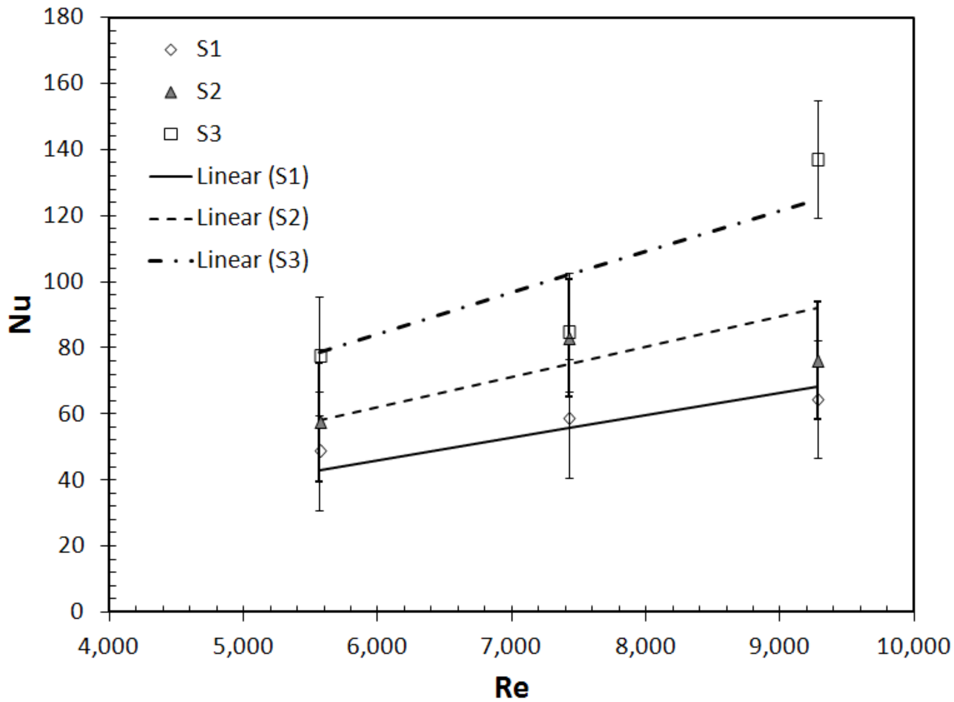

Figure 4-32 Nu versus Re, Single Phase Regime

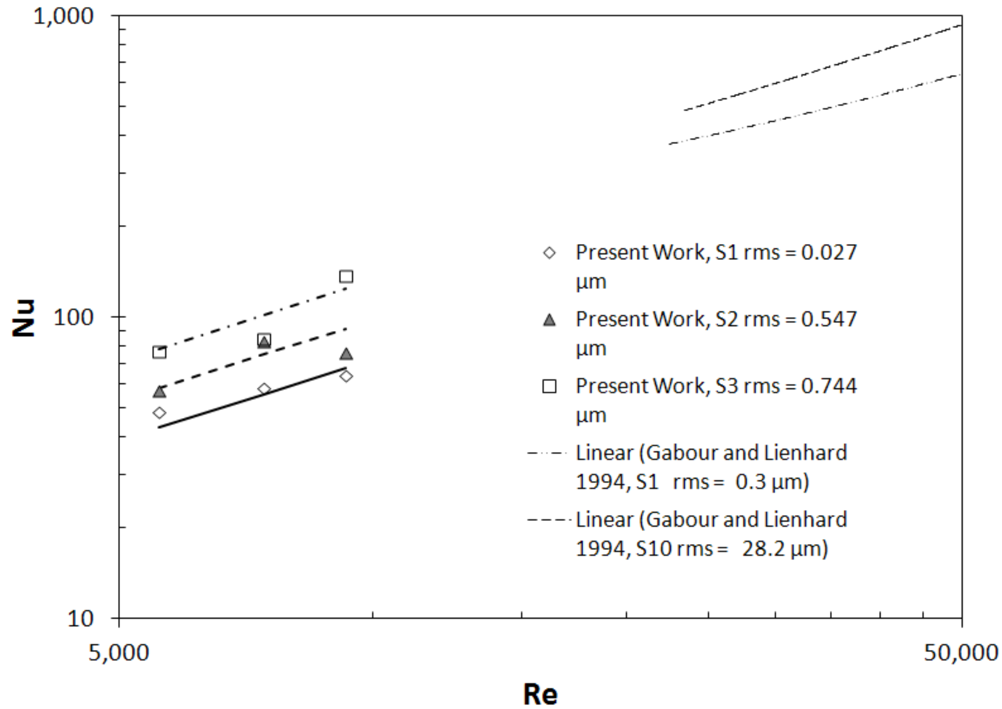

Figure 4-33 Comparison between the Current Study with Gabour & Lienhard (1994). Nu versus Re, Single Phase Regime

The Nu versus Re relationship is displayed through equations (4.4) to (4.6) for surfaces S1, S2 and S3 respectively. Gabour and Lienhard investigated a relationship between Re and Nu for the smooth surface S1 where Nu was proportional to $Re^{0.633}$.

For surface S1

$$Nu = 0.0183\ Re^{0.9} \qquad (4.4)$$

For surface S2

$$Nu = 0.0247\ Re^{0.9} \qquad (4.5)$$

For surface S3

$$Nu = 0.0335\ Re^{0.9} \tag{4.6}$$

Chapter 5 Summary, Conclusions and Recommendations

5.1 Summary and Conclusions

The reported study focused on the stagnation point. The conclusions from the current study are summarized in this section.

The existence of a hydraulic jump downstream the jet was confirmed by digital photos. For jet velocity V_j > 1.5 m/s, It was noticed that due to the high impact of the jet, a significant amount of water flowed along and across the side walls; which decreased the actual flow rate flowing on the heater surface and caused some discrepancies in the results. No flow measurements were recorded in the channel.

Although, the study focused on the stagnation region, some parameters were affected by the flow downstream the jet. The burn out heat flux BOF and the onset of nucleate boiling ONB are two of these variables. When the boiling starts anywhere downstream the jet, it propagates upstream quickly, by activating the closer potential nucleation site, affecting the ONB at the stagnation point. Flow restrictions due to the pressure drop resulting from bubble formation helps boiling to propagate more quickly. Similarly, when the BOF occurs anywhere downstream of the jet, the heating foil burns out causing the experiment to end.

Increasing jet velocity has a significant effect on the heat transfer under liquid jet impingement. Increasing jet velocity was found to increase the heat flux for the single phase regime insignificantly. ONB was found to be delayed with increasing jet velocity up to V_j = 1.5 m/s. These findings agree well with the literature (Omar 2010 and Robidou et al. 2003). Also increasing jet velocity was found to increase the BOF for jet velocities $V_j \leq 1.5$ m/s.

For jet velocities $V_j \leq 1.5$ m/s, increasing the surface roughness was found to increase the heat transfer in the single phase regime and increasing surface roughness also caused earlier ONB.

The effect of surface roughness on single phase heat transfer at the stagnation point was compared to Gabour and Lienhard (1994) and a good qualitative agreement was found.

5.2 Recommendations for Future Work

1. To ensure constant surface temperature, different power supplies with different controllers could be used, in order to decrease the temperature gradient on the heater surface. This will also help in protecting the foil from burnout by. In the current design where only one power supply is used, the controller cares about the controlled temperature regardless of what other thermocouples read. Burnout occurs at the location where burn out heat flux BOF is obtained first

2. Increasing the range of roughness parameters and creating more homogenous cavities on the surface. This could be obtained by electrical discharge machining EDM. Using special chemicals to manufacture the surface could result in a random cavity diameter distribution
3. In this study, foil burnout occurred earlier than expected. This could be avoided by:
    - Ensuring good contact between the surface and the Al_2O_3 layer. This could be done by using a layer with uniform thickness instead of spraying the foil
    - Allowing a space for foil expansion. When the foil expands, it wrinkles increasing the contact resistance
    - Increasing the foil thickness at the ends. Burn out usually occurs at one end of the foil
4. More homogeneous cavities could be also obtained by pressing sand paper into the surface. Different cavity diameters could be obtained by using different sand papers
5. Studying the effect of some other surface parameters that should be more significant than the surface roughness parameters, such as the cavity's mouth diameter, the cavity angle and the cavity shape. These parameters would affect the nucleation site density, the bubble size and bubble frequency

6. Studying the effect of surface curvature, which would be more closely related to some industrial applications such as those involve the processing of pipes
7. Studying the effect of the surface material (thermophysical properties). The ability of cavities to trap vapor is a function of the contact angle, while the surface superheat required to initiate boiling is function of the mouth diameter
8. Using high speed camera to collect data regarding bubble size, frequency and nucleation site density. This data would be useful to understand the physics of the surface roughness effect on boiling heat transfer. These data could be used also to derive a mechanistic model for the heat transfer under liquid jet impingement
9. As some industrial applications may not use water for cooling, the effect of changing the type of liquid could be investigated under jet impingement conditions
10. Studying the aging effect on the different surfaces. Surface cavities might be deactivated with time which is called the aging effect
11. If water has to be used, using smaller tank would help in degassing the water completely or using distilled water instead of tab water
12. Simpler test section could be used to focus on the stagnation regime without being affected by the downstream flow. This could be done by using jet larger than the heater surface

13. Wider channel could be used to avoid the flow profile occurred at high jet velocities. Wider channel with no sidewalls could be also used for the same reason
14. Using three rows of thermocouples instead of two will reduce the uncertainty in the surface temperature as well as the heat flux uncertainty
15. To avoid foil burn out, induction heating could be used to heat the copper block by radiation. In this case, the effect of the induction coil's electromagnetic field on the thermocouples should be taken into account. A number of cartridge heaters could be also used for the same reason

References

1. Bogdanic L., Auracher H., and Ziegler F., (May 2009). Two-Phase Structure above Hot Surfaces in Jet Impingement Boiling. *Heat and Mass Transfer*. Vol. 45. Issue 7, pp. 1019-1028

2. Gabour, L. A. and Lienhard, J. H., (1994). Wall Roughness Effects on Stagnation-Point Heat Transfer beneath an Impinging Liquid Jet. *Journal of Heat Transfer*, Vol. 116, Issue 1, pp. 81-87

3. Griffith, P., and Wallis, J. D., (1960). The Role of Surface Conditions in Nucleate Boiling. *Chem. Eng. Prog., Symp. Ser.*, Vol. 56, Issue 30, pp. 49–63

4. Guo, D., J.J. Wei, Y.H. Zhang. (2011). Enhanced Flow Boiling Heat Transfer with Jet Impingement on Micro-pin-finned Surfaces. *Applied Thermal Engineering*. Vol. 31, pp. 2042-2051

5. Ishigai, S., Nakanishi, S., and Ochi, T. (1978). Boiling Heat Transfer for a Plane Water Jet Impinging on a Hot Surface. *Proceedings of the 6th International Heat Transfer Conference*, Vol. 1, pp.445-450

6. Jones, B.J., McHale, J. P., and Garimella, S.V. (2009). The Influence of Surface Roughness on Nucleate Pool Boiling Heat Transfer. *Journal of Heat and Mass Transfer.* Vol. 131, pp. 1-14

7. Judd, R.L. and Hwang, K.S., (Nov.1976). Comprehensive Model for Nucleate Pool Boiling Heat Transfer Including Microlayer Evaporation. *Journal of Heat Transfer*. Vol. 98, Series C, No. 4, pp.623-629

8. Jung, Jung-Yeul and Kwak, Ho-Young., (2006). Effect of Surface Condition on Boiling Heat Transfer from Silicon Chip with Submicron-Scale Roughness. *International Journal of Heat and Mass Transfer, Vol. 49, pp. 4543-4551*

9. Kandlikar Satish G., Spiesman Paul H., (1998). Effect of Surface Finish on Flow Boiling Heat Transfer, *HTD, Vol. 361 issue 1, pp. 157-163*

10. Kugler S. and V.K. Dhir., (1996) Enhancement of Nucleate Boiling Heat Flux on Macro/micro Structured Surfaces Cooled by Multiple Impinging Jets. *AIChE Symposium Series.* Vol. 92, pp. 287-293

11. McHale, John P and Garimella S. V., (2010). Bubble Nucleation Characteristics in Pool Boiling of a Wetting Liquid on Smooth and Rough Surfaces. *International Journal of Multiphase Flow*. Vol. 36, pp. 249–260

12. Mpholo M., Mathaba T., and Bau H. H., (2010). A 2D Analysis of Surface Roughness for Prediction of Boiling Incipience*. International Journal of Heat and Mass Transfer.* Vol. 53, pp. 1313-1318

13. Nguyen, Cong Tam, Galanis, Nicolas, Polidori, Guillaume, Fohanno, Stéphane, Catalin V. Popa , and Arnaud Le Bechec (2009). An

Experimental Study of a Confined and Submerged Impinging Jet Heat Transfer Using Al_2O_3-water Nanofluid. *International Journal of Thermal Sciences.* Vol. 48, pp. 401-411

14. Omar A.M.T., Hamed M.S., Shoukri M., On The Bubble Dynamics Under An Impinging Free Planar Jet.*ECI International Conference on Boiling Heat Transfer*. 3-7 May 2009a, Florianopolis SC, Brazil

15. Omar A.M.T., Hamed M.S., and Shoukri M., Prediction of Wall Heat Flux to an Impinging Free Liquid Jet Using the Concept of Wall Flux Partitioning. *Fourth International Conference on Thermal Engineering: Theory and Applications*, January 12-14, 2009b. Abu Dhabi, UAE

16. Omar A.M.T., Hamed M.S., Shoukri M., Experimental Study of Steady State Nucleate Boiling Heat Transfer under Planar Jet Impingement. *The 12th International Topical Meeting on Nuclear Reactor Thermal Hydraulics (NURETH-12),* Sept. 30 - Oct. 4, 2007, Pittsburgh, Pennsylvania, U.S.A.

17. Omar, Ahmed (2010)., Experimental Study and Modeling of Nucleate Boiling Heat Transfer During Free Surface Planar Liquid Jet Impingement, *PhD Thesis, McMaster University, Canada.*

18. Robidou H., Auracher H., Gardin P., Lebouch M., and Bogdanic L. (2003). Local Heat Transfer from a Hot Plate to a Water Jet. *International Journal Heat and Mass Transfer*. Vol. 39, pp. 861-867

19. Sathe A M, and Mahajan S P. Effect of Surface Roughness and Subcooling in Pool Boiling Heat Transfer, *Indian Journal of Technology, Vol. 19, 1981, pp. 239-242*

20. Sinha, J. (2003). Effects of Surface Roughness, Oxidation Level, and Liquid Subcooling on the Minimum Film Boiling Temperature. *Experimental Heat Transfer*. Vol. 16, Issue 1, pp. 45 -60

21. Shoukri, Mamdouh. (1974)., Nucleation Site Activation in Saturated Boiling, *M.A.Sc. Thesis, McMaster University, Canada.*

22. Takata, Y., Hidaka, S., Kohno, M., Ishihara, N., Tagashira, K., and Kuroki, T., Behaviour of Small Water Droplets Impinging onto Hot Surface- Effects of Surface Roughness and Impinging Velocity. *7th ECI International Conference on Boiling Heat Transfer*, 2009, Florianopolis, Brazil

23. Vader, D. T., Incropera, F. P. , and Viskanta , R. (1992). Convective Nucleate Boiling on a Heated Surface Cooled by an Impinging Planer Jet of Water. *Journal Heat Transfer*. Vol.114, Issue 1, pp. 152-160

24. Watson, E. J., (1964). The Radical Spread of a Liquid Jet over a Horizontal Plane. *Journal of Fluid Mechanics*. Vol. 20, part 3, pp. 481-499

25. Webb, R. L., (2004). Odyssey of the Enhanced Boiling Surface. *Journal of Heat Transfer*. Vol. 126, Issue 6 , pp. 1051-1059

26. Wolf, D. H., Incropera F. P., and Viskanta R. (1993). Jet Impingement Boiling. *Advances in Heat Transfer*. Vol. 23, pp. 1-132

27. Wolf, D. H., Incropera F. P., and Viskanta R. (1996). Local Jet Impingement Boiling Heat Transfer. *International Journal of Heat and Mass Transfer.* Vol. 39, No. 7, pp 1395-1406

28. Yu J., Momoki S., Koyama S., (1999). Experimental Study of Surface Effect on Flow Boiling Heat Transfer in Horizontal Smooth Tubes, *International Journal of Heat and Mass Transfer*. Vol. 42, pp. 1909-1918

29. Zhen-Hua Liu and Yu-Hao Qiu, (2007). Boiling Heat Transfer Characteristics of Nanofluids Jet Impingement on a Plate Surface. *Heat Mass Transfer*. Vol. 43, pp. 699–706

Appendix A: Uncertainty Analysis and Repeatability Test

The uncertainty of the computed results was calculated using equation (A.1).

$$\frac{W_R}{R} = \sqrt{\left(\frac{\partial R}{\partial V_1}\cdot\frac{W_1}{R}\right)^2 + \left(\frac{\partial R}{\partial V_2}\cdot\frac{W_2}{R}\right)^2 + \ldots + \left(\frac{\partial R}{\partial V_n}\cdot\frac{W_n}{R}\right)^2} \qquad \text{(A.1)}$$

where

R	=	result computed
W_R	=	uncertainty in the result R
V_n	=	n^{th} variable
W_n	=	uncertainty in the n^{th} variable

A.1 Surface Temperature

The thermocouples were calibrated over the range of tested temperature with an error of ± 0.1°C. The surface temperature extrapolated using MATLAB was tested by Omar (2010) and it was exactly coinciding on the equation as will be seen in Appendix B. So, it is reasonable to assume that the surface temperature extrapolated by the MATLAB code is in accordance with that of the thermocouples readings at the interior locations, i.e.; ±0.1 °C.

The uncertainty in the surface temperatures is ± 0.1 °C. By assuming constant saturation temperature, the uncertainty in ΔT_{sat} could be assumed ± 0.1 °C. For low surface superheats, the uncertainty in ΔT_{sat} becomes ± 3%.

If the surface temperature would have been extrapolated from the linear temperature gradient, the error in surface temperature would have been ±0.5 °C. The existence of six thermocouples 0.5 mm could affect the uniformity of the heat transfer to the surface. However, its effect on the calculated values of surface temperature and heat flux could be neglected because of using two dimensional FDA.

A.2 Surface Heat Flux

The uncertainty in the average wall flux at the flat surface is based on the one-dimensional heat conduction analysis:

$$q'' = -k_{Cu} \frac{\Delta T}{\Delta y} \qquad \text{(A.2)}$$

Where y is the normal distance from the heater surface and k_{cu} is the copper thermal conductivity

The uncertainty in the copper thermal conductivity was within 3% over the operating temperature range. The uncertainty in the location of the thermocouples is ± 2.54E-6 m which is the precision of the machining device and the lower thermocouples row was located 2 mm below the surface. The uncertainty in the temperature difference would be twice as the uncertainty of thermocouples measurements, i.e. ± 0.2°C. From equation (A.1), the percentage uncertainty in the wall heat flux is estimated to be 19% at low values of heat flux (low temperature difference between the upper and lower thermocouples). This value decreases to be 1.87 % at BOF.

A.3 Nozzle hydraulic diameter

The hydraulic diameter was calculated from

$$D_h = \frac{4\, l.w}{2(l + w)} \qquad \text{(A.3)}$$

where

l	=	nozzle length
w	=	nozzle width
D_h	=	hydraulic diameter

The uncertainty in the nozzle width was equal to the uncertainty in the nozzle length and was equal to ± 2.5x10^{-6} m. By using equation (A.1), the uncertainty in the hydraulic diameter becomes less than 0.01%.

A.4 Nusselt number

Nu number was calculated from the equation:

$$Nu = \frac{\frac{q''}{T_s - T_w} . D_h}{k_f} \qquad \text{(A.4)}$$

where

q'' = computed heat flux

T_s = surface temperature

T_w = water temperature

k_f = fluid thermal conductivity at the film temperature

D_h = nozzle hydraulic diameter

The uncertainty in the nozzle hydraulic diameter was less than 0.01% for a hydraulic diameter 1.8 mm. The uncertainty in the temperature difference would be ± 0.2 °C while the temperature difference was in order of 10°C. Using the maximum error in heat flux (19 %) and heat flux of order 0.75 MW/m^2 in the single phase regime, the uncertainty in Nu would be ± 17.9 with a maximum error of 37%.

A.5 Reynolds number

Nu number was calculated from the equation:

$$\mathrm{Re} = \frac{\rho_f V_j D_h}{\mu_f} \qquad \text{(A.5)}$$

where

ρ_f = water density at the film temperature

μ_f = water viscosity at the film temperature

V_j = jet velocity

D_h = nozzle hydraulic diameter

The uncertainty in the nozzle hydraulic diameter was less than 0.01% for a hydraulic diameter 1.8 mm. The uncertainty in the jet velocity would be ± 0.05 m/s while the jet velocity was in order of 1 m/s. By assuming constant fluid properties, the uncertainty in Re number will be less than 0.1%.

A.6 Repeatability Test

Figure A-1shows a repeatability test done on surface S2 at a jet velocity Vj = 1.5 m/s on a log log scale. The difference between the two runs lies in the experimental error range. Results observed at jet velocities higher than 1.5 m/s was unrepeatable.

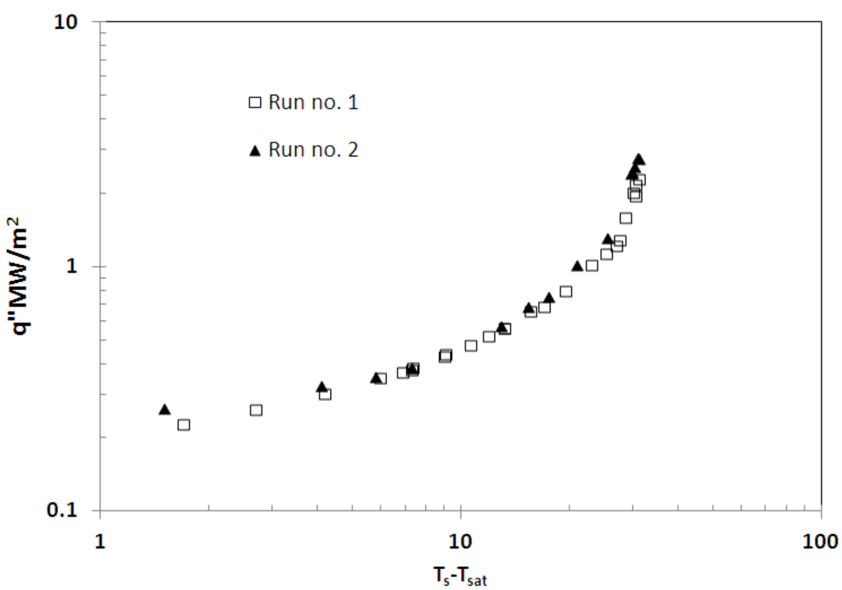

Figure A-1 Repeatability Test on Surface S2, Vj = 1.5 m/s, ΔTsub = 10˚C

Appendix B: FDA Used for Calculating Heat Flux

This appendix introduces the Finite Difference Algorithm and present the Code used to calculate surface temperature and surface heat flux. The code was produced by Omar, 2010 and copied from his thesis.

B.1 Nodalization of Boiling Module

Thermocouples readings were used to determine temperature spatial distribution and the heat flux at the boiling surface. Temperature measurements were taken at distances, x, from the jet stagnation equal to 0, 2, 4, 6, and 8 mm. Second degree polynomial fit of data at x = 6 and 8 mm, assuming zero temperature gradient at x=10 mm, were used to determine the temperature value at the insulated right side x = 10 mm. Then, the Data was used as input to a two dimensional finite difference algorithm (FDA) to determine the temperature distributions within the boiling block.

Figure B-1a shows the computational domain which represents half of the boiling block bounded by the two thermocouple rows at top and bottom. The left side at the stagnation line and ceramic insulated right side were treated as adiabatic boundary. Figure B-1b shows the intermediate nodes used for numerical calculations.

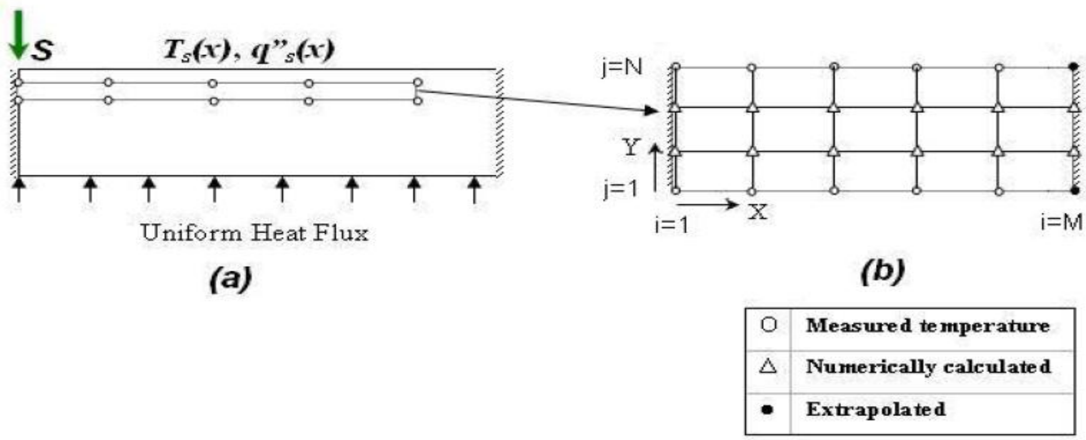

(a) Physical domain representing half the block, (b) Computational domain showing nodes of: measurement, measurement extrapolations, and numerical calculation

Figure B-1Discretization of Boiling Block, Omar, 2010

B.2 Determination of Surface Temperature and Heat Flux

By assuming constant thermal conductivity, the following two-dimensional, steady-state, heat conduction equation can represent the physical domain of interest within the boiling block

$$\frac{\partial^2 T}{\partial x^2} + \frac{\partial^2 T}{\partial y^2} = 0 \qquad (1)$$

and the boundary conditions are:

at x=X=0.01m

$$\frac{\partial T(0,y)}{\partial x} = 0 \qquad (2)$$

at x= 0

$$\frac{\partial T(X,y)}{\partial x} = 0 \qquad (3)$$

at y= Y= 0.0015 m

$$T(x,0) = F_1(x) \qquad (4)$$

at y= Y= 0 m

$$T(x,Y) = F_2(x) \qquad (5)$$

Where F_1 and F_2 are temperature values calculated at the top bottom boundary of the domain using cubic data fit of temperature readings.

The partial differential heat conduction equation (1) was converted into the following finite difference equation:

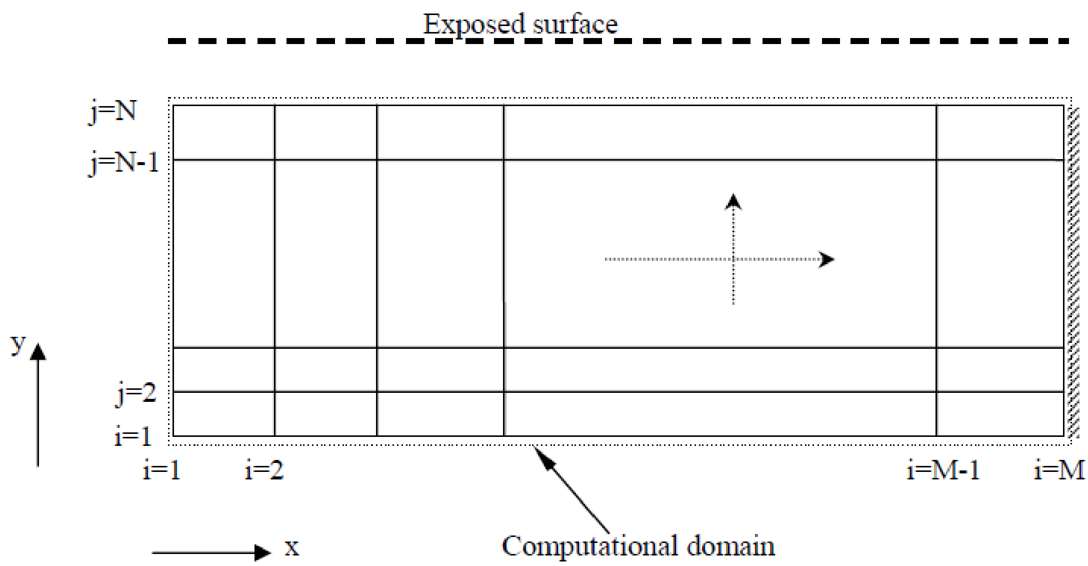

Figure B-2 Discretization scheme of the FDA domain, Omar, 2010

$$\frac{T_{i+1,j} - 2T_{i,j} + T_{i-1,j}}{(\Delta x)^2} + \frac{T_{i,j+1} - 2T_{i,j} + T_{i,j-1}}{(\Delta y)^2} = 0 \qquad (6)$$

And the boundary conditions were discretized to the form:

at x = 0

$$T_{-1,j} = T_{1,j} \qquad (7)$$

at x = 0.01 m

$$T_{M+1,j} = T_{M-1,j} \qquad (8)$$

at $y = 0$ m

$$T_{i,1} = T_{b,i} \tag{9}$$

at $y = 0.0015$ m

$$T_{i,N} = T_{t,i} \tag{10}$$

where subscripts ‘b’ and ‘t’ refer to temperature values, measured or interpolated, at the bottom and top thermocouple rows, respectively.

The surface was not included in the computational domain as shown in Figure B-3. The spatial variation of the surface temperature, $T_s(x)$ in the x-direction was calculated by extrapolating the interior temperature distribution in the y-direction to the surface using the second degree polynomial, Equation (3.11)

$$\mathrm{T_s}\,(\mathrm{x}) = \mathrm{a}_0(x) + \mathrm{a}_1(x)y + \mathrm{a}_2(x)y^2|_{y=0.002m} \tag{11}$$

where y = 2 mm, measured from the bottom thermocouple row.

The coefficients $a_o(x)$, $a_1(x)$, and $a_2(x)$ were determined using the interior temperature distribution in the y-direction. The accuracy of the chosen fit was found acceptable since R_2=1.

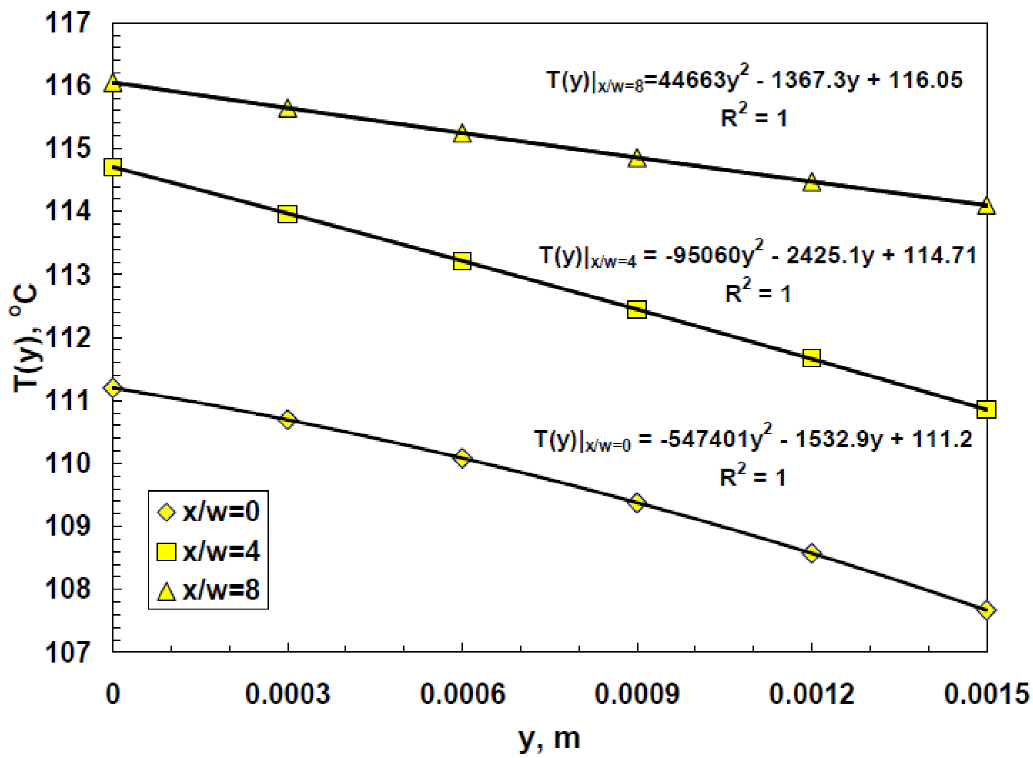

Figure B-3 Second Degree Polynomial Fit of the Interior Temperature Distribution between the Two Thermocouple Rows. Omar, 2010

The gradients of temperature functions represented by equation (11) were used to determine the spatial distribution of the surface heat flux using equation (12)

$$q_s^{"}(x) = -k_{Cu}\,\frac{\partial T(y)}{\partial y}\,|_{y=0.002m} = -k_{Cu}\left(\mathrm{a}_1 + 2\mathrm{a}_2(0.002)\right) \qquad (12)$$